2024

Biodistribution Comparison of Fentanyl and Morphine Following Acute and Repeated Expsoure

Rosamond M. Goodson
Virginia Commonwealth University

Biodistribution Comparison of Fentanyl and Morphine Following Acute and Repeated Exposure

A dissertation submitted in partial fulfillment of the requirements for the degree of Doctor of Philosophy in Pharmacology and Toxicology at the Virginia Commonwealth University School of Medicine.

by

Rosamond M. Goodson

Advisors: William L. Dewey, PhD

Professor and Chairman

Department of Pharmacology and Toxicology

Matthew S. Halquist, PhD

Associate Professor

Department of Pharmaceutics

Department of Pharmacology and Toxicology

Virginia Commonwealth University

Richmond, VA

April 2024

ACKNOWLEDGEMENTS

Much like the production of a musical or opera requires the combined time, talents, and effort of a diverse cast and crew, this dissertation could only reach the curtain call thanks to numerous contributions from faculty, colleagues, and loved ones. First and foremost, I would like to thank my mother, Anna Maria Goodson, for her steadfast love and support throughout my academic journey.

I am profoundly grateful to my mentors, Drs. William Dewey and Matthew Halquist, whose unflagging support and considerable joint expertise were vital to the development of my graduate career. It has been a privilege to work under their tutelage.

Many thanks are due as well to the other members of my committee, Drs. D. Matthew Walentiny, Michelle Peace, Carl Wolf, and Hamid Akbarali, for the valuable insights and suggestions they offered regarding my research and professional growth.

It is no hyperbole to state that this project would not have been possible without Justin Poklis, manager of the mass spectrometry lab in the Department of Pharmacology and Toxicology at Virginia Commonwealth University, and I am deeply indebted to his generosity and patience in helping me process the hundreds of tissue samples analyzed over the course of my work. I would also like to thank Melissa Morgan, David Stevens, and Dr. Minho Kang for the technical support they graciously provided.

Further thanks are owed to the Department of Pharmacology and Toxicology for securing the necessary financial and academic resources for my graduate education. In particular, I would like to extend my gratitude to Dr. Keith Shelton for his work as program director, to Laura Johnson and Robin Brannon (executive assistants past and present), and, once again, to Dr. William Dewey, for his tireless advocacy on behalf of the department.

Lastly, I would like to thank my “true, faithful, and loyal” Wesleyan sisters, my friends and fellow production team members on the Crossmodal podcast, and all the others whose kindness bolstered my morale and gave me the fortitude to persevere to the end.

This research was supported by the National Institute on Drug Abuse (T32 Training Grant 07727)

TABLE OF CONTENTS

LIST OF TABLES

Chapter 1

Chapter 3

Chapter 5

Appendix

LIST OF FIGURES

Chapter 1

Chapter 4

Chapter 5

LIST OF ABBREVIATIONS

4-ANPP	4-Anilino-N-Phenethylpiperidine, or Despropionyl Fentanyl
ANOVA	Analysis of Variance
AUC	Area Under the Curve
CDC	Centers for Disease Control and Prevention
CE	Collision Energy
C_{max}	Maximum Observed Concentration
CNS	Central Nervous System
DP	Declustering Potential
HPLC-ECD	High-Performance Liquid Chromatography Coupled to Electrochemical Detection
HPLC-MS/MS	High-Performance Liquid Chromatography Tandem Mass Spectrometry
f	Respiratory Rate, or Breath Frequency
FDA	Food and Drug Administration
GC/MS	Gas Chromatography/Mass Spectrometry
ip	intraperitoneal (route of drug administration)
iv	intravenous (route of drug administration)
LC/MS-MS	Liquid Chromatography Tandem Mass Spectrometry
LLOQ	Lower Limit of Quantification
LOD	Limit of Detection
LOQ	Limit of Quantification
M3G	Morphine-3-β-D-Glucuronide
M6G	Morphine-6-β-D-Glucuronide

mg/kg	milligrams/kilogram
min	Minutes
MRM	Multiple Reaction Monitoring
MVb	Minute Volume
NFLIS	National Forensic Laboratory Information System
ng/g	nanograms/gram
ng/mL	nanograms/milliliter
RPM	Revolutions/Minute
t_{max}	Time of Maximal Concentration
TVb	Tidal Volume
sc	subcutaneous (route of drug administration)
Q1	Quadrupole 1
Q3	Quadrupole 3
Qual.	Qualifying MRM transitions
Quant.	Quantifying MRM Transitions
UHPLC-MS/MS	Ultra-High Performance Liquid Chromatography Tandem Mass Spectrometry
UPLC-QTOF/MS	Ultra-High Performance Liquid Chromatography with Quadrupole Time-of-Flight Mass Spectrometry
UGT	Uridine Diphosphate Glucoronosyltransferases
(US)DEA	(United States) Drug Enforcement Administration
WONDER	Wide-ranging ONline Data for Epidemiologic Research

STATEMENT OF CONTRIBUTIONS

All studies reported in this dissertation were performed by Rosamond Morgan Goodson. Justin Poklis obtained raw analytical readings that quantified target analytes in blood and tissue samples. Further technical support was offered by Melissa Morgan, David Stevens, and Dr. Minho Kang, while Dr. Piyusha Pagare generously provided mice for repeated dosing studies. Data analyses were initially completed by Rosamond Morgan Goodson with additional input from Drs. Matthew Halquist and William Dewey. Manuscript was written by Rosamond Morgan Goodson, followed by critiques from Drs. Matthew Halquist and William Dewey. All work presented herein is original, and any figures or data from outside sources will be designated as such.

ABSTRACT

The ongoing opioid crisis constitutes a dire public health threat that has resulted in staggering loss of life. In 2021, opioids were implicated in over 75% of the approximately 107,000 deaths attributed to drug overdose (CDC), and synthetic opioids such as fentanyl and its analogues are key drivers of the surge in opioid fatalities in recent years. Although fentanyl is a μ opioid receptor agonist, it has several distinct attributes compared to other drugs in this category, such as morphine. These include enhanced lipophilicity, heightened potency to induce respiratory depression, more rapid entry into the central nervous system, reduced sensitivity to naloxone rescue after overdose, reduced cross-tolerance to fentanyl even with a previous history of opioid exposure, and promotion of skeletal muscle rigidity, or "wooden chest syndrome," which increases risk of overdose death. However, there are relatively few extensive comparisons of potential differences in biodistribution between fentanyl and classical opioids such as morphine in mouse models, despite the fact that mice are often used in preclinical studies of parameters relevant to the opioid crisis, i.e. respiratory depression. Therefore, the objective of the present dissertation was to compare acute biodistribution of fentanyl and morphine in blood and 12 murine tissues at doses demonstrated to cause respiratory depression and to gauge potential differences in biodistribution following repeated administration of these opioids. To this end, whole-body plethysmography studies were run to evaluate doses of fentanyl and morphine that produced comparable respiratory depression in male Swiss Webster mice. Then, an LC/MS-MS method was developed to quantify fentanyl, morphine, and select metabolites (norfentanyl and 4-ANPP, or despropionyl fentanyl, and morphine-3-β-D-glucuronide, respectively) in mouse whole blood, whole brain, lung, heart, kidney, small intestine, large intestine, spleen, stomach, muscle, fat, and skin. Afterwards, mice received acute doses of subcutaneous (sc) fentanyl (0.3 mg/kg) or

morphine (30 mg/kg) selected based on whole-body plethysmography studies, and samples were collected at 5, 15, 60, and 240 min. A separate cohort received repeated daily injections of these doses for 5 days prior to sample collection 60 min after the last treatment.

The data indicate that, after acute administration, time course of drug distribution varied by tissue, with fentanyl and morphine demonstrating similar time courses in tissues like lung, stomach, and small intestine, but differing in others, like brain and spleen. Moreover, fentanyl exhibits greater distribution out of the blood and into brain, liver, lung, and heart than morphine early after administration and accumulates out of blood into fat at later time points after administration to a greater extent than morphine. Ratios of total drug distribution (expressed as area under the curve) in tissue and blood over the observed acute administration time course suggest that fentanyl accumulation in tissue relative to blood in several regions of the body, such as lung, heart, kidney, spleen, fat, and small intestine, is greater than morphine. These findings indicate that, even though fentanyl's fatal effects are largely centrally-mediated, this synthetic opioid could potentially have deleterious effects on several organs to a larger degree than morphine, both those involved in respiration and those not directly involved in respiration. The data also suggest that temporary storage of fentanyl in adipose tissue is greater relative to opiates like morphine. Repeatedly-treated mice did not demonstrate tolerance or altered biodistribution compared to drug-naïve mice, implying that repeated fentanyl or morphine exposure that does not induce tolerance is not sufficient to modify tissue distribution. Broadly speaking, this body of work provides an assessment of fentanyl, morphine, and associated metabolite levels in diverse matrices of a model organism widely used for studying physiological and behavioral effects of synthetic opioids. In addition, a useful bioanalytical method was generated for measuring

fentanyl concentration in various mouse tissues, which could be applied to other preclinical studies conducting work related to the opioid crisis.

CHAPTER 1: INTRODUCTION

1.1. History and Epidemiology of Morphine

Although the precise date at which the opium poppy (*Papaver somniferum*) was integrated into human agriculture and medicine is unknown, Mesopotamian cuneiform tablets from 6000 BC lauded it as the "plant of joy," and its use was documented in ancient civilizations of the Mediterranean and Asia (Brook et al. 2017). Opium (whose name is derived from the Greek word ὀπός, or vegetable juice, on account of the latex harvested from the poppy plant [Brook et al. 2017]) commonly served both recreational and medicinal functions in the Middle Ages and through the Renaissance (Davenport-Hines 2002; Blakemore and White 2002), with Paracelsus inventing laudanum in 1525 (Wicks et al. 2021). Many prominent historical figures partook of the drug, including the military commander Napoleon (1769-1821), and writers such as Edgar Allan Poe (1809-1849) and Thomas de Quincey (1785-1859), whose influential book *Confessions of an English Opium Eater* chronicled his experiences with substance abuse (Brook 2017; de Quincey 1821).

While several attempts were made at isolating the natural alkaloid now known as morphine from opium (Bentley 1954; Davenport-Hines 2002; Trease 1964; University of the Sciences in Philadelphia, 2006), credit for this achievement is generally ascribed to Friedrich Sertürner, a German apothecary who published on isolating the compound in 1806 (Sertürner 1806). In 1819, C.F. Wilhelm Meissner would go on to correctly identify morphine as an alkaloid (Meissner 1819), and August Lauren successfully calculated the chemical formula for morphine in 1847 (Lauren 1847). Meanwhile, Sir Robert Robinson played an instrumental role in elucidating morphine's structure in the 1920s (Butora and Hudlicky 1998; Gulland and Robinson 1925).

Commercial production of morphine began in the 1820s (Europe) and 1830s (the United States) (Hodgson 2001), but the compound's popularity reached new heights in the 1850s thanks to Alexander Wood's and Charles-Gabriel Pravaz's contributions to the development of the hypodermic syringe. This device allowed morphine to be administered intravenously, which, along with morphine's greater potency compared with opium, promoted rapid, heightened analgesia, and the drug became a mainstay of battlefield medicine in conflicts like the American Civil War (1861-1865) (Hodgson, 2001). Patent medicines containing opiates were also widely used during the late nineteenth century, often with little regulatory oversight (Redford and Powell 2016). However, as wider understanding of the addictive potential of opium, morphine, and other opiates began to emerge, the federal government took a harsher stance, as with the 1909 Opium Exclusion Act, which banned the import of recreational smoking opium on a national scale, although opiates intended for medical use remained unaffected (Redford and Powell 2016). The subsequent International Opium Convention of 1912 and Harrison Act of 1914 placed further restrictions on the production, importation, and distribution of morphine and other opiates (Brook et al. 2017; Redford and Powell 2016).

Though no longer regarded as a panacea, morphine is authorized for clinical use as a Food and Drug Administration (FDA)-approved medication for acute or chronic instances of moderate-to-severe pain, such as ongoing cancer treatment, emergency care, and palliative care. As with most opioids, however, its use comes with a host of adverse or even life-threatening side effects, including respiratory depression, constipation, bradycardia, nausea, and vomiting (Murphy et al. 2024).

1.2. History and Epidemiology of Fentanyl

Fentanyl was first synthesized in Belgium by Janssen in 1960 as part of an initiative to develop high-potency, rapidly-acting analgesics that could serve as viable alternatives to morphine (Jannetto et al. 2019; Kuczyńska 2018; Stanley 2014). Introduced in Europe as an intravenous analgesic in 1963, fentanyl was also utilized for intravenous anesthesia, both alone and in combination with other drugs (i.e. neuroleptanalgesia, combination of fentanyl and the butyrophenone droperidol, and neuroleptanesthesia, combination of fentanyl, droperidol, and nitrous oxide) (Stanley 2014). Although the FDA eventually approved fentanyl for clinical use in the United States, as well, it was initially only permitted in combination with droperidol at a 50:1 ratio (droperidol to fentanyl), officially termed Innovar (Stanley 2014).

While morphine showed promise as an intravenous anesthetic for patients requiring cardiac surgery (Lowenstein et al. 1969), whose suboptimal cardiovascular and pulmonary condition placed them at heightened risk under the anesthetic techniques of the time, adverse effects such as histamine-mediated bronchoconstriction and hypotension diminished its utility (Stanley 1992). Fentanyl emerged as a desirable alterative to morphine for intravenous anesthesia because, in addition to its increased potency relative to morphine, rapid onset, and short duration of action, it generally did not disrupt cardiovascular function to the same extent (Grell 1970; Lunn et al. 1979). Demand for the synthetic opioid grew to the point that, when it first went off-patent in 1981, fentanyl sales in the United States increased ten-fold (Stanley in Egar et al. 2014). Even in the early years of fentanyl's use, however, its tendency to cause muscle rigidity was observed (Grell 1970).

Based on the specific formulation, fentanyl is currently FDA-approved as an adjunct for general and regional anesthesia, as an analgesic, and for persistent, moderate-to-severe chronic pain that requires continuous administration for an extended period of time that cannot be

provided by other analgesics (Raffa et al. 2018). Besides injectable formulations, pharmaceutical fentanyl products taken via other routes of administration are also available, including those intended for transmucosal (buccal tablets, lozenges, sublingual tablets), intranasal (nose spray), and transdermal (fentanyl patches) delivery (Kuczyńska et al. 2018). Like other μ opioid receptor agonists, fentanyl can cause sedation, euphoria, drowsiness, constipation, nausea, vomiting, and respiratory depression (Kuczyńska et al. 2018). Fentanyl use, particularly misuse and/or overdose, can also produce symptoms atypical for opioids, such as seizure-like activity, immediate blue discoloration of the lips, foaming at the mouth, gurgling sounds with breathing, and confusion or strange affect before unresponsiveness (Sommerville et al. 2017). Pulmonary alveolar proteinosis after smoking fentanyl (Chapman et al. 2012), diffuse alveolar hemorrhage in response to snorting fentanyl powder (Ruzycki et al. 2016), and acute anterograde amnesia associated with fentanyl abuse (Barash et al. 2018) have also been reported.

Though not on the scale of the present opioid crisis, abuse of pharmaceutical and illicit fentanyl prior to 2013 was certainly not unheard of. In the 1970s, heroin adulterated with or completely replaced by fentanyl and its analogues (sold under street names like “China White” and “Tango and Cash”) began to appear on the illicit drug market in North America (United Nations Office on Drugs and Crime 2017). In 2006, the United States experienced a public health crisis in which, unbeknownst to the drug users purchasing it, heroin was adulterated with fentanyl, leading to overdose deaths. However, lethal overdoses and fentanyl seizures declined after the clandestine laboratory in Toluca, Mexico producing this fentanyl was shut down (USDEA 2016). From 2002-2005, the National Forensic Laboratory Information System (NFLIS) reported only gradual increases in fentanyl encounters, and reported fentanyl encounters remained fairly stable between the end of the 2006 fentanyl crisis and 2013 (Janetto et al. 2019).

Healthcare professionals, especially anesthesiologists, were a common demographic among whom pharmaceutical fentanyl abuse was observed in the early 2000s due to ease of access to the drug within their work environment (Booth et al. 2002; Kintz et al. 2005).

From 2013 onward, use of and overdose deaths attributed to fentanyl increased at an alarming rate. For example, NFLIS reported that fentanyl drug seizures went from 618 in 2012 to 945 in 2013 and 4,585 in 2014 (CDC 2015). By 2016, estimated national fentanyl reports had reached 34,199 (NFLIS 2017). Meanwhile, overdose deaths in the United States attributable to fentanyl climbed from 1,605 in 2012 to 1,905 in 2013 and 4,200 in 2014 (Warner et al. 2016). These troubling trends have persisted to the present day. The rate of drug overdose deaths involving fentanyl in the United States increased from 5.7 per 100,000 standard population in 2016 to 21.6 per 100,000 standard population in 2021—in other words, a 279% increase (Spencer et al. 2023). According to CDC WONDER, almost 71,000 overdose deaths attributable to synthetic opioids (including fentanyl) other than methadone occurred in the United States in 2021, entailing a 22% increase from 2020. Much of the illicit fentanyl entering the United States is smuggled in from China and, to an extent, from Mexico (USDEA 2016, 2017). Illicit fentanyl is sold in a variety of forms, such as pills, powder, capsules, and patches, and may be administered via injection (intravenous or intramuscular), by smoking, transdermally, intranasally, sublingually, or orally (Abdulrahim et al. 2018). Since fentanyl is often clandestinely mixed with other drugs like heroin and cocaine, users are frequently unaware of ingesting the drug (Griswold et al. 2018; Macmadu et al. 2017; Volkow 2021). This leads to heightened risk of overdose due to fentanyl's increased potency relative to other opioids such as heroin (CDC 2023), especially in users lacking opioid tolerance (Volkow 2021).

1.3. Unique Properties of Fentanyl

Like morphine, fentanyl is a μ-opioid receptor agonist, but it possesses several distinctive characteristics compared to these classical opioids. For instance, fentanyl's elongated chemical structure and rotatable bonds confer greater flexibility than morphine's interconnected rings (Kelly et al. 2021). Moreover, in contrast to most other opioids, fentanyl's protonated nitrogen (which interacts with $Asp147^{3.32}$ within the μ opioid receptor) is positioned in the middle of the molecule (Kelly et al. 2021). This may permit multiple binding poses for fentanyl within the orthosteric binding pocket of the μ opioid receptor (Dosen-Micovic et al., 2006; Ellis et al., 2018; de Waal et al., 2020; Vo et al., 2021), while morphine only appears to adopt one binding pose within the μ opioid receptor (Kapoor et al., 2017). Structural differences between fentanyl and morphine are illustrated in greater detail in **Figure 1.1** below.

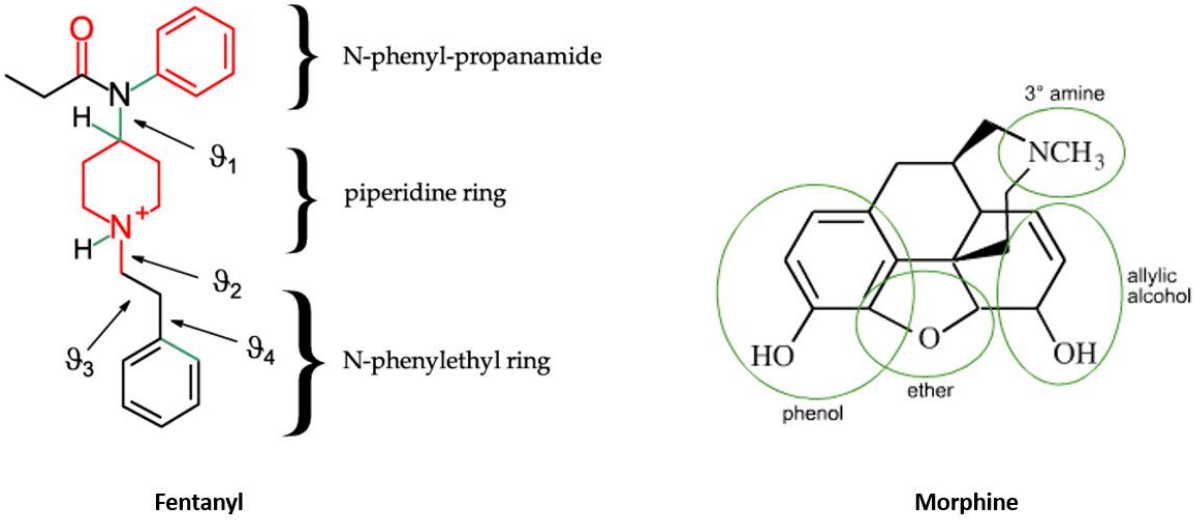

Figure 1.1: Chemical Structures of Fentanyl and Morphine. Note the central position of fentanyl's protonated nitrogen and greater flexibility (indicated by torsion angles) compared to morphine's rigid ring structure. Adapted from Lipiński et al. 2019 (fentanyl) and Florida State University (morphine).

Fentanyl also exhibits greater lipophilicity than morphine (Kelly et al. 2019; Roy and Flynn 1988). This could contribute to fentanyl's rapid CNS entry (and, by extension, rapid onset of centrally-mediated effects) compared to morphine (Hill et al. 2020) and also supports intriguing findings *in silico* which suggest that fentanyl may penetrate the cell membrane to a greater depth than morphine and enter the μ opioid receptor orthosteric binding pocket through a lipid route (the cell membrane) as well as the conventional aqueous route (Sutcliffe et al. 2021). **Table 1.1** provides a brief comparison of fentanyl's and morphine's chemical properties.

Table 1.1: Chemical Properties of Fentanyl and Morphine

Fentanyl	**Morphine**
Synthetic Opioid	Opiate (Natural Alkaloid)
XlogP[3]: 3.94	XlogP[3]: 0.49
pKa[1]: 8.43	pKa[1]: 7.9
Solubility (water, 25 ˚C)[2]: 0.200	Solubility (water, 25 ˚C)[2]: 0.345
Solubility (hexane, 35˚C)[2]: 31.96	Solubility (hexane, 35˚C)[2]: 1.3×10^{-4}

XlogP: Expression of octanol:water partition coefficient (logP), a measure of lipophilicity

1. Mather 1983 (after Meuldermans et al. 1982)

2. Roy and Flynn 1988

3. https://www.guidetopharmacology.org/

As depicted in **Figure 1.2**, fentanyl and morphine undergo distinct metabolic routes. Fentanyl is metabolized by cytochrome P450 enzymes, primarily CYP3A4, which break it down into various phase I metabolites such as norfentanyl (through N-dealkylation) and despropionyl fentanyl (through hydrolysis) (Iula 2017). In contrast, morphine undergoes glucuronidation by uridine diphosphate glucuronosyltransferases (UGTs), which convert it into the phase II metabolites morphine-3-β-D-glucuronide and morphine-6-β-D-glucuronide (Gabel et al. 2023).

In humans, this function is chiefly carried out by UGT2B7 (Gabe et al. 2023). However, this enzyme is absent in mice, which instead generate morphine-3-β-D-glucuronide via enzymes such as UGT2B36 (Kurita et al. 2017) and generally do not produce morphine-6-β-D-glucuronide at readily detectable levels (Grung et al. 1998; Handal et al. 2002; Lawrence et al. 1992).

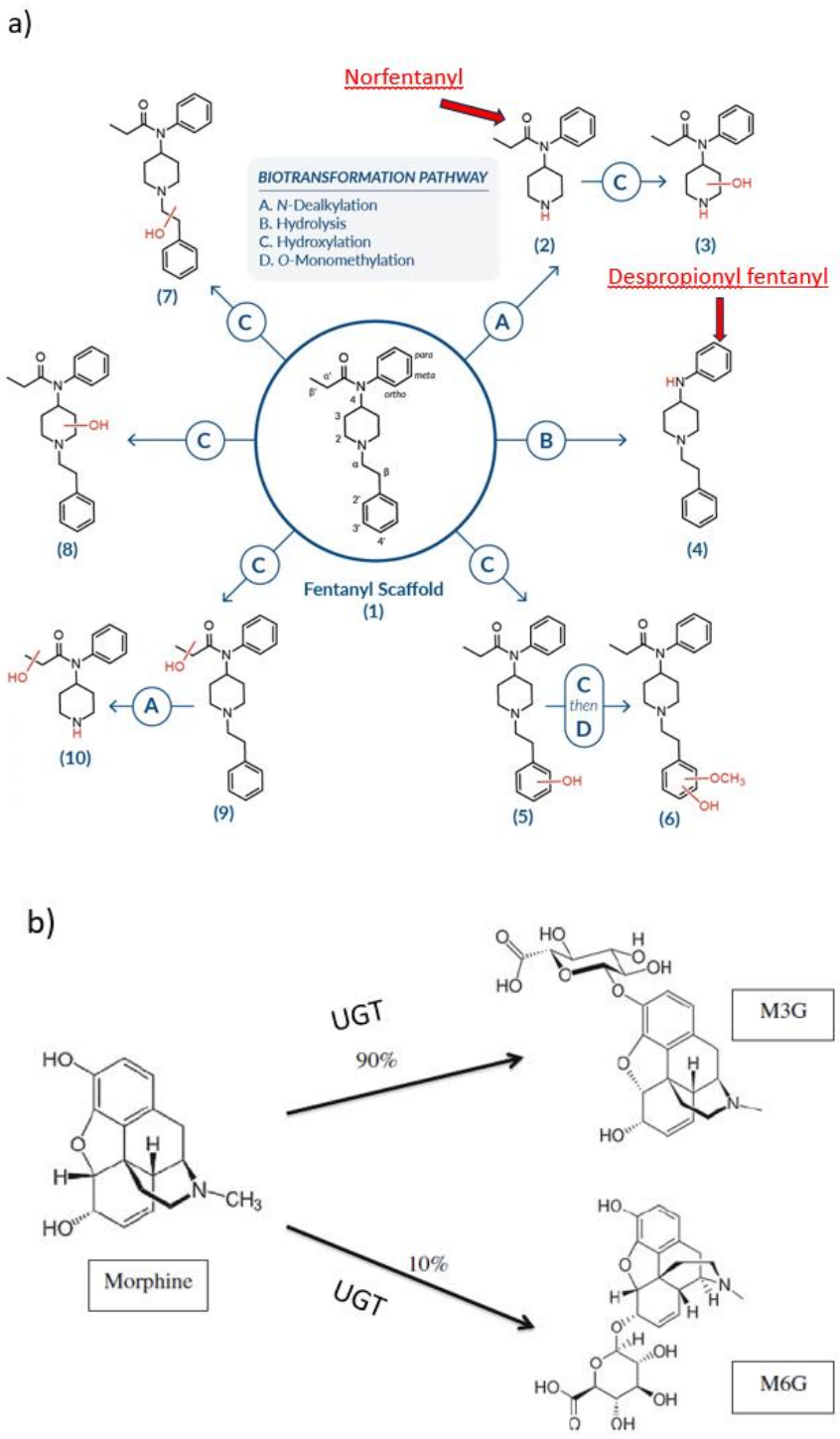

Figure 1.2: Metabolism of Fentanyl and Morphine. M3G: Morphine-3-β-D-glucuronide; M6G: Morphine-6-β-D-glucuronide. Modified from Iula 2017 (fentanyl) and De Gregori et al. 2012 (morphine).

Studies such as a 2007 paper by Kalvass et al. point to other pharmacokinetic differences between fentanyl and morphine in mice, including absorption rate constant (min^{-1}; 0.07 ± 0.07 for fentanyl, 0.27 ± 0.04 for morphine) and brain equilibration half-life (min; 4.9 ± 1.3 for fentanyl, 74 ± 45 for morphine). The authors also noted that, in contrast to morphine and the five other opioids studied, a two-compartment model was required to adequately describe fentanyl systemic pharmacokinetics based on brain and serum data (Kalvass et al. 2007).

Moreover, several characteristics of fentanyl enhance its impact on respiratory depression, contributing to its increased lethality. For instance, fentanyl is 50-100 times more potent than morphine (CDC 2023). As stated above, fentanyl also enters the brain more quickly, driving rapid onset of central nervous system effects such as respiratory depression (Hill et al. 2020). Compared to heroin overdose death, which may occur within 20-30 min of administration (Dark and Duflou 2016), fentanyl overdose death can, depending on the route, occur within 2 min after administration (Kuczyńska 2018), leaving a dangerously narrow window of intervention for victims of fentanyl overdose. This problem is further compounded by fentanyl's reduced sensitivity to naloxone antagonism (Hill et al. 2020; Mahonski et al. 2020; Mayer et al. 2018; Moe et al. 2020; Somerville et al. 2017; Sutter et al. 2017), which impedes responders' ability to reverse an overdose. In addition, subjects that have been rendered tolerant to other opioids, such as chronic morphine, exhibit reduced cross-tolerance to fentanyl-induced respiratory depression (Hill et al. 2020). Yet another unique attribute of fentanyl is its ability to promote skeletal muscle rigidity (Comstock et al. 1981; Grell et al. 1970), including sustained diaphragm/intercostal muscle contractions (Benthyusen et al. 1986) and obstruction of the glottic and supraglottic airway (Abrams et al. 1996; Bennet et al. 1997). This phenomenon, dubbed

‘wooden chest syndrome,’ further exacerbates fentanyl-induced respiratory depression (Kelly et al. 2021).

1.4. Whole-Body Plethysmography: An Assay of Respiratory Depression

The pilot experiments that informed choice of fentanyl and morphine doses for biodistribution studies were run using a technique known as whole-body plethysmography. In brief, whole-body plethysmography is a non-invasive method for recording respiration in small animal subjects like mice (Prada-Dacasa et al. 2020). Specifically, as air enters and leaves the mouse’s lungs during inspiration and expiration, concomitant changes in air humidity, temperature, and pressure occur within the recording chamber, enabling measurement of tidal volume, respiratory rate, etc. (Lim et al. 2014). Because mice are conscious during experimental sessions and can move freely within the confines of the chamber, whole-body plethysmography is unencumbered by the confounds associated with other methodologies for measuring murine respiration (Prada-Dacasa et al. 2020). Forced oscillation technique requires anesthetizing and performing tracheotomies on subjects to provide mechanical ventilation for assessing lung function (McGovern et al., 2013), which automatically introduces artificial constructs that are not representative of the mouse’s natural baseline state (Prada-Dacasa et al. 2020). Although double-chamber plethysmography does not involve anesthesia, it entails immobilizing the mouse by securing its head and thorax in two different chambers (Mailhot-Larouche et al. 2018), thus causing restraint stress.

Besides avoiding these pitfalls, body plethysmography also possesses a certain level of translatability due to its proven use for measuring respiration in humans (Criée et al. 2011). The effectiveness of whole-body plethysmography for assessing respiration in mice has been demonstrated across several contexts, from the influence of inflammatory signaling

(Giannakopoulou et al. 2019) to the role of central pattern generators on respiratory cycles (Crone et al. 2012). Most relevant to the current research, however, is the established use of whole-body plethysmography by other laboratories to examine the effects of drugs, including opioids, on respiration in mouse models (Baird et al. 2022; Elder et al. 2023; Hill et al. 2016; Glovak et al. 2022; Hill et al. 2020; Hill et al. 2023; Newman et al. 2024; Varshneya et al. 2022; Wiese et al. 2021; Zavala et al. 2021). Thus, there is appreciable support in the literature for measuring opioid-induced respiratory depression with the whole-body plethysmography assay.

1.5: Opioid Analytical Methods

As summarized in **Table 1.2**, various analytical methods have been developed to measure concentrations of fentanyl and morphine in mouse blood and tissue samples. Notably, however, these protocols are often intended to measure either fentanyl *or* morphine rather than both opioids simultaneously and may not include their metabolites. Also, barring a few exceptions (Heydari et al. 2021; Schinkel et al. 1995; Zelcer 2005) analytical methods such as the ones listed below only quantify fentanyl and/or morphine in a limited number of murine matrices, such as blood and brain. Thus, development of a bioanalytical method capable of quantifying both fentanyl and morphine in multiple murine tissues would represent a useful contribution to the literature.

Table 1.2: Analytical Methods for Quantifying Fentanyl and Morphine in Mice.

Author, Year	Mouse Strain/Sex	Matrices	Analytes Measured	Method Type	LOQ/LOD
Appelgren et al. 1973	Both sexes (strain not stated)	Brain, gall bladder, intestine, placental barrier, urine	^{3}H-labelled fentanyl, dihydromorphine	Whole-body autoradiography	N/A
Ishikawa et al. 1983	Male ICR	Brain	Morphine	HPLC-ECD	Not stated
Jin et al. 1986	Not specified	Blood, lung, heart, kidney, brain, liver, fat	3-methyl[carbonyl-14C]fentanyl	Radioimmunoassay	N/A
Schinkel et al. 1995	*mdr1a*(+/+) & (-/-)	Plasma, brain, muscle, heart, kidney, liver, gall bladder, lung, stomach, small intestine, colon, testis, spleen, thymus	[^{3}H]Morphine	Liquid scintillation counting	N/A
Bian and Bhargava 1998	Male Swiss Webster	Lung, liver, kidney, spleen, urine	Morphine	Radioimmunoassay	LOD: 0.8 ng/mL
Bhargava and Bian 1998	Male Swiss Webster	Serum, brain, spinal cord, lung, liver, kidneys, spleen, urine	Morphine	Radioimmunoassay	LOD: 0.8 ng/mL
Stout et al. 1998	Male BALB/c	Hair	Fentanyl	GC/MS	LOQ: 0.2 ng/mL
Zelcer et al. 2005	*Mrp3*(+/+) and (-/-)	Plasma, lung, brain, liver, gall bladder, kidney, urine bladder, stomach, stomach contents, small intestine, colon + cecum, intestinal contents	[^{3}H]Morphine	Liquid scintillation counting	N/A
Leal et al. 2006	C57 (both sexes)	Serum	Fentanyl	LC-MS/MS	LOQ: 2.0 ng/mL
Kalvass et al. 2007	Male CF-1 *mdr1a*(+/+)	Serum, brain	Fentanyl, Morphine	HPLC-MS/MS	Not stated
Karinen et al. 2009	C59BL/6J-Bom	Blood, brain	Morphine, M3G, M6G	Reversed-phased LC-MS/MS	Blood LOQ: 0.0012 (morphine) mg/L, 0.019 (M3G) mg/L, 0.0014 mg/L (M6G); Brain LOQ: 0.0036 μg/g (morphine),

Yang et al. 2016	Male ICR	Brain	Morphine, M3G, M6G	UHPLC-MS/MS	0.059 μg/g (M3G), 0.004 μg/g (M6G) LLOQ: 0.05 ng/mL (all analytes)
Bremer et al. 2016	Male Swiss Webster	Serum, brain	Fentanyl	LC-MS	Not stated
Weinsanto et al. 2018	Male C57BL/6 mice	Plasma, brain, urine, liver	Morphine, M3G	LC-MS/MS	Plasma LOQ: 130.13 ± 39.93 fmol (morphine), 7.12 ± 0.98 (M3G) Brain LOQ: 10.02 ± 3.45 fmol (morphine), 8.32 ± 0.44 fmol (M3G) Liver LOQ: 92.13 ± 4.12 fmol (morphine), 6.19 ± 0.01 fmol (M3G) Urine LOQ: 2.02 ± 0.29 fmol (morphine), 5.44 ± 0.36 fmol (M3G)
Zhu et al. 2018	C57BL/6J	Plasma, liver, kidney	Morphine	[^{3}H]Morphine	N/A
Chen et al. 2019	Male C57BL/6	Plasma, liver	Morphine, M3G	UPLC-QTOF/MS	Not stated
Raleigh et al. 2019	Male BALB/c	Serum, brain	Fentanyl	GC-MS	Not stated
Smith et al. 2019	Male Swiss Webster	Plasma	Fentanyl	LC-MS/MS	LOD: 1.6 ng/mL
Ban et al. 2021	Female BALB/c	Blood, brain	Fentanyl	LC-MS/MS	LOQ: 0.25 ng/mL
Heydari et al. 2021	Wild-type FVB/NRj mice	Plasma, brain, spleen, kidney, small intestine, liver	Morphine, M3G, M6G	UPLC-MS/MS	LLOQ: 1 ng/mL (morphine), 10 ng/mL (M3G), 0.5 ng/mL (M6G)(human plasma)
Powers et al. 2023	Female BALB/c	Serum, brain	Fentanyl	LC-MS/MS	Not stated

Abbreviations
LOQ: limit of quantification
LLOQ: lower limit of quantification
LOD: limit of detection
M3G: morphine-3-β-D-glucuronide
M6G: morphine-6-β-D-glucuronide

CHAPTER 2: SPECIFIC AIMS

Despite the common use of mice as a model for studying fentanyl-induced respiratory depression (Elder et al. 2023; Hill et al. 2020; Varshneya et al. 2022), little extensive research has been done into widespread distribution of fentanyl in murine tissue or comparing said distribution with that of traditional opiates like morphine. Although one whole-body radiography study reported greater fentanyl distribution in the central nervous system, gallbladder, and intestines relative to dihydromorphine in mice (Appelgren et al. 1973), mouse research comparing equipotent doses of fentanyl and morphine typically limits sample collection to blood and brain (Kalvass et al. 2007).

However, in male Charles River F344 rats infused for 6 hr with 0.15-0.30 μg/min·kg fentanyl, higher concentrations of fentanyl were observed in fat compared to kidney, liver, and muscle (Björkman and Stanski 1988). Moreover, male F1 hybrid rats given 6 hr infusion of 13 μg/kg/hr infusions of fentanyl demonstrated noticeably higher steady-state tissue-blood partition coefficients in fat compared to vessel-rich tissues like brain, heart, and lungs (Björkman et al. 1990). In Sprague-Dawley rats given 50 μg/kg tritium-labelled fentanyl intravenously (iv) and sacrificed at several time points from 1.5-240 min after injection, well-perfused tissues such as brain, lung, and heart displayed parallel changes in concentration over time with plasma, suggesting these tissues could be grouped into the central compartment of a pharmacokinetic model for fentanyl, while fentanyl uptake and elimination were delayed in muscle and fat, implying they belonged in a peripheral pharmacokinetic compartment (Hug and Murphy 1981).

Meanwhile, in time-course autoradiography (Schneider and Brune 1985) and high performance thin-layer chromatography studies (Schneider and Brune 1986) on biodistribution of iv fentanyl infusions in female Wistar rats, fentanyl concentration was highest in brain, heart,

and lungs shortly after administration, while redistribution of fentanyl into stomach, intestines (Schneider and Brune 1985, 1986), and/or fat (Schneider and Brune 1986) occurred at later time points. That being said, these studies did not compare fentanyl biodistribution with biodistribution of equivalent doses of traditional opioids such as morphine. Some of these rat experiments also used routes of drug administration, i.e. continuous infusion (Björkman and Stanski 1988; Björkman et al. 1990) more in line with fentanyl's clinical use as an anesthetic than its abuse within the context of recreational drug seeking (Abdulrahim et al. 2018).

Thus, there is a need for a more comprehensive examination of fentanyl and morphine biodistribution in multiple tissues within a preclinical mouse model at doses that induce respiratory depression. The experiments described below seek to address this gap in the literature. It was hypothesized that fentanyl would undergo more rapid distribution than morphine, with greater accumulation in fat and similar tissues due to its greater lipophilicity. It was also hypothesized that, following repeated administration, fentanyl accumulation in fat in opioid-experienced mice would be greater than in opioid-naïve mice, while observed differences in morphine accumulation in fat between repeatedly-treated and acutely-treated mice would not be as prominent since morphine is less lipophilic. Specific aims were as follows:

Aim 1: Validate a bioanalytical method for measuring concentrations of fentanyl, morphine, and select metabolites in a comprehensive, diverse array of murine tissues, including blood, brain, liver, lung, heart, kidney, spleen, small and large intestine, stomach, muscle, fat, and skin. This will permit simultaneous assessment of fentanyl and morphine concentrations in a mouse model to a more thorough extent than much of the prior literature.

Aim 2: Compare the biodistribution of fentanyl and morphine in opioid-naïve mice at multiple time points after acute treatment with doses demonstrated to induce similar levels of respiratory

depression. Based on previous literature, it is hypothesized that more rapid uptake of fentanyl into central compartments and greater storage in adipose tissue will be observed.

a) Use whole-body plethysmography, a well-established assay for evaluating respiratory depression in mice, to run pilot studies assessing dose-response of fentanyl- and morphine-induced respiratory depression in opioid-naïve mice. These data will assist in identifying doses of fentanyl and morphine that produce comparable respiratory depressant effects, thus informing our choice of doses for subsequent biodistribution studies.
b) Harvest and analyze blood and tissue samples collected at 4 different time points (5, 15, 60, and 240 min) after acute fentanyl or morphine injection for the purpose of determining peak concentrations of fentanyl, morphine, and their metabolites in various murine tissues. This will generate a comprehensive profile for acute biodistribution of fentanyl and morphine across numerous mouse tissues while also tracking the acute time course of this tissue distribution.

Aim 3: Compare biodistribution of fentanyl and morphine in opioid-experienced mice to evaluate whether and to what extent tissue distribution of these opioids is impacted by repeated exposure. Based on alterations in fentanyl or morphine effects on respiratory depression (Hill et al. 2019; Laferrière et al. 2005) and antinociception (Bilsky et al. 1996; Marcus et al. 2015) observed by other laboratories following repeated treatment regimens, it is hypothesized that repeated opioid exposure will alter physiological parameters like biodistribution, as well. It is also hypothesized that fentanyl will accumulate in fat following repeated administration to a greater extent than in mice repeatedly treated with morphine or in opioid-naïve mice given acute fentanyl.

a) Administer repeated daily injections (once every 24 hr) to mice and harvest and analyze blood and tissue samples collected at a specific time point after the final injection, determined based on Aim 2 results, during which appreciable quantities of target opioids can be observed in several tissues. The resulting data will enable biodistribution comparisons of fentanyl and morphine in drug-naïve (Aim 2) and drug-experienced (Aim 3) mice to evaluate potential changes in tissue accumulation caused by this repeated injection schedule.

b) Evaluate the above repeated fentanyl and morphine injection schedule in a model of thermal nociception, specifically, warm-water tail withdrawal, to determine whether this treatment regimen induces opioid tolerance. Since the intent of Aim 3 is to investigate the effects of repeated opioid exposure on biodistribution, not to model chronic opioid use, it is predicted that mice placed on this injection schedule will not exhibit tolerance to fentanyl or morphine.

CHAPTER 3: OPIOID ANALYTICAL METHOD VALIDATION FOR FENTANYL, MORPHINE, AND SELECT METABOLITES

3.1. Objective.

The aim of the experiments outlined below was to validate a bioanalytical method for the purpose of simultaneously measuring fentanyl, norfentanyl, 4-ANPP, morphine, and morphine-3-β-D-glucuronide in murine tissue. As stated above, morphine-6-β-D glucuronide is not typically measured in mice treated with morphine (Grung et al. 1998; Handal et al. 2002; Lawrence et al. 1992). However, it was included in the method to serve as a negative control in bioanalytical studies, i.e. if tissue samples from opioid distribution experiments had returned sizable readings for morphine-6-β-D glucuronide, this would be indicative of potential technical errors that might otherwise confound the results.

3.2. Materials and Methods.

3.2.1. Standards and Reagents

Certified reference materials and internal standards for mass spectroscopy studies, including 100 µg/mL fentanyl (N-Phenyl-N-[1-(2-phenylethyl)-4-piperidinyl]propanamide; Lot No. FE03012201; CAS No. 437-38-7) in methanol, 100 µg/mL fentanyl-d5 (N-(Pentadeuterophenyl)-N-[1-(2-phenylethyl)-4-piperidinyl]propanamide; Lot No. FE08312117; CAS No. 118357-29-2) in methanol, 1 mg/mL norfentanyl oxalate (N-Phenyl-N-(4-piperidinyl)propanamide oxalate; Lot No. FE02172249; CAS No. 1211527-24-0) in methanol, 1 mg/mL norfentanyl-d5 oxalate (N-(4-Piperidinyl)-N-pentadeuterophenylpropionamide oxalate; Lot No. FE10092001; CAS No. 1435933-84-8) in methanol, 100 µg/mL 4-ANPP (N-Phenyl-1-(2-phenethyl)-4-piperidinamine; Lot No. FE07272146; CAS No. 21409-26-7) in methanol, 100 µg/mL 4-ANPP-d5 (N-phenyl-D5-1-(2-phenethyl)-4-piperidinamine; Lot No. FE12172036; CAS

No. 1189466-15-6) in methanol, 1 mg/mL morphine ((5α, 6α)-7,8-Didehydro-4,5-epoxy-17-methylmorphinan-3,6-diol; Lot No. FE03252112; CAS No.57-27-2) in methanol, 100 µg/mL morphine-d3 (7,8-Didehydro-4,5-epoxy-17-trideuteromethylmorphinan-3,6-diol; Lot No. FE08312130; CAS No. 67293-88-3) in methanol, 1 mg/mL morphine-3-β-d-glucuronide ((5α, 6α)-7,8-didehydro-4,5-epoxy-6-hydroxy-17-methylmorphinan-3-yl-β-D-glucopyranosiduronic acid; Lot No. FE01142007, CAS No. 20290-09-9) in methanol with 0.05% NaOH, 100 µg/mL morphine-3-β-d-glucuronide-d3 (7,8-Didehydro-4,5-epoxy-17-trideuteromethylmorphinan-6-ol-3beta-glucuronic acid; Lot No. FE07162006; CAS No. 136765-44-1) in methanol with 0.05% NaOH, 1 mg/mL morphine-6-β-d-glucuronide ((5α, 6α)-7,8-didehydro-4,5-epoxy-3-hydroxy-17-methylmorphinan-6-yl-β-D-glucopyranosiduronic acid; Lot No. FE11172134; CAS No. 20290-10-2) in water:methanol (80:20), and 100 µg/mL morphine-6-β-d-glucuronide-d3 ((5α, 6α)-7,8-didehydro-4,5-epoxy-3-hydroxy-17(methyl-D3)morphinan-6-yl-β-D-glucopyranosiduronic acid; Lot No. FE03012203; CAS No. 219533-69-4) in water:methanol (50:50) were purchased from the Cerilliant Corporation (Round Rock, TX, USA).

HPLC-grade water, HPLC-methanol, and formic acid were purchased from Fisher Chemical.

3.2.2. Samples

Samples for most method validation procedures were obtained from sterile-filtered, heat-inactivated mouse serum stock (SKU: 30611146-3; Lot No. V20082500) purchased from bioWORLD (Dublin, OH, USA). Samples for quality controls (brain, lung, etc.) were harvested from drug-naïve male Swiss Webster mice that could be used as sources of blank tissue. Mice were decapitated by guillotine, and trunk blood and tissue samples (brain, liver, lung, heart, kidney, spleen, small intestine, large intestine, stomach, muscle, fat, and skin) were immediately harvested on ice. After collection, samples were stored at –80˚C.

3.2.3. Solid-Phase Extraction

Tissue samples were homogenized in a 1:4 dilution in water (except for muscle and skin, which were diluted 1:8). 100 µL aliquots of homogenate were placed in a glass culture tube along with 50 µL of internal standard solution (0.2 µg/mL morphine-d3, 1 µg/mL morphine-3-β-D-glucuronide-d3 & morphine-6-β-D-glucuronide-d3, 0.02 µg/mL fentanyl-d5, 0.1 µg/mL norfentanyl-d5 & 4-ANPP-d5) and 300 µL HPLC water. Samples were then centrifuged (Allegra X-15R centrifuge, Beckman Coulter, Inc., Indianapolis, IN, USA) at 3,000 RPM for 10 minutes.

Extraction was performed with a 48-position positive pressure manifold (United Chemical Technologies, Inc., Bristol, PA, USA) connected to a N2 gas tank. SPE-Phenomenex Strata-x 33 µ Polymeric Reversed Phase columns (Phenomenex Inc.) were conditioned with 1 mL of methanol followed by 1 mL of water, and samples subsequently loaded. This was followed by a 5% methanol wash (1 mL). Samples were then eluted with 0.400 mL (2X) of 95% methanol.

Eluted samples were transferred to a 96 deep-well plate, evaporated under nitrogen (25 psi) 30-45 min at 55˚C on an SPE Dry 96 (Biotage) and reconstituted with 65 µL methanol. In addition to method validation samples, each run also included a calibration curve (in mouse serum), blanks, and quality controls (see **Appendix** for specific concentrations). Calibrators were prepared at 1, 2, 5, 10, 20, 50, and 100 ng/mL (fentanyl and 4-ANPP), 5, 10, 20, 50, 100, 200, and 500 ng/mL (norfentanyl), 10, 20, 50, 100, 200, 500, and 1000 ng/mL (morphine), and 50, 100, 200, 500, 1000, 2000, and 5000 ng/mL (morphine-3 and morphine-6-β-D-glucuronide).

3.2.4. Quantitation of Fentanyl, Morphine, and Their Metabolites

Chromatographic separation was performed with a SCIEX ExionLC 2.0 liquid chromatograph using an Agilent Polaris SI-A column (180 Å, 5 µm, 50 x 3.0 mm). Autosampler

injection volume was 5 µL with a duration of 5.50 minutes. Mobile phases were kept on an isocratic gradient (90 % Mobile Phase A, 10% Mobile Phase B), where Phases A and B consisted of 1% formic acid in water and 1% formic acid in acetonitrile, respectively. Column oven temperature was maintained at 40˚C.

Mass spectrometry was performed by a SCIEX QTRAP 6500+ high-throughput mass spectrometer run on Analyst 1.7.2 analytical software. Source temperature was set to 600˚C, while curtain gas and Gases 1 and 2 flow rates were set to 40 mL/min. Electrospray voltage was 5500 eV, and dwell time was 100 msec.

Ion mass/charge ratios (*m/z*) for Q1 and Q3, as well as collision energy and declustering potential, are listed in **Table 3.1**.

Table 3.1: Parent Ion (Q1) and Product Ion (Q3) Mass-to-Charge Ratios, MRM Transitions, Collision Energy (CE) and Declustering Potential (DP) for Spectrometric Analysis.

Compound	Q1 (*m/z*)	Q3 (*m/z*)	CE (eV)	DP (V)
Fentanyl (Quant.)	337	188	30	62
Fentanyl (Qual.)	337	105	42	62
Fentanyl-d5 (Quant).	342	188	30	62
Fentanyl-d5 (Qual.)	342	105	42	62
Norfentanyl (Quant.)	233	84	22	67
Norfentanyl (Qual.)	233	150	24	67
Norfentanyl-d5 (Quant.)	238	84	22	67
Norfentanyl-d5 (Qual.)	238	155	24	67
4-ANPP (Quant.)	281	188	22	63
4-ANPP (Qual.)	281	105	38	63
4-ANPP-d5 (Quant.)	286	188	22	63
4-ANPP-d5 (Qual.)	286	105	38	63
Morphine (Quant.)	286	185	41	127
Morphine (Qual.)	286	157	54	127
Morphine-d3 (Quant.)	289	185	45	127
Morphine-d3 (Qual.)	289	157	54	127
Morphine-3β-d-glucuronide (Quant.)	462	286	40	30
Morphine-3β-d-glucuronide (Qual)	462	201	56	30
Morphine-3β-d-glucuronide	462	165	71	30
Morphine-3β-d-glucuronide-d3 (Quant.)	465	289	40	30
Morphine-3β-d-glucuronide-d3 (Qual.)	465	204	56	30
Morphine-3β-d-glucuronide-d3	465	165	71	30

Quant.: Quantifying MRM transitions (Q1→Q3)

Qual.: Qualifying MRM transitions (Q1→Q3)

CE: Collision Energy; rate of acceleration at which ions collide with inert gas in Quadrupole 2

DP: Declustering Potential; applied voltage that prevents ion clustering

Summary tables of method validation criteria for each analyte are listed below. Further detail on absolute between- and within-run accuracy and precision, recovery of analytes and internal standards, matrix effects, analyte stability over time and under different storage conditions, and

quality controls for each analyte in different matrices can be found in the **Appendix**. Method validation procedures were informed by Version M10 of the Bioanalytical Method Validation and Study Sample Analysis guidelines from the International Council for Harmonisation of Technical Requirements for Pharmaceuticals for Human Use.

Table 3.2: Validation Summary Table for Fentanyl

Method Description	
Short description of method	Solid-phase extraction with reverse-phase HPLC with MS/MS detection
Matrix	Mouse serum
Analyte	Fentanyl
Internal standard (IS)	Fentanyl-d5 (deuterated Fentanyl)
Calibration concentrations	1 ng/mL to 100 ng/mL
QC concentrations	1 ng/mL (LLOQ), 3 ng/mL (Low QC), 7.5 ng/mL (Med QC), and 75 ng/mL (High QC)
Selectivity	No peaks
Lower limit of quantification	1 ng/mL Between-run absolute bias (accuracy): 11% Between-run precision: 15% Within-run absolute bias (accuracy): 2-16% Within-run precision: 4-22%
Between-run absolute bias (accuracy)*	4%-11%
Between-run precision	7%-16%
Within-run absolute bias (accuracy)*	Run 1: 3-14% Run 2: 8-15% Run 3: 2-11%
Within-run precision	Run 1: 4-16% Run 2: 3-22% Run 3: 4-14%
Matrix effect	Low QC: 45% (18 %CV) High QC: 15% (7 %CV)
Recovery of analyte	66% -93%
Recovery of IS	93%
Auto-sampler storage stability	Confirmed for up to 72 hr at 40˚C nominal 24 hr: Bias (accuracy) 8% for LLOQ, 4% for Low QC, 7% for Med QC, and 8% for High QC 48 hr: Bias (accuracy) 7% for LLOQ, 7% for Low QC, 5% for Med QC, and 10% for High QC 72 hr: Bias (accuracy) 1% for LLOQ, 3% for Low QC, 10% for Med QC, and 2% for High QC
Freeze-thaw stability	Confirmed up to 3 cycles Bias (accuracy) 5% for Low QC and 12% for High QC
Bench top stability	Confirmed up to 24 hours at room temperature Bias (accuracy) 4% for Low QC and 9% for High QC
Injector Carryover	No carryover was observed
Long Term Storage Stability	Confirmed up to 138 days Bias (accuracy) 13% for Low QC, 0.1% for Med QC, and 18% for High QC

* Low bias = high accuracy

Table 3.3: Validation Summary Table for Norfentanyl

Method Description	
Short description of method	Solid-phase extraction with reverse-phase HPLC with MS/MS detection
Matrix	Mouse serum
Analyte	Norfentanyl
Internal standard (IS)	Norfentanyl-d5 (deuterated Norfentanyl)
Calibration concentrations	5 ng/mL to 500 ng/mL
QC concentrations	5 ng/mL (LLOQ), 15 ng/mL (Low QC), 40 ng/mL (Med QC), and 400 ng/mL (High QC)
Selectivity	No peaks
Lower limit of quantification	5 ng/mL Between-run absolute bias (accuracy): 4% Between-run precision: 11% Within-run absolute bias (accuracy): 3-16% Within-run precision: 2-7%
Between-run absolute bias (accuracy):	0.5%-4%
Between-run precision	9-15%
Within-run absolute bias (accuracy):	Run 1: 4-16% Run 2: 3-13% Run 3: 3-9%
Within-run precision	Run 1: 6-18% Run 2: 5-7% Run 3: 3-7%
Matrix effect	Low QC: 15% (13 %CV) High QC: 6% (14 %CV)
Recovery of analyte	101-139%
Recovery of IS	118%
Auto-sampler storage stability	Confirmed for up to 72 hr at 40˚C nominal 24 hr: Bias (accuracy) 11% for LLOQ, 6% for Low QC, 2% for Med QC, and 9% for High QC 48 hr: Bias (accuracy) 7% for LLOQ, 6% for Low QC, 3% for Med QC, and 8% for High QC 72 hr: Bias (accuracy) 6% for LLOQ, 15% for Low QC, 5% for Med QC, and 5% for High QC
Freeze-thaw stability	Confirmed up to 3 cycles Bias (accuracy) 10% for Low QC and 5% for High QC
Bench top stability	Confirmed up to 24 hours at room temperature Bias (accuracy) 19% for Low QC and 0% for High QC
Injector Carryover	No carryover was observed
Long Term Storage Stability	Confirmed up to 138 days Bias (accuracy) 15% at Low QC, 2% at Med QC, and 13% at High QC

* Low bias = high accuracy

Table 3.4: Validation Summary Table for 4-ANPP

Method Description	
Short description of method	Solid-phase extraction with reverse-phase HPLC with MS/MS detection
Matrix	Mouse serum
Analyte	N-Phenyl-1-(2-phenethyl)-4-piperidinamine
Internal standard (IS)	4-ANPP-d5 (deuterated 4-ANPP)
Calibration concentrations	1 ng/mL to 100 ng/mL
QC concentrations	1 ng/mL (LLOQ), 3 ng/mL (Low QC), 7.5 ng/mL (Med QC), and 75 ng/mL (High QC)
Selectivity	No peaks
Lower limit of quantification	1 ng/mL Between-run absolute bias (accuracy): 8% Between-run precision: 10% Within-run absolute bias (accuracy): 1-16% Within-run precision: 6-9%
Between-run absolute bias (accuracy)*	6-14%
Between-run precision	6-13%
Within-run absolute bias (accuracy)*	Run 1: 3-8% Run 2: 15-20% Run 3: 1-18%
Within-run precision	Run 1: 4-14% Run 2: 1-7% Run 3: 6-9%
Matrix effect	Low QC: 90% (9 %CV) High QC: 14% (5 %CV)
Recovery of analyte	69% -88%
Recovery of IS	85%
Auto-sampler storage stability	Confirmed for up to 72 hr at 40˚C nominal 24 hr: Bias (accuracy) 1% for LLOQ, 4% for Low QC, 7% for Med QC, and 11% for High QC 48 hr: Bias (accuracy) 10% for LLOQ, 5% for Low QC, 5% for Med QC, and 19% for High QC 72 hr: Bias (accuracy) 4% for LLOQ, 8% for Low QC, 18% for Med QC, and 13% for High QC
Freeze-thaw stability	Confirmed up to 3 cycles Bias (accuracy) 3% for Low QC and 8% for High QC
Bench top stability	Confirmed up to 24 hours at room temperature Bias (accuracy) 8% for Low QC and 12% for High QC
Injector Carryover	No carryover was observed**
Long Term Storage Stability	Confirmed up to 138 days Bias (accuracy) 18% for Low QC, 0.3% for Mid QC, and 19% for High QC

* Low bias = high accuracy

** Single exception: 50 ng/mL measured in double blank during Run 1

Table 3.5: Validation Summary Table for Morphine

Method Description	
Short description of method	Solid-phase extraction with reverse-phase HPLC with MS/MS detection
Matrix	Mouse serum
Analyte	Morphine
Internal standard (IS)	Morphine-d3 (deuterated Morphine)
Calibration concentrations	10 ng/mL to 1000 ng/mL
QC concentrations	10 ng/mL (LLOQ), 30 ng/mL (Low QC), 75 ng/mL (Med QC), and 750 ng/mL (High QC)
Selectivity	No peaks
Lower limit of quantification	10 ng/mL Between-run absolute bias (accuracy): 4% Between-run precision: 13% Within-run absolute bias (accuracy): 3-10% Within-run precision: 5-19%
Between-run absolute bias (accuracy)*	1-10%
Between-run precision	5-13%
Within-run absolute bias (accuracy)*	Run 1: 1-11% Run 2: 10-15% Run 3: 5-10%
Within-run precision	Run 1: 5-18% Run 2: 2-8% Run 3: 5-7%
Matrix effect	Low QC: 19% (13% CV) High QC: 11% (1% CV)
Recovery of analyte	77-90%
Recovery of IS	93%
Auto-sampler storage stability	Confirmed for up to 72 hr at 40˚C nominal 24 hr: Bias (accuracy) 1% for LLOQ, 7% for Low QC, 14% for Med QC, and 12% for High QC 48 hr: Bias (accuracy) 8% for LLOQ, 8% for Low QC, 12% for Med QC, and 8% for High QC 72 hr: Bias (accuracy) 1% for LLOQ, 10% for Low QC, 12% for Med QC, and 10% for High QC
Freeze-thaw stability	Confirmed up to 3 cycles Bias (accuracy) 12% for Low QC and 11% for High QC
Bench top stability	Confirmed up to 24 hours at room temperature Bias (accuracy) 9% for Low QC and 11% for High QC
Injector Carryover	No carryover was observed
Long Term Storage Stability	Confirmed up to 138 days Bias (accuracy) 9% for Low QC, 16% for Mid QC, and 15% for High QC

* Low bias = high accuracy

Table 3.6: Validation Summary Table for Morphine-3-β-D-glucuronide

Method Description	
Short description of method	Solid-phase extraction with reverse-phase HPLC with MS/MS detection
Matrix	Mouse serum
Analyte	Morphine-3-β-D-glucuronide
Internal standard (IS)	Morphine-3-β-D-glucuronide -d3 (deuterated Morphine-3-β-D-glucuronide)
Calibration concentrations	50 ng/mL to 5000 ng/mL
QC concentrations	50 ng/mL (LLOQ), 150 ng/mL (Low QC), 400 ng/mL (Med QC), and 4,000 ng/mL (High QC)
Selectivity	No peaks
Lower limit of quantification	50 ng/mL Between-run absolute bias (accuracy): 12% Between-run precision: 15% Within-run absolute bias (accuracy): 5-30% Within-run precision: 5-8%
Between-run absolute bias (accuracy)*	4-12%
Between-run precision	7-15%
Within-run absolute bias (accuracy)*	Run 1: 2-9% Run 2: 9-19% Run 3: 0.1-6%
Within-run precision	Run 1: 4-10% Run 2: 1-8% Run 3: 5-12%
Matrix effect	Low QC: 26% (16 %CV) High QC: 12% (3% CV)
Recovery of analyte	66-81%
Recovery of IS	84%
Auto-sampler storage stability	Confirmed for up to 72 hr at 40˚C nominal 24 hr: Bias (accuracy) 4% at LLOQ, 0.3% at Low QC, 3% at Med QC, and 3% at High QC 48 hr: Bias (accuracy) 1% at LLOQ, 6% at Low QC, 9% at Med QC, and 1% at High QC 72 hr: Bias (accuracy) 10% at LLOQ, 18% at Low QC, 12% at Med QC, and 7% at High QC
Freeze-thaw stability	Confirmed up to 3 cycles Bias (accuracy) 16% for Low QC and 17% for High QC
Bench top stability	Confirmed up to 24 hours at room temperature Bias (accuracy) 6% for Low QC and 16% for High QC
Injector Carryover	No carryover was observed
Long Term Storage Stability	Confirmed up to 138 days Bias (accuracy) 3% for Low QC, 2% for Med QC, and 8% for High QC

* Low bias = high accuracy

Table 3.7: Validation Summary Table for Morphine-6-β-D-glucuronide

Method Description	
Short description of method	Solid-phase extraction with reverse-phase HPLC with MS/MS detection
Matrix	Mouse serum
Analyte	Morphine-6-β-D-glucuronide
Internal standard (IS)	Morphine-6-β-D-glucuronide-d3 (deuterated Morphine-6-β-D-glucuronide)
Calibration concentrations	50 ng/mL to 5000 ng/mL
QC concentrations	50 ng/mL (LLOQ), 150 ng/mL (Low QC), 400 ng/mL (Med QC), and 4,000 ng/mL (High QC)
Selectivity	No peaks
Lower limit of quantification	50 ng/mL Between-run absolute bias (accuracy): 10% Between-run precision: 8% Within-run absolute bias (accuracy): 8-13% Within-run precision: 3-11%
Between-run absolute bias (accuracy)*	1-10%
Between-run precision	8-14%
Within-run absolute bias (accuracy)*	Run 1: 4-11% Run 2: 8-14% Run 3: 1-9%
Within-run precision	Run 1: 4-11% Run 2: 5-6% Run 3: 6-11%
Matrix effect	Low QC: 26% (16 %CV) High QC: 15% (3% CV)
Recovery of analyte	52-62%
Recovery of IS	59%
Auto-sampler storage stability	Confirmed for up to 72 hr at 40˚C nominal 24 hr: Bias (accuracy) 8% at LLOQ, 1% at Low QC, 2% at Med QC, and 5% at High QC 48 hr: Bias (accuracy) 11% at LLOQ, 2% at Low QC, 10% at Med QC, and 1% at High QC 72 hr: Bias (accuracy) 11% at LLOQ, 21% at Low QC, 10% at Med QC, and 8% at High QC
Freeze-thaw stability	Confirmed up to 3 cycles Bias (accuracy) 2% for Low QC and 2% for High QC
Bench top stability	Confirmed up to 24 hours at room temperature Bias (accuracy) 8% for Low QC and 2% for High QC
Injector Carryover	No carryover was observed**
Long Term Storage Stability	Confirmed up to 138 days Bias (accuracy) 8% for Low QC, 11% for Med QC, and 13% for High QC

* Low bias = high accuracy

**Two exceptions: 3660 ng/mL measured in double blank during Run 1; 25.1 ng/mL carryover between Calibrator 7 and blank in 10/19/23 run (spleen/small int./large int.)

CHAPTER 4: DOSE RESPONSE OF FENTANYL- AND MORPHINE-INDUCED RESPIRATORY DEPRESSION

4.1. Objective

The aim of these pilot studies was to evaluate dose response of fentanyl-and morphine-induced respiratory depression in a mouse model in order to identify doses of fentanyl and morphine that produced comparable respiratory depressant effects. These equipotent doses were subsequently used in the biodistribution studies described in Chapter 5.

4.2. Materials and Methods

4.2.1. Drugs

Fentanyl hydrochloride and morphine sulfate pentahydrate were provided by the National Institute on Drug Abuse (Bethesda, MD, USA) Drug Supply Program. Drugs were dissolved in sterile saline and administered sc at a volume of 10 mL/kg body weight.

4.2.2. Subjects

Adult male Swiss Webster mice (Envigo; 80 total) weighing between 27-44 g (mean ± standard deviation = 33.1 ± 3.72 g) were group housed (4-5/cage) in Association for Assessment and Accreditation of Laboratory Animal Care-accredited facilities at Virginia Commonwealth University. Animals were kept on a 12-hr reverse light/dark cycle and allowed at least one week to acclimate to vivarium conditions prior to experiments. Mice had access to food (Teklad 7012 Rodent Diet; Envigo, Madison, WI, USA) and tap water *ad libitum* in the home cage. Assays were run during the dark period, when mice were more likely to be active. To avoid confounding effects of previous drug history, all mice remained drug-naïve until the day of testing, and each mouse was only used once for a single study.

All experiments were performed in accordance with the National Research Council's Guide for Care and Use of Laboratory Animals (2011), and associated protocols were approved by Virginia Commonwealth University's Institutional Animal Care and Use Committee.

4.2.3. Apparatus

Lighting for laboratory space was provided by custom 660 nM-emitting T8-style ceiling-mounted light tubes, each with 96 0.2-watt Epistar 2835 SMD LEDs (Shenzhen Benwei Electronics Co., Ltd., Longhua District, Shenzhen, China). Since mice demonstrate reduced sensitivity to this wavelength compared to humans (Peirson et al. 2018), these lights ensured minimal disruption of the dark cycle while providing visibility for research personnel. An example image of these experimental conditions is provided in **Figure 4.1**.

Figure 4.1: Whole-Body Plethysmography Chambers under 660 nM Lighting Conditions. One mouse run in each chamber. Chambers connected to gas source (5 % CO_2, 21 % O_2, and balance N_2).

Mice were placed in individual whole-body plethysmograph chambers (FinePointe WBP Chamber with Halcyon Technology, Data Sciences International, St. Paul, MN, USA) with a volume of 0.5 L (adjustable 0.5 L/min room air bias flow) that allowed unrestrained movement. To enhance the assay's ability to measure drug-induced respiratory effects and reduce variation caused by ambient air conditions, a standardized gas mixture comprised of 5 % CO_2, 21 % O_2, and balance N_2 was continuously delivered into the chambers (Elder et al. 2023; Varshneya et al. 2022).

4.2.4. Whole-Body Plethysmography Protocol

Animals were run on a 3-phase protocol, lasting a total of 90 min, modified from Elder et al. 2023. During the Baseline Phase (20 min), animals were placed in the plethysmography chambers to acclimate to the novel environment, and baseline respiration (in the absence of drug treatment) was monitored. At the conclusion of the Baseline Phase, mice were removed from the chamber, given a subcutaneous (sc) injection of either saline, fentanyl (0.03-1 mg/kg), or morphine (1-30 mg/kg), and immediately returned to the chamber to record respiration during the second phase, or Agonist Phase (35 min). At the end of the Agonist Phase, mice were removed from the chamber, given a sc injection of saline, and immediately returned to the chamber to record respiration during the Reversal Phase (35 min). Ordinarily, a μ opioid receptor (MOR) antagonist such as naloxone would be administered at the start of the Reversal Phase (see Elder et al. 2023). However, since the main purpose of the above pilot was to compare fentanyl and morphine dose response in respiratory depression, all mice received saline for the Reversal Phase. A schematic of this protocol is provided in **Figure 4.2**.

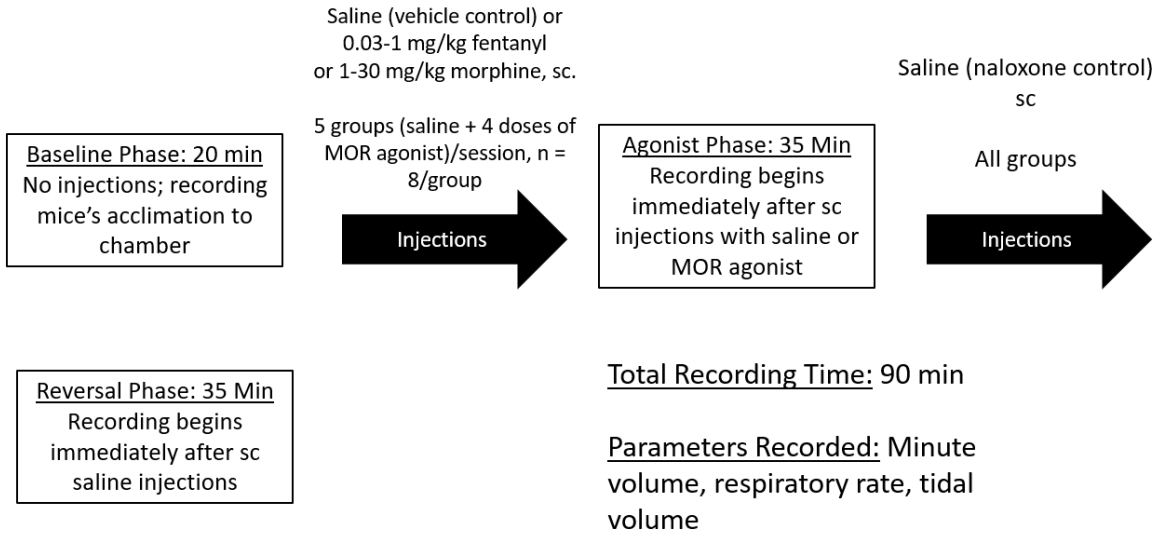

Figure 4.2: Diagram of Three-Phase Whole-Body Plethysmography Protocol.

Frequency (f; respiratory rate, or number of breaths per minute), tidal volume (TVb; the volume of air displaced from the lungs between inspiration and expiration), and minute volume (MVb; the volume of air inhaled or exhaled from the lungs in a minute, defined as the product of frequency x tidal volume) were recorded with FinePointe software (version 2.7.0.11788).

4.2.5. Statistics

Statistical analysis was performed with GraphPad Prism software (version 6.01). Whole-body plethysmography data (MVb, f, and TVb) was normalized within-subject to percent baseline to control for potential variation from differences in raw baseline values. Specifically, raw data for these parameters from individual subjects was grouped into five-minute bins, and these five-minute averages were divided by the average MVb, f, or TVb measured during the Baseline Phase, then multiplied by 100%. Afterwards, normalized individual averages were used to calculate normalized average MVb, f, and TVb for each treatment group during each five-minute bin. Normalized group averages underwent two-way analysis of variance (ANOVA) with time as the within-subjects factor and treatment as the between-subjects factor, followed by Holm-Šídák post-hoc for multiple comparisons as needed. Significance was defined as $p < 0.05$ for all statistical tests.

4.3. Results

4.3.1. Fentanyl-induced respiratory depression

2-way repeated-measures ANOVA revealed significant effects of dose and time ($P<0.0001$) on MVb, f, and TVb in drug-naïve mice treated with a range of acute fentanyl doses (0-1.0 mg/kg sc). Detailed comparisons of different fentanyl doses to saline are provided in **Figures 4.3-4.5**. There was a temporary increase in respiratory parameters (MVb, f, and TVb) 5 min after mice received the Reversal Phase injection (60 min into total session runtime) and,

primarily in control mice or groups receiving lower doses, the 5 min after mice received the Agonist Phase injection. This behavioral artifact has also been observed by other groups (Elder et al. 2023) and is thought to potentially stem from the mice's response to the dual stressors of handling and injection experienced immediately before the start of the Agonist and Reversal Phases.

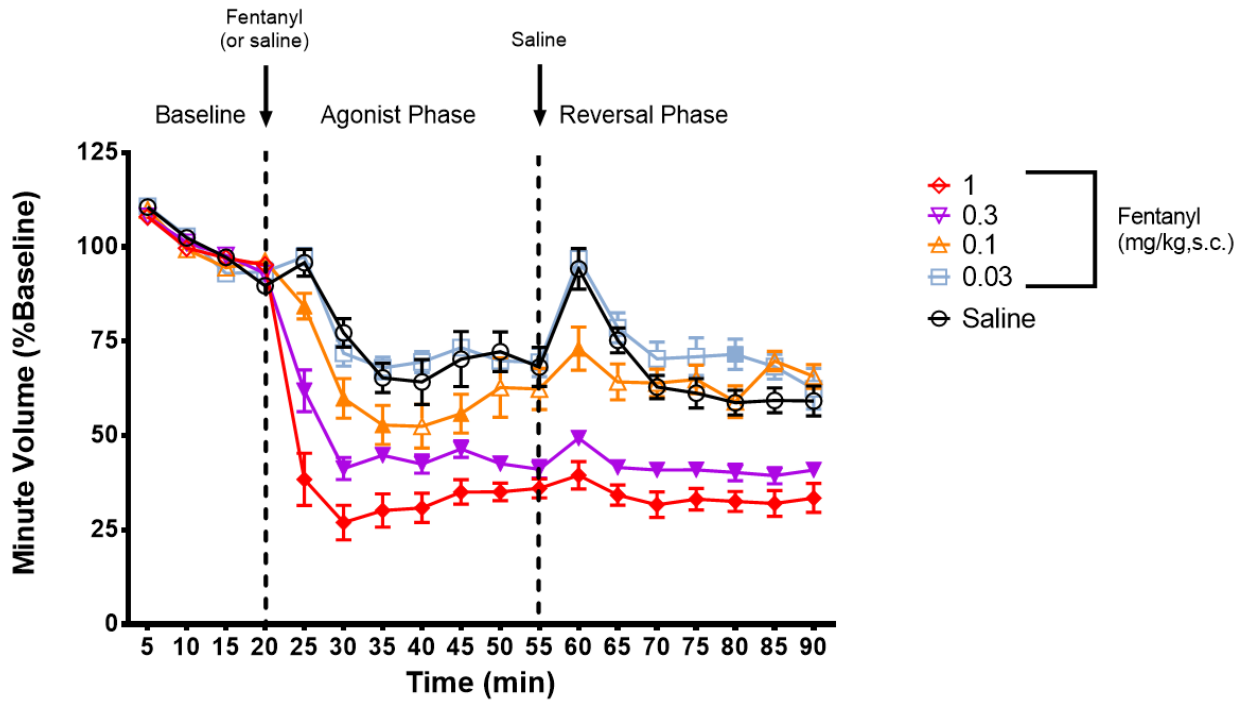

Figure 4.3: Fentanyl Demonstrates Dose Response Effects in Induction of Respiratory Depression (Specifically, MVb) in Mice, with Sustained Respiratory Depression at 0.3 mg/kg and Higher. After the first 20 min (Baseline Phase), during which baseline respiration was established, male Swiss Webster mice were injected with either vehicle control (saline) or 0.03-1.0 mg/kg fentanyl sc and MVb (minute volume; product of frequency and tidal volume), measured for 35 min (Agonist Phase). Mice then received a saline injection, and MVb was measured for an additional 35 min (Reversal Phase). 2-way repeated-measures ANOVA revealed a significant effect of dose ($P<0.0001$) and time ($P<0.0001$), with differences from control

further evaluated by Holm-Šídák post hoc. Filled symbols denote significant difference from saline (p≤0.05). Data are presented as mean normalized MVb (5-min bins), expressed as percent baseline ± SEM. n = 8/group

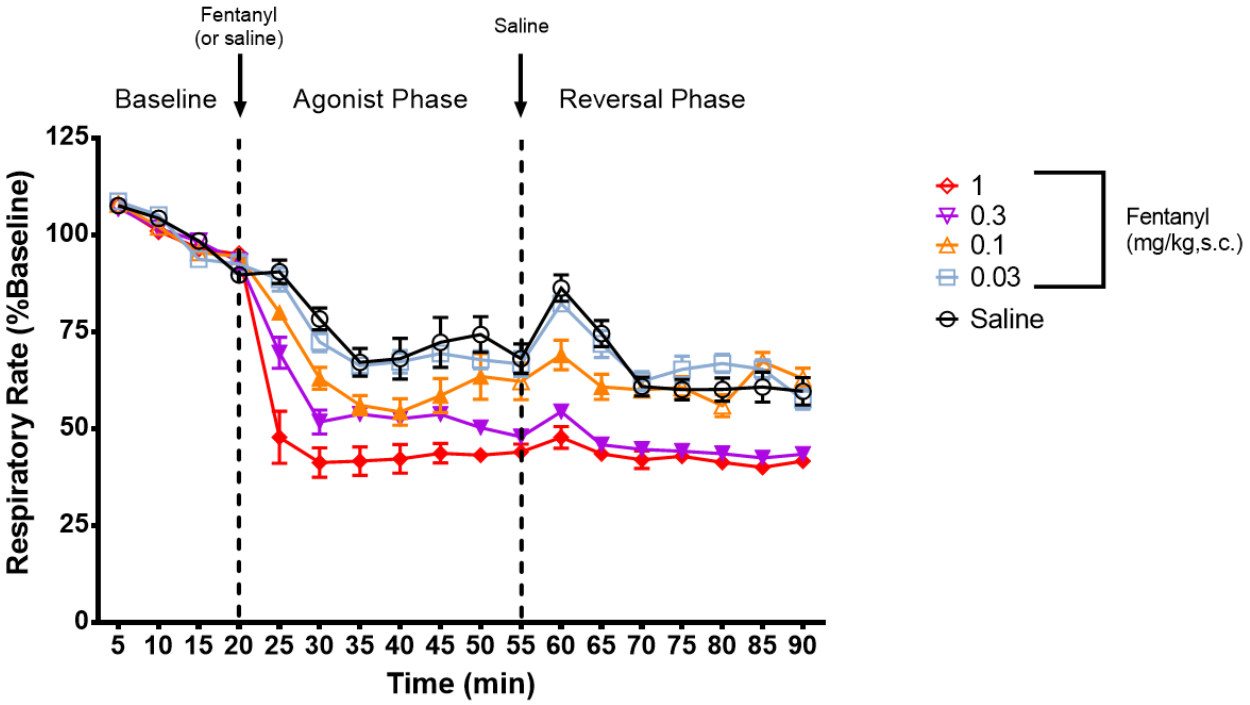

Figure 4.4: Fentanyl Demonstrates Dose Response Effects in Induction of Respiratory Depression (Specifically, f) in Mice, with Sustained Respiratory Depression at 0.3 mg/kg and Higher. After the first 20 min (Baseline Phase), during which baseline respiration was established, male Swiss Webster mice were injected with either vehicle control (saline) or 0.03-1.0 mg/kg fentanyl sc and f (frequency, or respiratory rate; breaths/minute) measured for 35 min (Agonist Phase). Mice then received a saline injection, and f was measured for an additional 35 min (Reversal Phase). 2-way repeated-measures ANOVA revealed a significant effect of dose ($P<0.0001$) and time ($P<0.0001$), with differences from control further evaluated by Holm-Šídák post hoc. Filled symbols denote significant difference from saline (p≤0.05). Data are presented as mean normalized f (5-min bins), expressed as percent baseline ± SEM. n = 8/group

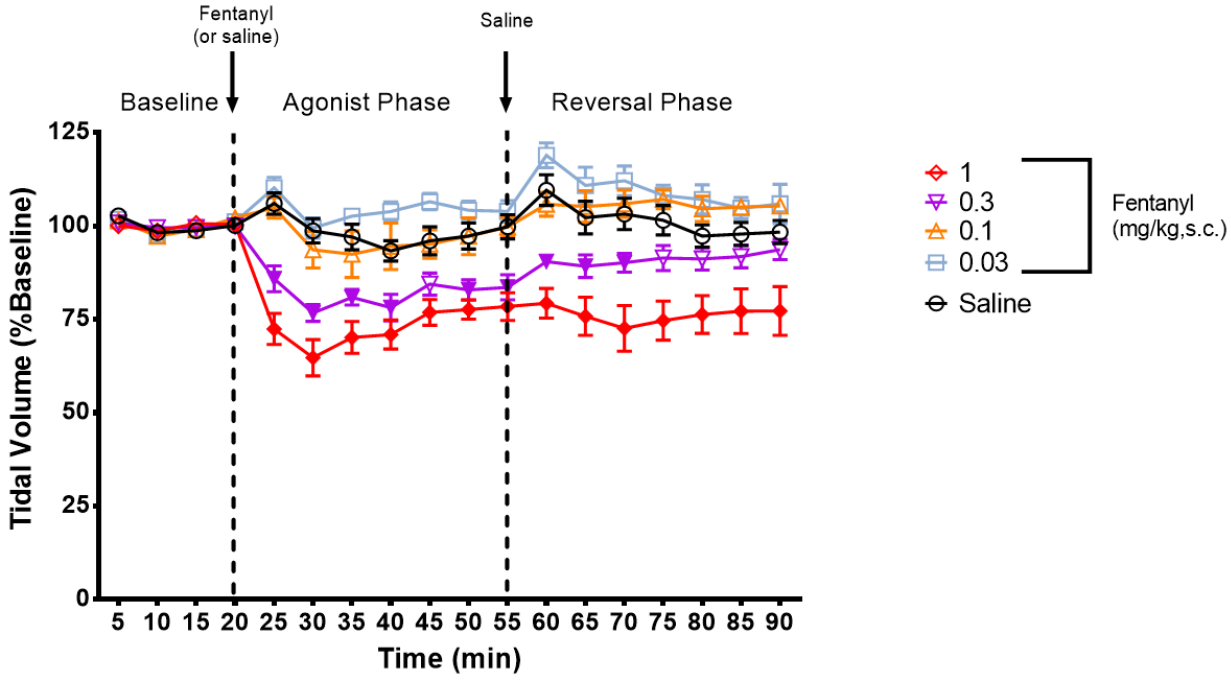

Figure 4.5: Fentanyl Demonstrates Dose Response Effects in Induction of Respiratory Depression (Specifically, TVb) in Mice, with Sustained Respiratory Depression at 0.3 mg/kg and Higher. After the first 20 min (Baseline Phase), during which baseline respiration was established, male Swiss Webster mice were injected with either vehicle control (saline) or 0.03-1.0 mg/kg fentanyl sc and TVb (tidal volume; volume of air displaced from the lungs/respiratory cycle) measured for 35 min (Agonist Phase). Mice then received a saline injection, and TVb was measured for an additional 35 min (Reversal Phase). 2-way repeated-measures ANOVA revealed a significant effect of dose ($P<0.0001$) and time ($P<0.0001$), with differences from control further evaluated by Holm-Šídák post hoc. Filled symbols denote significant difference from saline ($p\leq0.05$). Data are presented as mean normalized TVb (5-min bins), expressed as percent baseline ± SEM. n = 8/group

4.3.2. Morphine-induced respiratory depression

2-way repeated-measures ANOVA revealed significant effects of dose and time ($P<0.0001$) on MVb, f, and TVb in drug-naïve mice treated with a range of acute morphine doses (0-30 mg/kg sc). Detailed comparisons of different morphine doses to saline are provided in **Figures 4.6-4.8**.

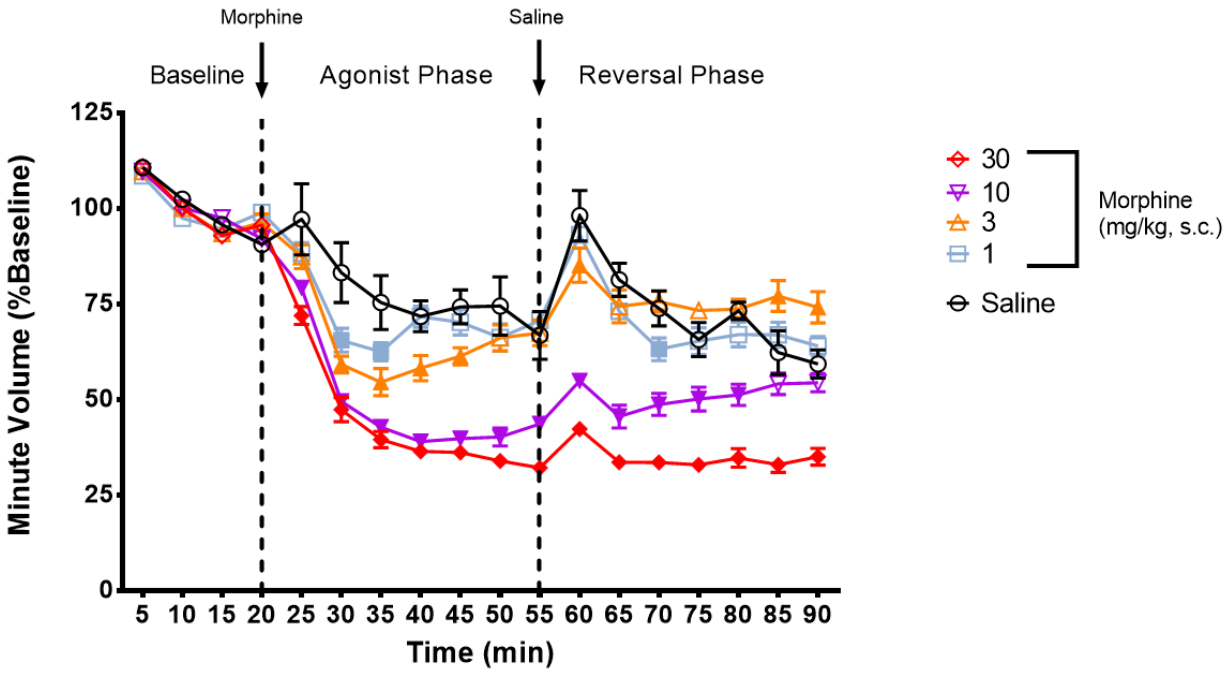

Figure 4.6: Morphine Demonstrates Dose Response Effects in Induction of Respiratory Depression (Specifically, MVb) in Mice, with Sustained Respiratory Depression at 30 mg/kg. After the first 20 min (Baseline Phase), during which baseline respiration was established, male Swiss Webster mice were injected with either vehicle control (saline) or 1-30 mg/kg morphine sc and MVb (minute volume; product of frequency and tidal volume) measured for 35 min (Agonist Phase). Mice then received a saline injection, and MVb was measured for an additional 35 min (Reversal Phase). 2-way repeated-measures ANOVA revealed a significant effect of dose ($P<0.0001$) and time ($P<0.0001$), with differences from control further evaluated

by Holm-Šídák post hoc. Filled symbols denote significant difference from saline ($p \leq 0.05$). Data are presented as normalized mean MVb (5-min bins), expressed as percent baseline ± SEM. n = 8/group

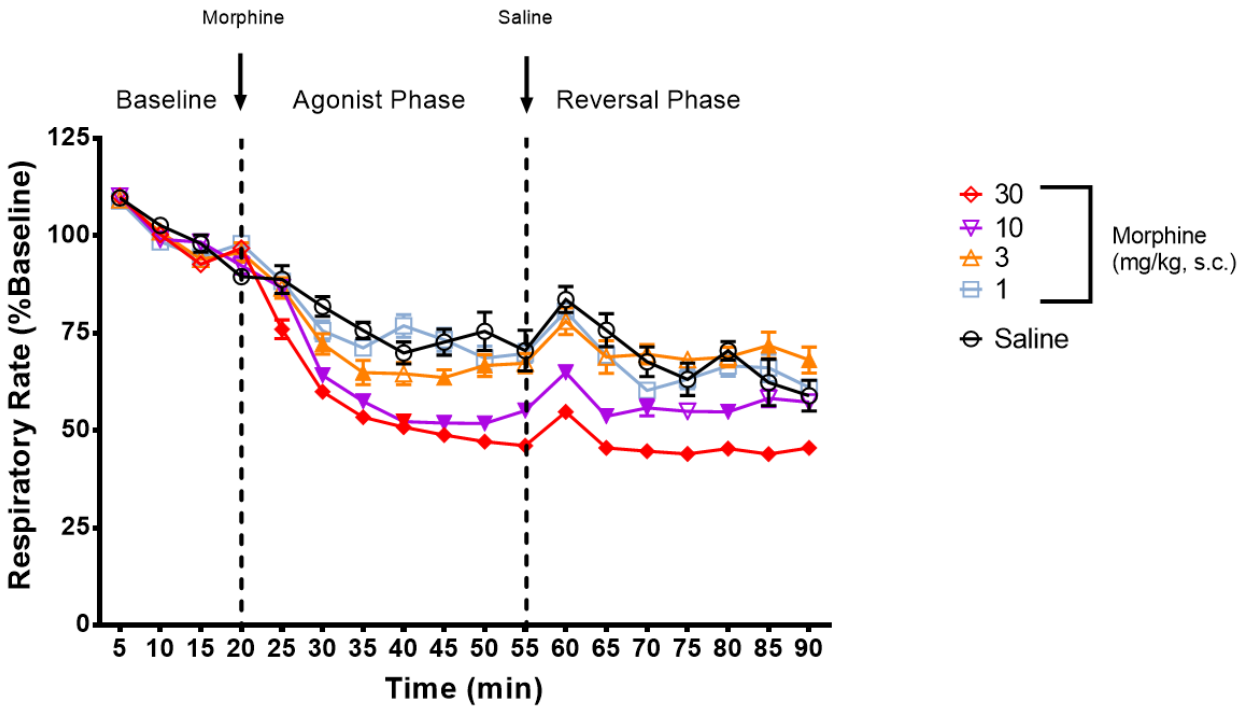

Figure 4.7: Morphine Demonstrates Dose Response Effects in Induction of Respiratory Depression (Specifically, f) in Mice, with Sustained Respiratory Depression at 30 mg/kg. After the first 20 min (Baseline Phase), during which baseline respiration was established, male Swiss Webster mice were injected with either vehicle control (saline) or 1-30 mg/kg morphine sc and f (frequency, or respiratory rate; breaths/minute) measured for 35 min (Agonist Phase). Mice then received a saline injection, and f was measured for an additional 35 min (Reversal Phase). 2-way repeated-measures ANOVA revealed a significant effect of dose ($P<0.0001$) and time ($P<0.0001$), with differences from control further evaluated by Holm-Šídák post hoc. Filled

symbols denote significant difference from saline (p≤0.05). Data are presented as normalized f (5-min bins), expressed as percent baseline ± SEM. n = 8/group

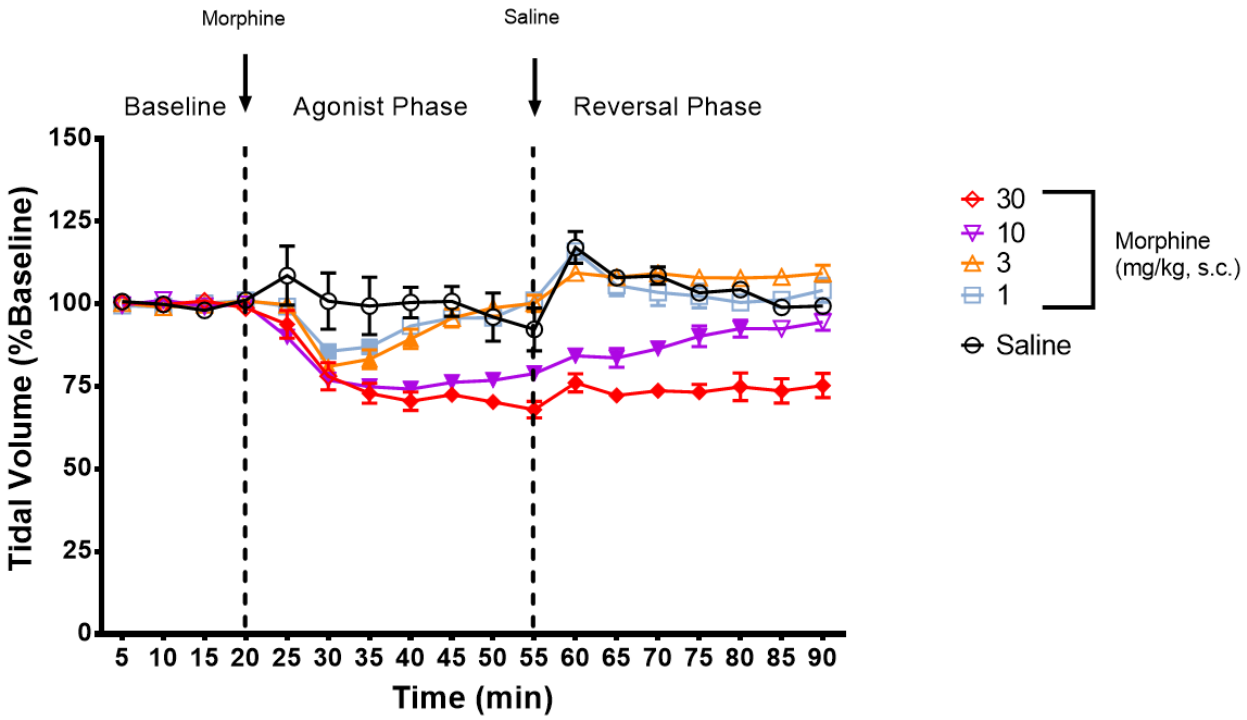

Figure 4.8: Morphine Demonstrates Dose Response Effects in Induction of Respiratory Depression (Specifically, TVb) in Mice, with Sustained Respiratory Depression at 30 mg/kg. After the first 20 min (Baseline Phase), during which baseline respiration was established, male Swiss Webster mice were injected with either vehicle control (saline) or 1-30 mg/kg morphine sc and TVb (tidal volume; volume of air displaced from the lungs/respiratory cycle) measured for 35 min (Agonist Phase). Mice then received a saline injection, and TVb was measured for an additional 35 min (Reversal Phase). 2-way repeated-measures ANOVA revealed a significant effect of dose (P<0.0001) and time (P<0.0001), with differences from control further evaluated by Holm-Šídák post hoc. Filled symbols denote significant difference from saline (p≤0.05). Data

are presented as normalized mean TVb (5-min bins), expressed as percent baseline ± SEM. n = 8/group

4.3.3. Doses of fentanyl and morphine equipotent in inducing respiratory depression

As demonstrated in the above figures, 0.3 mg/kg fentanyl and 30 mg/kg morphine (doses with a 100-fold difference in concentration) induced similar significant respiratory depression compared to vehicle control. Direct comparison of MVb (**Figure 4.9**), f (**Figure 4.10**), and TVb (**Figure 4.11**) at these two doses further highlights their similarities of effect, barring moderate (though statistically significant) differences in MVb at 25 and 45-55 min (**Figure 4.9**) and TVb at 45-90 min (**Figure 4.11**). Based on these findings, as well as the established 50-100-fold difference in potency between these opioids reported by the CDC, these two doses were selected for use in biodistribution studies.

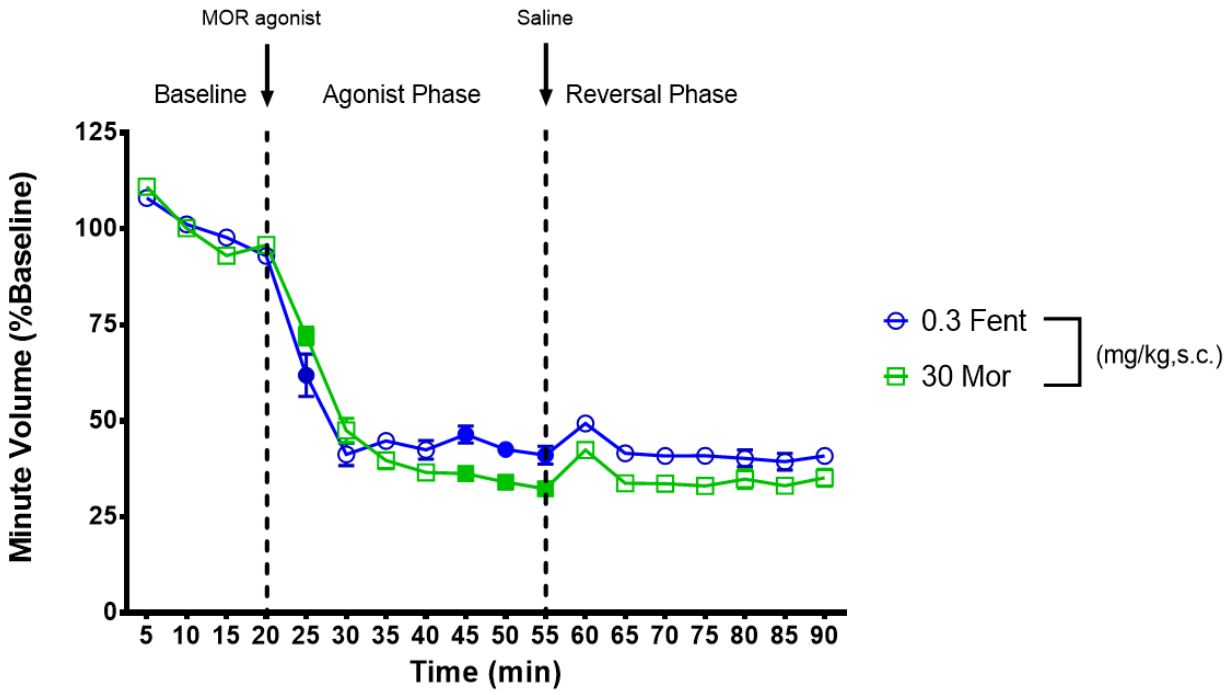

Figure 4.9: Comparison of Respiratory Depressant Effects (Specifically, MVb) of 0.3 mg/kg Fentanyl sc and 30 mg/kg Morphine sc in Mice. Data taken from Figures 4.4 and 4.7,

respectively. All phases as described in previous figure legends. 2-way repeated-measures ANOVA with Holm-Šídák post hoc as needed. Filled symbols denote significant difference between groups ($p \leq 0.05$). Data are presented as normalized mean MVb (5-min bins), expressed as percent baseline ± SEM. n = 8/group

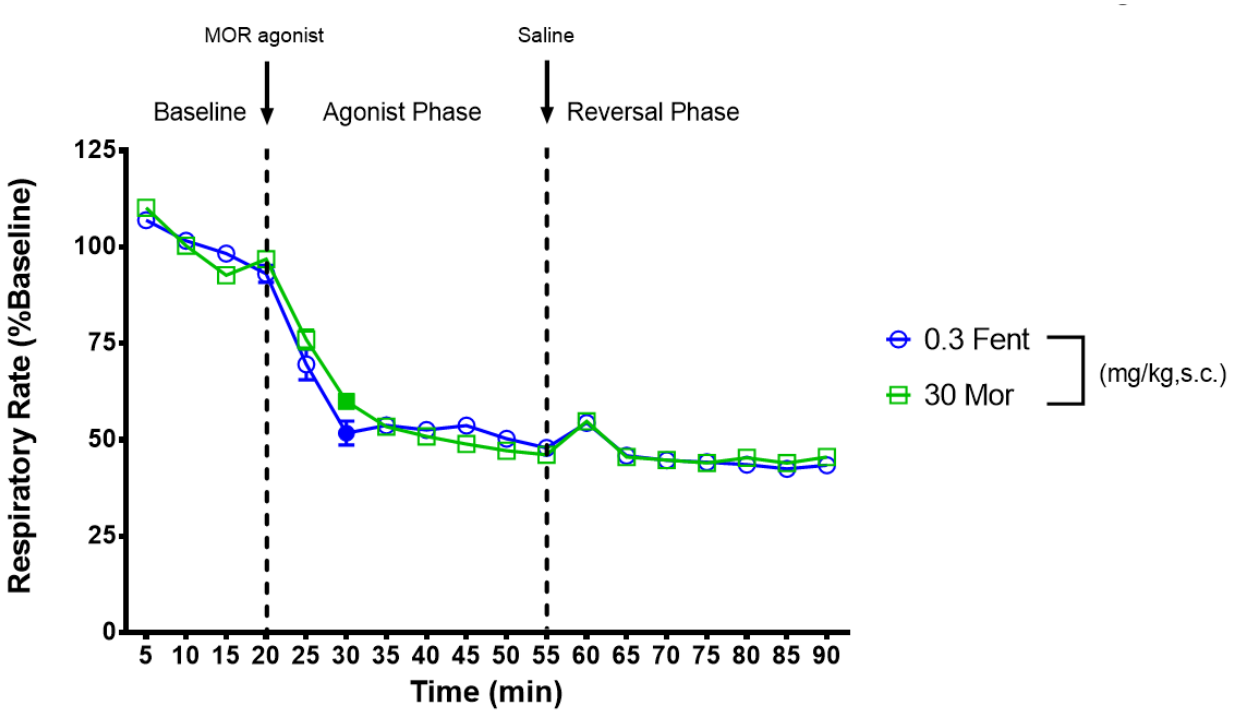

Figure 4.10: Comparison of Respiratory Depressant Effects (Specifically, f) of 0.3 mg/kg Fentanyl sc and 30 mg/kg Morphine sc in Mice. Data taken from Figures 4.5 and 4.8, respectively. All phases as described in previous figure legends. 2-way repeated-measures ANOVA with Holm-Šídák post hoc as needed. Filled symbols denote significant difference between groups ($p \leq 0.05$). Data are presented as normalized mean f (5-min bins), expressed as percent baseline ± SEM. n = 8/group

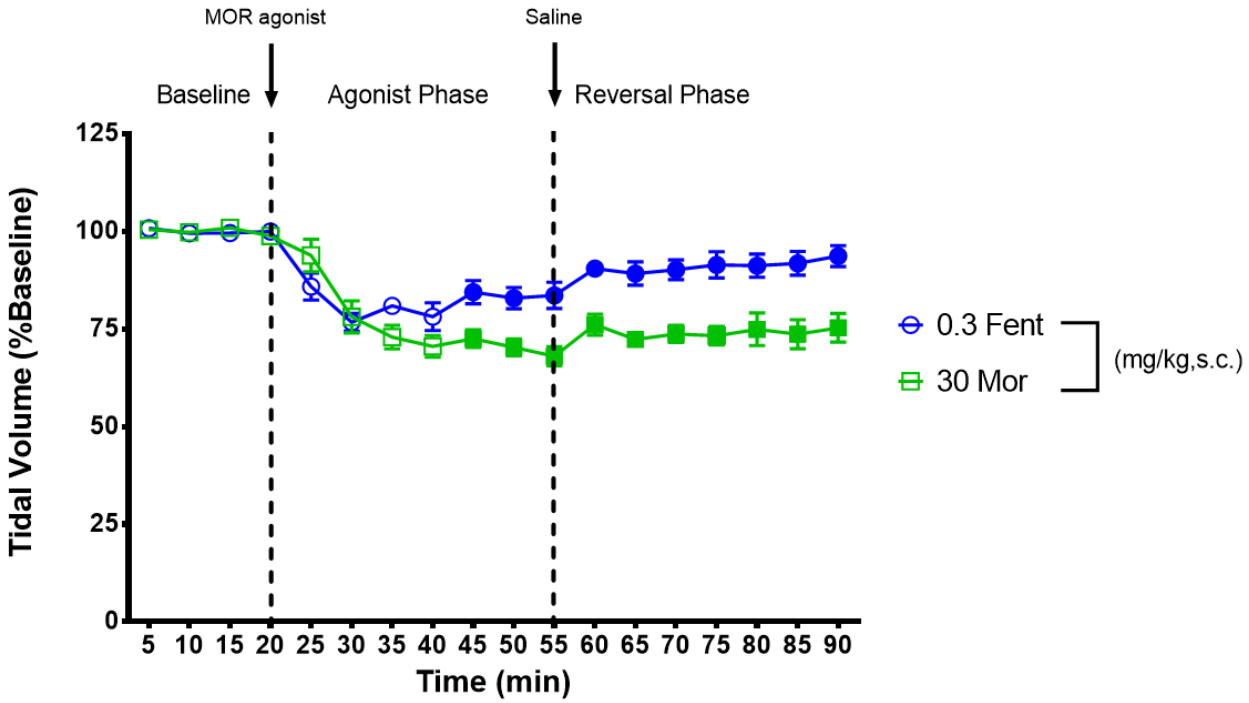

Figure 4.11: Comparison of Respiratory Depressant Effects (Specifically, TVb) of 0.3 mg/kg Fentanyl sc and 30 mg/kg Morphine sc in Mice. Data taken from Figures 3 and 6, respectively. All phases as described in previous figure legends. 2-way repeated-measures ANOVA with Holm-Šídák post hoc as needed. Filled symbols denote significant difference between groups ($p \leq 0.05$). Data are presented as normalized mean TVb (5-min bins), expressed as percent baseline ± SEM. n = 8/group

To evaluate potential pre-existing differences in baseline respiration, average MVb, f, and TVb were calculated from raw Baseline Phase values for each treatment group in fentanyl and morphine dose-response studies. One-way ANOVA did not reveal significant differences in baseline f or TVb for either the fentanyl (**Figure 4.12b-c**) or morphine (**Figure 4.13b-c**) studies. However, one-way ANOVA detected significant differences in baseline MVb in both the fentanyl study (**Figure 4.12a**; P = 0.0486) and the morphine study (**Figure 4.13a**; P = 0.0444), although further examination with Holm-Šídák post-hoc did not indicate significant differences between

any of the treatment groups at Baseline Phase. Therefore, the data as a whole indicate that there were no differences in baseline MVb, f, or TVb between treatment groups within either dose-response study.

a)

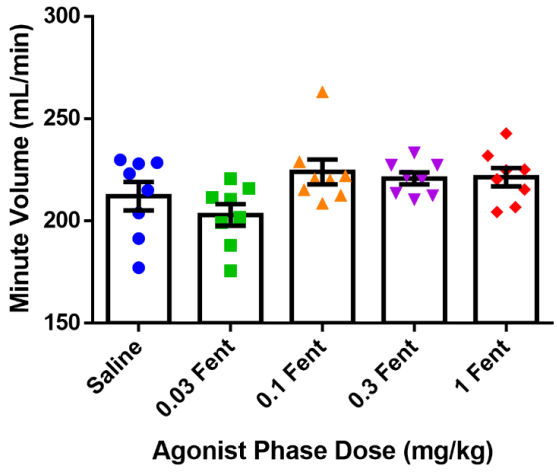

b)

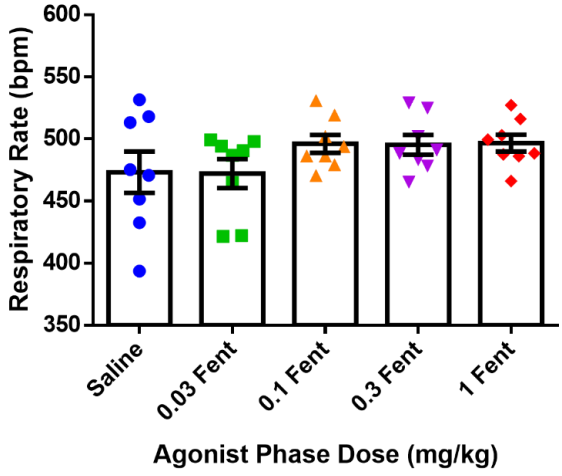

c)

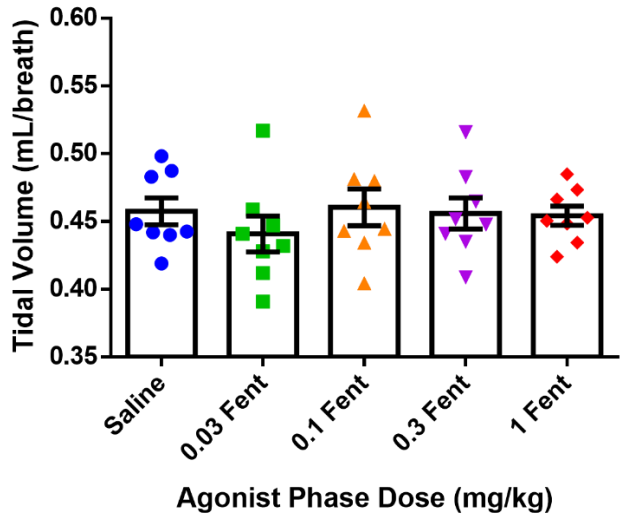

Figure 4.12: Baseline Respiration in Fentanyl Dose-Response Whole-Body Plethysmography Study Prior to Agonist Phase. Mice organized based on dose received at the start of the Agonist Phase. a) Average MVb over the course of 20-min Baseline Phase.

Significant differences between treatment groups at baseline detected through ANOVA (P = 0.0486), but no further significant differences in post-hoc. b) Average f over the course of 20-min Baseline Phase. No significant differences between treatment groups at baseline (P = 0.2444). c) Average TVb over the course of 20-min Baseline Phase. No significant differences between treatment groups at baseline (P = 0.7703). One-way ANOVA followed by Holm-Šídák post hoc as needed. Data are presented as mean ± SEM. n = 8/group

a)

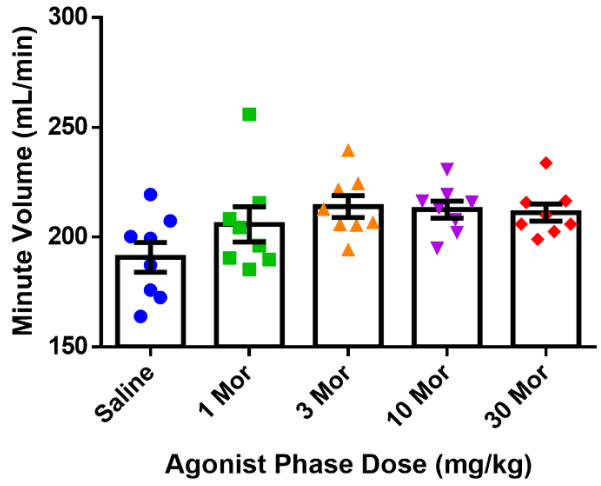

b)

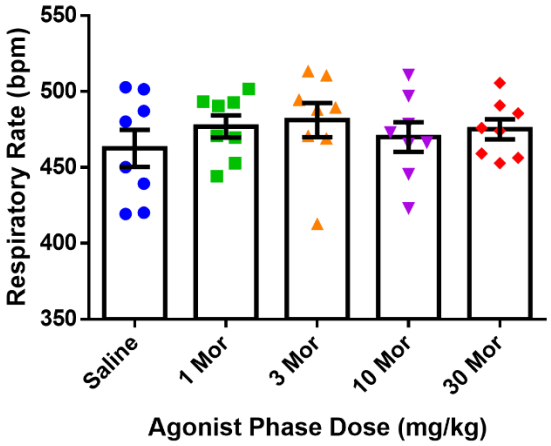

c)

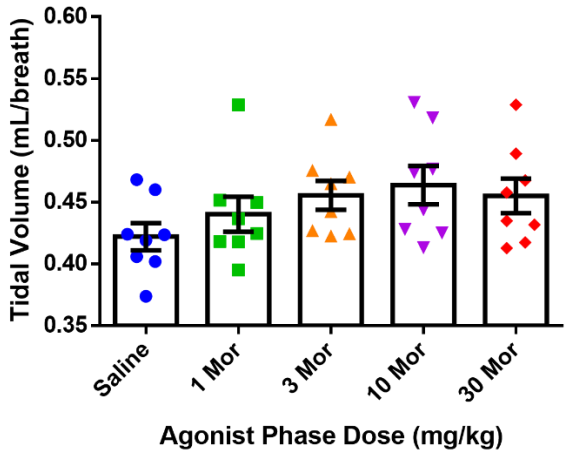

Figure 4.13: Baseline Respiration in Morphine Dose-Response Whole-Body Plethysmography Study Prior to Agonist Phase. Mice organized based on dose received at the start of the Agonist Phase. a) Average MVb over the course of 20-min Baseline Phase. Significant differences between treatment groups at baseline detected through ANVOA (P = 0.0486), but no further significant differences in post-hoc. b) Average f over the course of 20-min Baseline Phase. No significant differences between treatment groups at baseline (P = 0.2444). c) Average TVb over the course of 20-min Baseline Phase. No significant differences between

treatment groups at baseline (P = 0.7703). One-way ANOVA followed by Holm-Šídák post hoc as needed. Data are presented as mean ± SEM averaged over the 20-min Baseline Phase. n = 8/group

CHAPTER 5: BIODIDSTRIBUTION OF ACUTE- AND REPEATED-DOSE FENTANYL AND MORPHINE

5.1. Objective

The aim of these studies was to quantify and compare biodistribution of fentanyl, morphine, and select metabolites (norfentanyl, 4-ANPP, and morphine-3-β-D-glucuronide) in mice acutely treated with equipotent doses of fentanyl or morphine at 5, 15, 60, or 240 minutes after administration and to evaluate levels of these compounds in blood and tissue in mice repeatedly treated with the same doses of fentanyl or morphine used in acute studies.

5.2. Materials and Methods

5.2.1. Drugs

Fentanyl hydrochloride and morphine sulfate pentahydrate were provided by the National Institute on Drug Abuse (Bethesda, MD, USA) Drug Supply Program. Drugs were dissolved in sterile saline and administered sc at a volume of 10 mL/kg body weight.

5.2.2. Standards and Reagents

Certified reference materials and internal standards for mass spectroscopy studies, including 100 µg/mL fentanyl (N-Phenyl-N-[1-(2-phenylethyl)-4-piperidinyl]propanamide; Lot No. FE03012201; CAS No. 437-38-7) in methanol, 100 µg/mL fentanyl-d5 (N-(Pentadeuterophenyl)-N-[1-(2-phenylethyl)-4-piperidinyl]propanamide; Lot No. FE08312117; CAS No. 118357-29-2) in methanol, 1 mg/mL norfentanyl oxalate (N-Phenyl-N-(4-piperidinyl)propanamide oxalate; Lot No. FE02172249; CAS No. 1211527-24-0) in methanol, 1 mg/mL norfentanyl-d5 oxalate (N-(4-Piperidinyl)-N-pentadeuterophenylpropionamide oxalate; Lot No. FE10092001; CAS No. 1435933-84-8) in methanol, 100 µg/mL 4-ANPP (N-Phenyl-1-(2-phenethyl)-4-piperidinamine; Lot No. FE07272146; CAS No. 21409-26-7) in methanol, 100

μg/mL 4-ANPP-d5 (N-phenyl-D5-1-(2-phenethyl)-4-piperidinamine; Lot No. FE12172036; CAS No. 1189466-15-6) in methanol, 1 mg/mL morphine ((5α, 6α)-7,8-Didehydro-4,5-epoxy-17-methylmorphinan-3,6-diol; Lot No. FE03252112; CAS No.57-27-2) in methanol, 100 μg/mL morphine-d3 (7,8-Didehydro-4,5-epoxy-17-trideuteromethylmorphinan-3,6-diol; Lot No. FE08312130; CAS No. 67293-88-3) in methanol, 1 mg/mL morphine-3-β-d-glucuronide ((5α, 6α)-7,8-didehydro-4,5-epoxy-6-hydroxy-17-methylmorphinan-3-yl-β-D-glucopyranosiduronic acid; Lot No. FE01142007, CAS No. 20290-09-9) in methanol with 0.05% NaOH, 100 μg/mL morphine-3-β-d-glucuronide-d3 (7,8-Didehydro-4,5-epoxy-17-trideuteromethylmorphinan-6-ol-3beta-glucuronic acid; Lot No. FE07162006; CAS No. 136765-44-1) in methanol with 0.05% NaOH, 1 mg/mL morphine-6-β-d-glucuronide ((5α, 6α)-7,8-didehydro-4,5-epoxy-3-hydroxy-17-methylmorphinan-6-yl-β-D-glucopyranosiduronic acid; Lot No. FE11172134; CAS No. 20290-10-2) in water:methanol (80:20), and 100 μg/mL morphine-6-β-d-glucuronide-d3 ((5α, 6α)-7,8-didehydro-4,5-epoxy-3-hydroxy-17(methyl-D3)morphinan-6-yl-β-D-glucopyranosiduronic acid; Lot No. FE03012203; CAS No. 219533-69-4) in water:methanol (50:50) were purchased from the Cerilliant Corporation (Round Rock, TX, USA).

HPLC-grade water, HPLC-methanol, and formic acid were purchased from Fisher Chemical.

5.2.3. Subjects

For acute opioid biodistribution studies, 48 adult male Swiss Webster mice (Envigo) weighing between 27-41 g (mean ± standard deviation = 33.7 ± 3.15 g) were group housed (5/cage) in Association for Assessment and Accreditation of Laboratory Animal Care-accredited facilities at Virginia Commonwealth University. Mice were kept on a standard 12-hr light/dark cycle and given at least one week to acclimate to vivarium conditions prior to experiments. Mice had access to food (Teklad 7012 Rodent Diet; Envigo, Madison, WI, USA) and tap water ad

libitum in the home cage. All animals were drug-naïve prior to day of sacrifice to prevent confounding effects of previous drug history.

For repeated opioid biodistribution studies, 16 adult male Swiss Webster mice (Envigo) weighing between 27-36 g (mean ± standard deviation = 30.4 ± 2.34 g) at time of sacrifice were used. Vivarium and housing conditions were as described for acute studies. During experiments, animals were housed out-of-vivarium up to day of sacrifice to prevent undue stress from repeated transport to and from the vivarium and to ensure that mice were acclimated to the laboratory space where injections were administered. Weights were taken daily both to determine necessary injection volume and to monitor animal health over the course of the study. While mice experienced moderate weight loss (1.31 g on average) during the five-day period, this was not severe enough to warrant concern, and no significant differences in weight loss were observed between pretreatment groups.

For studies of antinociceptive tolerance following repeated opioid injection, 16 adult male Swiss Webster mice (Envigo) weighing between 31-39 g (mean ± standard deviation = 33.7 ± 2.05 g) at time of testing were used. Vivarium and housing conditions were as described above. As with repeated opioid biodistribution studies, mice were housed out-of-vivarium for the duration of the study to ensure acclimation to laboratory and to prevent stress from repeated transport to and from vivarium. Mice were weighed daily to determine necessary injection volume and to monitor health. Although moderate weight loss (1.38 g on average) occurred over the five-day experimental period, this was not severe enough to warrant concern.

All experiments were performed in accordance with the National Research Council's Guide for Care and Use of Laboratory Animals (2011), and associated protocols were approved by Virginia Commonwealth University's Institutional Animal Care and Use Committee.

5.2.4. Tissue Collection

For acute opioid biodistribution studies, mice were randomly sorted into three treatment groups: Saline (vehicle control), 0.3 mg/kg fentanyl, or 30 mg/kg morphine. These groups were further divided based on time of sacrifice post-injection (5, 15, 60, or 240 min; n = 4/treatment/time point). All injections were delivered sc. The above doses of fentanyl and morphine were chosen based on the ~100-fold difference in potency between these drugs (CDC) and their ability to produce robust respiratory depression in plethysmography studies. After the designated time had elapsed, mice were decapitated by guillotine, and trunk blood and tissue samples (brain, liver, lung, heart, kidney, spleen, small intestine, large intestine, stomach, muscle, fat, and skin) were harvested on ice. Immediately after collection, samples were stored at –80˚C.

For repeated opioid biodistribution studies, mice were randomly sorted into four treatment groups: Repeated fentanyl + saline injection (F/S; 0.3 mg/kg fentanyl once daily for four days + acute saline injection on the fifth day), repeated morphine + saline injection (M/S; 30 mg/kg morphine once daily for four days + acute saline injection on the fifth day), repeated fentanyl + fentanyl injection (F/F; 0.3 mg/kg fentanyl once daily for four days + acute fentanyl injection [0.3 mg/kg] on the fifth day), or repeated morphine + morphine injection (M/M; 30 mg/kg morphine once daily for four days + acute morphine injection [30 mg/kg] on the fifth day) (n = 4/group). All injections were delivered sc.

On the fifth day, animals were sacrificed 60 minutes after the acute injection. This time was chosen based on the results from acute opioid biodistribution studies as a window during which sizable quantities of the target opioids could be observed in several tissues. Mice were decapitated by guillotine, and trunk blood and tissue samples (brain, liver, lung, heart, kidney,

spleen, small intestine, large intestine, stomach, muscle, fat, skin, spine, and diaphragm) were harvested on ice. Immediately after collection, samples were stored at –80˚C.

5.2.5. Solid-Phase Extraction

Tissue samples were homogenized in a 1:4 dilution in water (except for muscle and skin, which were diluted 1:8). 100 µL aliquots of homogenate were placed in a glass culture tube along with 50 µL of internal standard solution (0.2 µg/mL morphine-d3, 1 µg/mL morphine-3-β-D-glucuronide-d3 & morphine-6-β-D-glucuronide-d3, 0.02 µg/mL fentanyl-d5, 0.1 µg/mL norfentanyl-d5 & 4-ANPP-d5) and 300 µL HPLC water. Samples were then centrifuged (Allegra X-15R centrifuge, Beckman Coulter, Inc., Indianapolis, IN, USA) for 10 minutes.

Extraction was performed with a 48-position positive pressure manifold (United Chemical Technologies, Inc., Bristol, PA, USA) connected to a N2 gas tank. SPE-Phenomenex Strata-x 33 µ Polymeric Reversed Phase columns (Phenomenex Inc.) were conditioned with 1 mL of methanol followed by 1 mL of water, and samples subsequently loaded. This was followed by a 5% methanol wash (1 mL). Samples were then eluted with 0.400 mL (2X) of 95% methanol.

Eluted samples were transferred to a 96 deep-well plate, evaporated under nitrogen (25 psi) 30-45 min at 55˚C on an SPE Dry 96 (Biotage) and reconstituted with 65 µL methanol. In addition to experimental samples, each run also included a calibration curve (in mouse serum; see **Section 3.2.2** for product details), blanks, and quality controls for the tissue types being analyzed. Calibrators were prepared at 1, 2, 5, 10, 20, 50, and 100 ng/mL (fentanyl and 4-ANPP), 5, 10, 20, 50, 100, 200, and 500 ng/mL (norfentanyl), 10, 20, 50, 100, 200, 500, and 1000 ng/mL (morphine), and 50, 100, 200, 500, 1000, 2000, and 5000 ng/mL (morphine-3 and morphine-6-β-D-glucuronide).

5.2.6. Quantitation of Fentanyl, Morphine, and Their Metabolites

The analytical method was validated in accordance with version M10 of the guidelines laid out by the International Council for Harmonisation of Technical Requirements for Pharmaceuticals for Human Use (see Chapter 3).

Chromatographic separation was performed with a SCIEX ExionLC 2.0 liquid chromatograph using an Agilent Polaris SI-A column (180 Å, 5 µm, 50 x 3.0 mm). Autosampler injection volume was 5 µL with a duration of 5.50 minutes. Mobile phases were kept on an isocratic gradient (90 % Mobile Phase A, 10% Mobile Phase B), where Phases A and B consisted of 1% formic acid in water and 1% formic acid in acetonitrile, respectively. Column oven temperature was maintained at 40˚C.

Mass spectrometry was performed by a SCIEX QTRAP 6500+ high-throughput mass spectrometer run on Analyst 1.7.2 analytical software. Source temperature was set to 600˚C, while curtain gas and Gases 1 and 2 flow rates were set to 40 mL/min. Electrospray voltage was 5500 eV, and dwell time was 100 msec.

5.2.7. Warm-Water Tail Withdrawal.

Mice were given repeated injections of 0.3 mg/kg fentanyl or 30 mg/kg morphine sc (once every 24 hr for 5 days) or, in the case of vehicle controls, repeated saline injections (once every 24 hr for 4 days) followed by acute 0.3 mg/kg fentanyl or 30 mg/kg morphine sc 24 hr later (the fifth experimental day).

The basic tail withdrawal protocol is outlined in **Figure 5.1**. In short, on the fifth experimental day, baseline tail withdrawal latencies were measured by partially submerging the mice's tails in warm water (56˚C; Thermo Precision Microprocessor Controlled 280 Series Water Bath) and recording the time elapsed (s) before the tail was fully withdrawn from the bath. Mice

displaying baseline latencies between 2-4 s were deemed acceptable for further testing. In the aforementioned repeated opioid biodistribution study, tissue samples were collected 60 min after injection. Therefore, tail withdrawal latency was measured again 60 min after the final injection (test latency). If mice did not remove their tails from the water after 10 s, testing was concluded to minimize tissue damage.

Opioid antinociception was defined as percent maximum possible effect (%MPE; Harris and Pierson, 1964) and calculated using the equation below (based on Welch and Dewey 1986):

$$\%\text{MPE} = \frac{(\text{test latency} - \text{baseline latency})}{(10 - \text{baseline latency})}$$

with 10 representing the 10-s cutoff time.

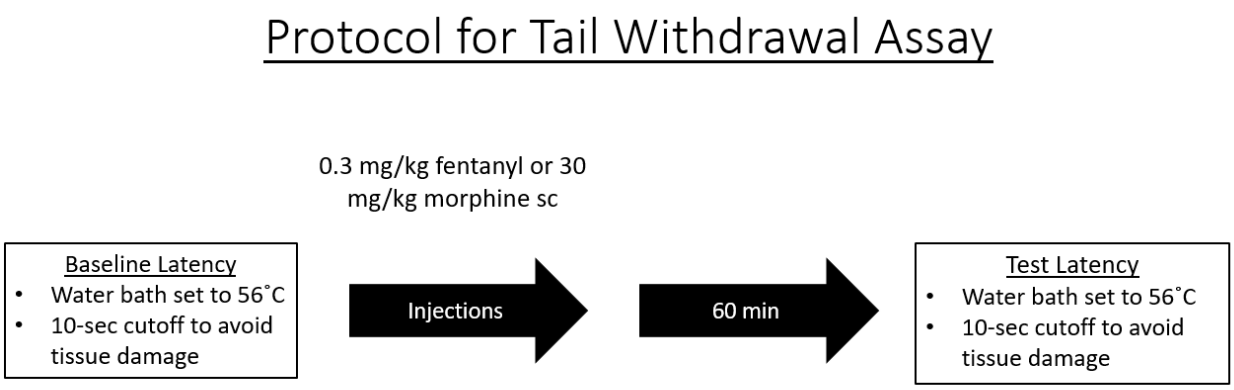

Figure 5.1: Schematic of Basic Procedure for Warm-Water Tail Withdrawal Assay.

5.2.8. Statistics

Statistical analysis was performed with GraphPad Prism software (version 6.01). Acute biodistribution data was analyzed using two-way ANOVA and, if significant differences were detected between analytes, Šídák's post-hoc for multiple comparisons. One-way ANOVA could not be performed on tail withdrawal data due to a standard error of zero for all groups. Unpaired 2-tailed T-tests were used to compare AUC tissue:blood ratios and, when appropriate, for

analyzing biodistribution data from repeated injection studies. Significance was defined as $p<0.05$ for all statistical tests.

5.3. Results

5.3.1. Biodistribution of Fentanyl, Morphine, and their Metabolites over Time after Acute Injection.

Following acute sc injection with vehicle control (saline), 0.3 mg/kg fentanyl, or 30 mg/kg morphine, mice were sacrificed at 5 min, 15 min, 60 min, or 240 min after administration and tissues harvested for bioanalytical analysis as described above. Observed analyte t_{max} (time at which maximal concentration was observed) and C_{max} (maximal concentration observed) for each tissue are summarized in **Table 5.1**, while fentanyl and morphine tissue:blood concentration ratios are displayed in **Table 5.2** and **Table 5.3**, respectively. Comparisons of fentanyl and morphine tissue:blood area under the curve (AUC) are summarized in **Table 5.4**, while original AUC values (both individual subjects and group averages) for fentanyl and morphine are provided in **Table 5.5** and **Table 5.6**. A detailed breakdown of tissue:blood AUC ratios (both individual subjects and group averages) is listed in **Table 5.7** and **Table 5.8**. AUC values were used as a noncompartmental method to better represent drug concentration over the total acute time course studied.

Table 5.1: Observed t_{max} and C_{max} of Acute Fentanyl and Morphine in Blood and 12 Tissues

Tissue	Analyte	t_{max} (min)	C_{max} (ng/mL or ng/g)
Whole blood	Fentanyl	15	47
	Norfentanyl	60	6.63
	4-ANPP	5	1.12
	Morphine	15	17825
	Morphine-3-β-D-glucuronide	60	19900
Brain	Fentanyl	15	158
	Norfentanyl	5	9.9
	4-ANPP	60	11.4
	Morphine	60	1880
	Morphine-3-β-D-glucuronide	60	1561.5
Liver	Fentanyl	15	19.1
	Nofentanyl	60	21
	4-ANPP	60	2.7
	Morphine	15	1280
	Morphine-3-β-D-glucuronide	60	12202.5
Lung	Fentanyl	15	398.5
	Norfentanyl	60	14.5
	4-ANPP	60	2.5
	Morphine	15	38200
	Morphine-3-β-D-glucuronide	60	15570
Heart	Fentanyl	15	202
	Norfentanyl	240	21.1
	4-ANPP	15	10.6
	Morphine	5	782
	Morphine-3-β-D-glucuronide	60	5490
Kidney	Fentanyl	15	413.5
	Norfentanyl	60	33.9
	4-ANPP	240	21.1
	Morphine	60	59390
	Morpine-3-glucuronide	60	203900
Spleen	Fentanyl	60	282.4
	Norfentanyl	60	19.03
	4-ANPP	N/A	N/A
	Morphine	15	30588.29
	Morphine-3-β-D-glucuronide	60	2623.2
Small Intestine	Fentanyl	60	90.7

	Norfentanyl	60	30.1
	4-ANPP	N/A	N/A
	Morphine	60	14170
	Morphine-3-β-D-glucuronide	15	32790
Large Intestine	Fentanyl	60	88.9
	Norfentanyl	N/A	N/A
	4-ANPP	N/A	N/A
	Morphine	240	22534
	Morphine-3-β-D-glucuronide	N/A	N/A
Stomach	Fentanyl	60	105.7
	Norfentanyl	60	18.35
	4-ANPP	N/A	N/A
	Morphine	60	20350
	Morphine-3-β-D-glucuronide	60	8835
Muscle	Fentanyl	15	30.8
	Norfentanyl	60	31.1
	4-ANPP	N/A	N/A
	Morphine	60	4362.5
	Morphine-3-β-D-glucuronide	60	4335
Fat	Fentanyl	60	163.8
	Norfentanyl	60	10.6
	4-ANPP	N/A	N/A
	Morphine	60	2195
	Morphine-3-β-D-glucuronide	60	1980
Skin	Fentanyl	60	95.5
	Norfentanyl	N/A	N/A
	4-ANPP	N/A	N/A
	Morphine	5	64075
	Morpine-3-glucuronide	60	16900

Table 5.2: Acute Fentanyl Tissue:Blood Ratios in 12 Tissue Types

	Tissue:Blood Concentration Ratio			
Tissue	**5 min**	**15 min**	**60 min**	**240 min**
Brain	2.9	3.4	3.3	3.6
Liver	0.32	0.41	0.55	0.84
Lung	3.0	8.5	9.8	9.3
Heart	3.8	4.3	4.8	12
Kidney	4.5	8.8	18	17
Spleen	1.2	3.3	16	14
Small intestine	1.1	1.7	5.3	10
Large intestine	0.69	1.2	5.2	9.3
Stomach	0.67	1.6	6.1	23
Muscle	0.16	0.66	0.28	1.3
Fat	0.42	1.0	9.5	37
Skin	1.9	1.9	5.6	10

Table 5.3: Acute Morphine Tissue:Blood Ratios in 12 Tissue Types

	Tissue:Blood Ratio			
Tissue	**5 min**	**15 min**	**60 min**	**240 min**
Brain	0.091	0.076	0.34	5.3
Liver	0.072	0.072	0.20	2.0
Lung	0.75	2.1	2.0	4.4
Heart	0.081	0.042	0.051	3.7
Kidney	2.9	3.1	11	14
Spleen	1.2	1.7	4.2	6.5
Small intestine	0.66	0.73	2.6	8.7
Large intestine	0.33	0.37	2.6	268
Stomach	0.48	0.85	3.7	39
Muscle	-	0.059	0.80	-
Fat	0.057	0.080	0.40	5.0
Skin	6.7	3.0	4.0	6.2

Morphine not detected in muscle at 5 and 240 min

Table 5.4: Comparison of Acute Fentanyl and Morphine Tissue:Blood AUC in 12 Tissue Types.

Tissue	Difference in Concentration Ratio (Tissue AUC:Blood AUC)
Brain	Fentanyl > Morphine ($p<0.0001$)
Liver	Fentanyl > Morphine ($p=0.0013$)
Lung	Fentanyl > Morphine ($p=0.0008$)
Heart	Fentanyl > Morphine ($p<0.0001$)
Kidney	Fentanyl > Morphine ($p=0.0002$)
Spleen	Fentanyl > Morphine ($p=0.0012$)
Small intestine	Fentanyl > Morphine ($p=0.0276$)
Large intestine	No significant difference ($p=0.2833$)
Stomach	Fentanyl > Morphine ($p=0.0064$)
Muscle	No significant difference ($p=0.8740$)
Fat	Fentanyl > Morphine ($p=0.0009$)
Skin	No significant difference ($p=0.8954$)

No morphine detected in muscle at 5 or 240 min

Table 5.5: Fentanyl AUC Values (Average and by Subject) in Blood and 12 Tissues

	AUC (ng/mL*min or ng/g*min)				
Tissue	**Subject #1**	**Subject #2**	**Subject #3**	**Subject #4**	**Average**
Blood	4719	3829	3640	2972	3790
Brain	14654	11862	12709	10957	12545
Liver	2258	1480	1884	1907	1882
Lung	34250	28658	42601	26605	33028
Heart	17391	20166	22227	15441	18806
Kidney	54849	52815	51797	46476	51484
Spleen	36738	36262	46554	38297	39463
Small intestine	11509	13561	20210	15181	15115
Large intestine	15885	10755	13756	14795	13798
Stomach	18580	18373	22782	17741	19369
Muscle	1547	524	2752	1045	1467
Fat	30551	24128	25136	32574	28097
Skin	17187	22002	17018	8778	16246

Table 5.6: Morphine AUC Values (Average and by Subject) in Blood and 12 Tissues

	AUC (ng/mL*min or ng/g*min)				
Tissue	**Subject #1**	**Subject #2**	**Subject #3**	**Subject #4**	**Average**
Blood	968106	1816140	1156793	792614	1183413
Brain	248860	393160	269930	267908	294964
Liver	214603	159278	172923	167490	178573
Lung	2496570	2985520	2410700	1677650	2392610
Heart	85361	65771	64372	126620	85531
Kidney	6773940	12431680	9560000	5247660	8503320
Spleen	3094169	4601706	3892459	2635961	3556074
Small intestine	2628740	2697500	1416700	1514920	2064465
Large intestine	2359010	6846860	3861810	2302660	3842585
Stomach	2858225	3390050	3282000	2631900	3040544
Muscle	281475	1566000	137800	93818	519773
Fat	587278	245980	302968	176148	328093
Skin	2880090	3785650	6737030	4336150	4434730

Table 5.7: Acute Fentanyl Tissue:Blood AUC (Average and by Subject) in 12 Tissue Types

	AUC Tissue:Blood Ratio				
Tissue	**Subject #1**	**Subject #2**	**Subject #3**	**Subject #4**	**Average**
Brain	3.1	3.1	3.5	3.7	3.3
Liver	0.48	0.39	0.52	0.64	0.51
Lung	7.3	7.5	12	9	8.8
Heart	3.7	5.3	6.1	5.2	5.1
Kidney	12	14	14	16	14
Spleen	8	9	13	13	11
Small intestine	2.4	3.5	5.6	5.1	4.2
Large intestine	3.4	2.8	3.8	5.0	3.7
Stomach	3.9	4.8	6.3	6.0	5
Muscle	0.33	0.14	0.76	0.35	0.39
Fat	6.5	6.3	6.9	11	8
Skin	3.6	5.7	4.7	3.0	4.3

Table 5.8: Acute Morphine Tissue:Blood AUC (Average and by Subject) in 12 Tissue Types

	AUC Tissue:Blood Ratio				
Tissue	**Subject #1**	**Subject #2**	**Subject #3**	**Subject #4**	**Average**
Brain	0.26	0.22	0.23	0.34	0.26
Liver	0.22	0.088	0.15	0.21	0.17
Lung	2.6	1.6	2.1	2.1	2.1
Heart	0.088	0.036	0.056	0.16	0.085
Kidney	7.0	6.8	8.3	6.6	7.2
Spleen	3.2	2.5	3.4	3.3	3.1
Small intestine	2.7	1.5	1.2	1.9	1.8
Large intestine	2.4	3.8	3.3	2.9	3.1
Stomach	3.0	1.9	2.8	3.3	2.7
Muscle	0.29	0.86	0.12	0.12	0.35
Fat	0.61	0.14	0.26	0.22	0.31
Skin	3.0	2.1	5.8	5.5	4.1

Opioid analytes were not detected in samples from saline control mice at any of the time points studied. Morphine-6-β-D-glucuronide was not detected at quantifiable levels in samples from morphine-treated mice.

For the purpose of better visualizing time course of fentanyl and morphine distribution to scale, average morphine concentrations were normalized to account for the hundred-fold difference in dose between 0.3 mg/kg fentanyl and 30 mg/kg morphine. For comparisons between morphine and its metabolite, morphine-3-β-D-glucuronide, average morphine concentration was calculated from raw data.

Figure 5.2a demonstrates that, in whole blood, normalized morphine concentration was greater than fentanyl at 15 min post-administration ($p<0.0001$), although both opioids exhibited a t_{max} of 15 min. Average fentanyl AUC was 3790 ng/mL*min, while average morphine AUC (with original concentrations) was 1183413 ng/mL*min ($p=0.0019$). Fentanyl was detected at significantly higher concentrations than its metabolite norfentanyl in blood at 5 and 15 min ($p<0.0001$), and significantly exceeded 4-ANPP at 5 ($p<0.0001$), 15 ($p<0.0001$), and 60 min ($p<0.05$) (**Figure 5.2b**). No significant differences were observed between morphine and its metabolite, morphine-3-β-D-glucuronide, at any of the time points studied (**Figure 5.2c)**.

a)

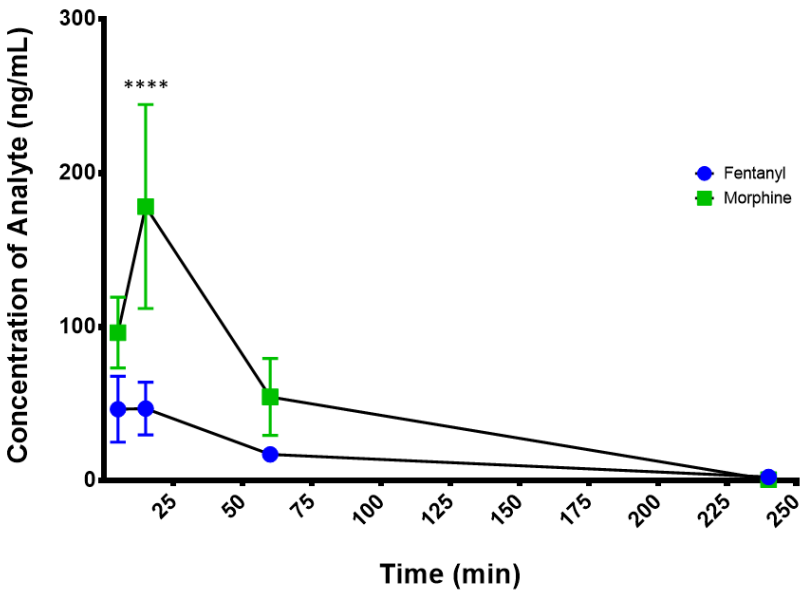

b)

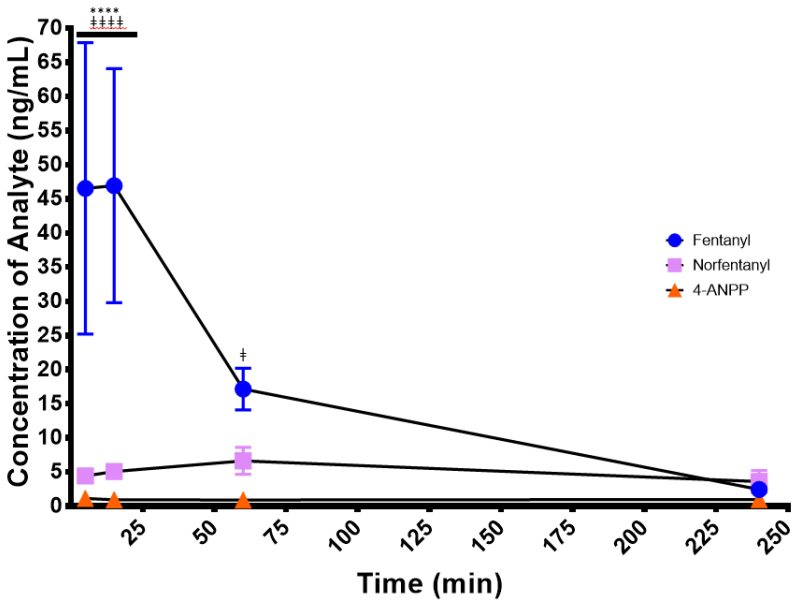

c)

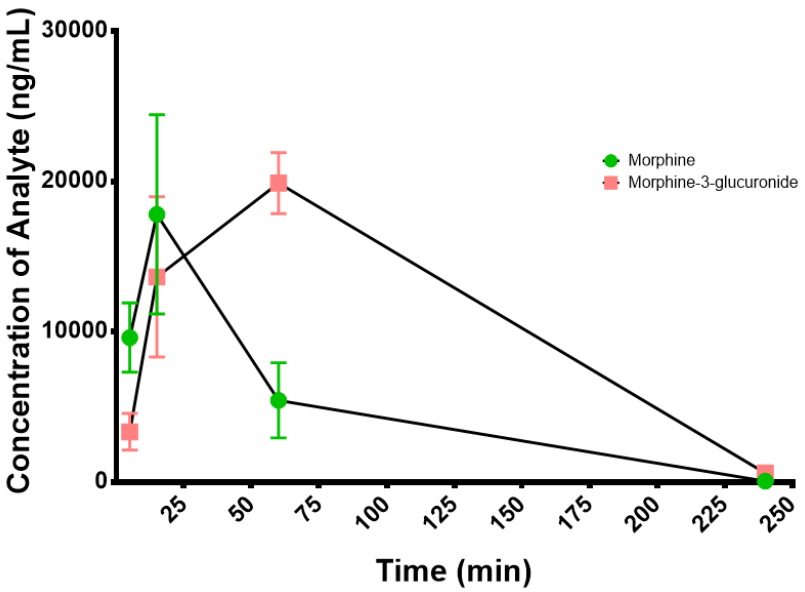

Figure 5.2: Concentration of Fentanyl, Morphine, and Select Metabolites in Whole Blood from 5-240 Min in Mice. a) Average whole blood concentration of fentanyl and morphine in mice injected with either 0.3 mg/kg fentanyl sc or 30 mg/kg morphine sc Morphine averages normalized by hundredfold division to account for difference in dosage. Significant effect of treatment ($P = 0.0046$; $F(1, 6) = 19.36$), significant effect of time ($P<0.0001$; $F(3, 18) = 28.05$), and significant interaction between time and treatment ($P=0.0005$; $F(3, 18) = 9.652$). ****: $p<0.0001$(fentanyl vs morphine). Fentanyl AUC: 3790 ng/mL*min; morphine AUC (original data): 1183413 ng/mL*min ($p=0.0019$)
b) Average concentration of fentanyl and its metabolites, norfentanyl and 4-ANPP, in whole blood. Significant difference in analyte concentration ($P<0.0001$; $F(2, 9) = 43.98$), significant effect of time ($P<0.0001$; $F(3, 27) = 11.29$), and significant interaction of time and analyte concentration ($P<0.0001$; $F(6, 27) = 11.04$). ****: $p<0.0001$ (fentanyl vs norfentanyl); ǂ: $p<0.05$ (fentanyl vs 4-ANPP); ###: $p<0.0001$ (fentanyl vs 4-ANPP)

In brain, fentanyl was detected at higher concentrations than normalized morphine at 5 min ($p<0.0001$) and 15 min ($p<0.0001$) (**Figure 5.3a**). Average fentanyl AUC was 12545 ng/g*min, while average morphine AUC (with original concentrations) was 294964 ng/g*min ($p=0.0001$). Over the time points studied, fentanyl t_{max} = 15 min, while morphine exhibited a t_{max} of 60 min. Fentanyl concentrations in brain were greater than norfentanyl at 5 min ($p<0.0001$), 15 min ($p<0.0001$), and 60 min ($p<0.01$) and greater than 4-ANPP at 5 min ($p<0.0001$), 15 min ($p<0.0001$), and 60 min ($p<0.05$) (**Figure 5.3b**). No significant differences were observed between morphine and morphine-3-β-D-glucuronide in brain at any of the four time points (**Figure 5.3c**).

a)

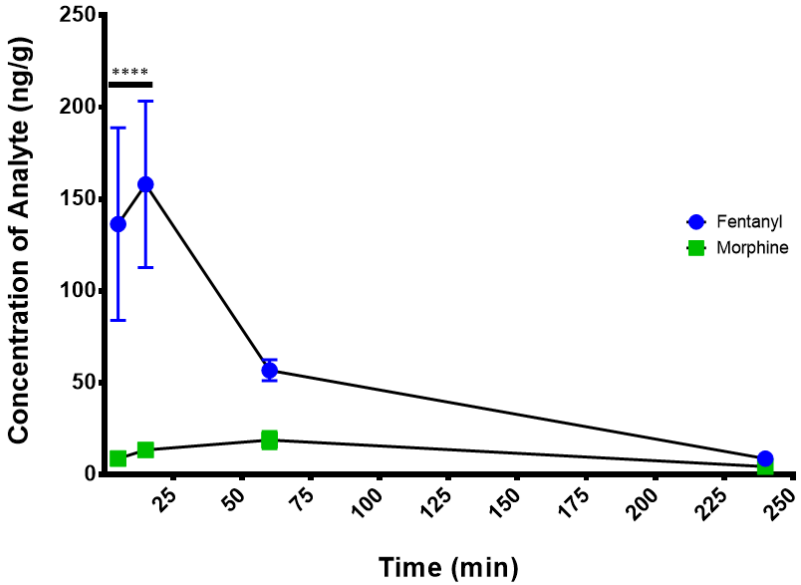

b)

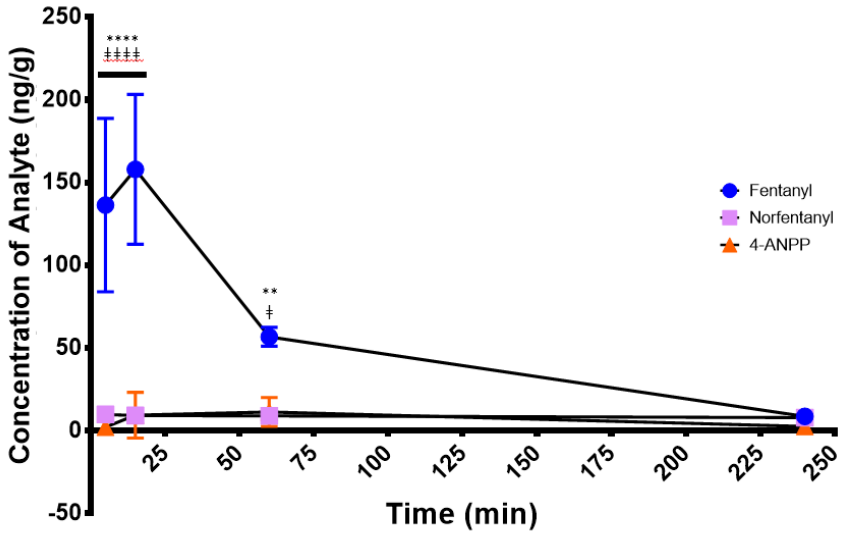

c)

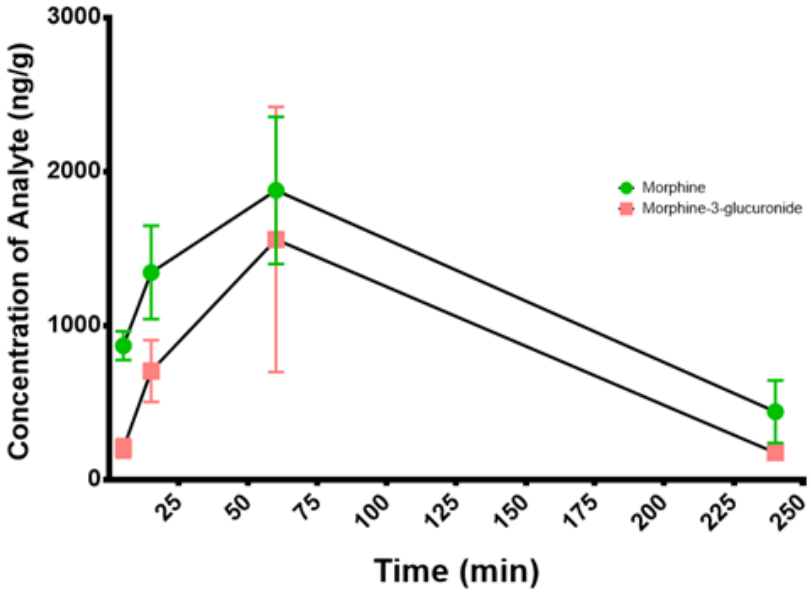

Figure 5.3: Concentration of Fentanyl, Morphine, and Select Metabolites in Whole Brain from 5-240 Min in Mice. a) Average fentanyl and morphine concentration in brain in mice injected with either 0.3 mg/kg fentanyl sc or 30 mg/kg morphine sc. Morphine averages normalized by hundredfold division to account for the difference in dosage. Significant effect of treatment ($P = 0.0001$; $F(1, 6) = 80.64$), significant effect of time ($P<0.0001$; $F(3, 18) = 16.74$), and significant interaction of time and treatment ($P<0.0001$; $F(3, 18) = 15.26$). ****: $p<0.0001$ (fentanyl vs morphine) Fentanyl AUC: 12545 ng/g*min; morphine AUC (original data): 294964 ng/g*min ($p<0.0001$) b) Average concentration of fentanyl and its metabolites, norfentanyl and 4-ANPP, in brain. Significant difference in analyte concentration ($P = 0.0005$; $F(2, 9) = 80.40$), significant effect of time ($P<0.0001$; $F(3, 27) = 16.01$), and significant interaction of time and analyte concentration ($P<0.0001$; $F(6, 27) = 15.09$). **: $p<0.01$ (fentanyl vs norfentanyl); ****:$p<0.0001$ (fentanyl vs norfentanyl); ǂ:$p<0.05$ (fentanyl vs 4-ANPP); ǂǂǂǂ: $p<0.0001$ (fentanyl vs 4-ANPP)

Figure 5.6 cont. c) Average concentration of morphine and its metabolite, morphine-3-β-D-glucuronide, in brain. Significant difference in analyte concentration ($P = 0.0180$; $F(1, 6) = 10.42$ and significant effect of time ($P<0.0001$; $F(3, 18) = 23.00$), but no significant interaction of time and treatment ($P = 0.5934$; $F(3, 18) = 0.6496$). Data expressed as mean ± SD and analyzed by 2-way repeated-measures ANOVA, with Šídák's post hoc for multiple comparisons as needed. n = 4/group

In liver, fentanyl concentration was greater than normalized morphine at 5 min ($p<0.01$) and 15 min ($p<0.05$) (**Figure 5.4a**). Average fentanyl AUC was 1882 ng/g*min, while average morphine AUC (with original concentrations) was 178573 ng/g*min ($p<0.0001$). Both opioids displayed a t_{max} of 15 min. Fentanyl concentration was greater than norfentanyl at 5 min ($p<0.0001$) and 15 min ($p<0.05$), although norfentanyl concentration exceeded fentanyl at 60 min ($p<0.0001$) (Figure 12b). Fentanyl was measured at higher levels than 4-ANPP at 5 min ($p<0.0001$), 15 min ($p<0.0001$), and 60 min ($p<0.01$) (**Figure 5.4b**). Concentration of morphine-3-β-D-glucuronide exceeded morphine at 5 min ($p<0.05$), 15 min ($p<0.0001$), and 60 min ($p<0.0001$) (**Figure 5.4c**).

a)

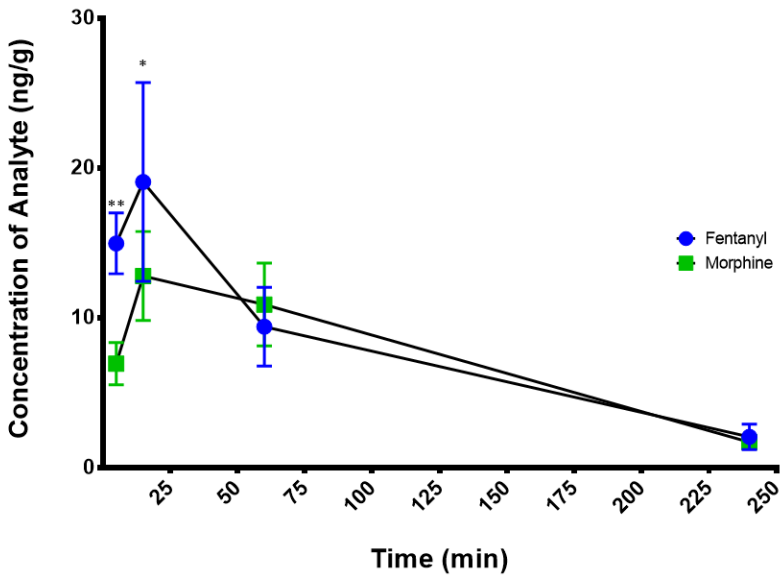

b)

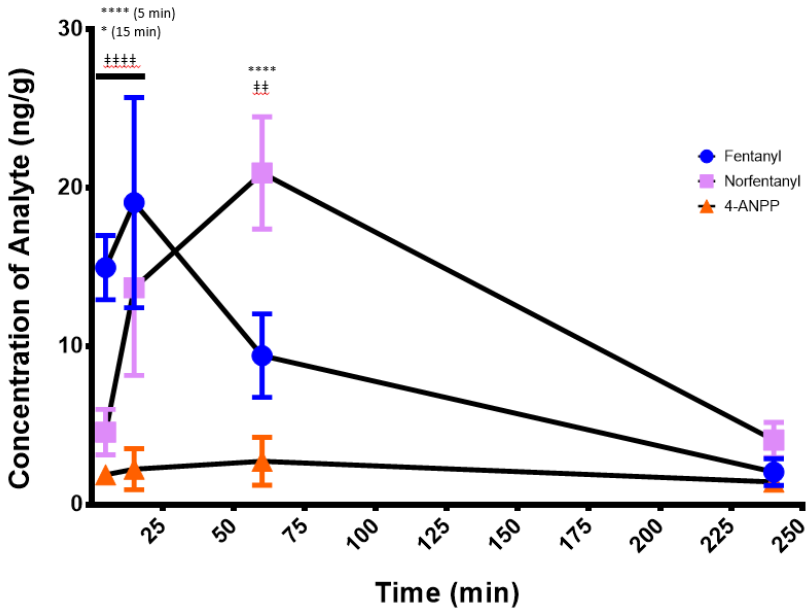

c)

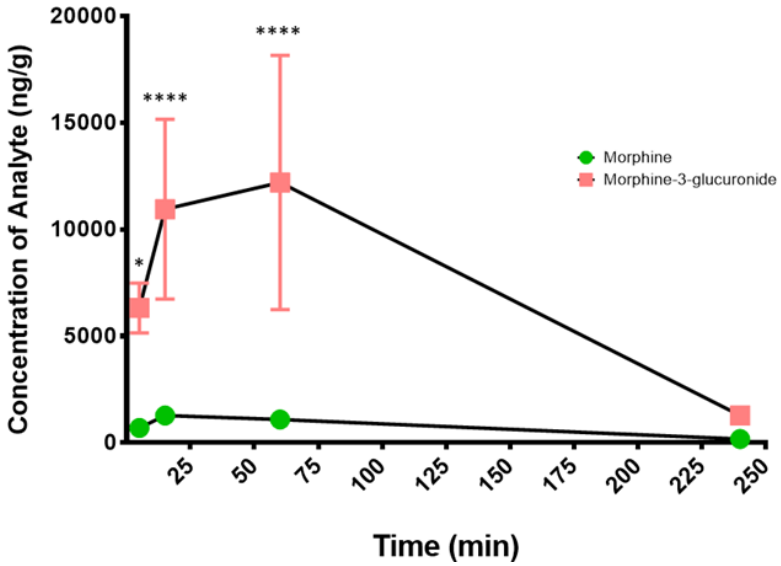

Figure 5.4: Concentration of Fentanyl, Morphine, and Select Metabolites in Liver from 5-240 Min in Mice. a) Average fentanyl and morphine concentration in liver in mice injected with either 0.3 mg/kg fentanyl sc or 30 mg/kg morphine sc. Morphine averages normalized by hundredfold division to account for the difference in dosage. Significant effect of treatment ($P=0.0093$; $F(1, 6) = 14.20$), significant effect of time ($P<0.0001$; $F(3, 18) = 26.21$), and significant interaction of time and treatment ($P=0.0231$; $F(3, 18) = 4.050$). *: $p<0.05$ (fentanyl vs morphine); **: $p<0.01$ (fentanyl vs morphine). fentanyl AUC: 1882 ng/g*min; morphine AUC (original data): 178573 ng/g*min ($p<0.0001$) b) Average concentration of fentanyl and its metabolites, norfentanyl and 4-ANPP, in liver. Significant difference in analyte concentration ($P<0.0001$; $F(2, 9) = 75.85$), significant effect of time ($P<0.0001$; $F(3, 27) = 21.43$), and significant interaction of time and analyte concentration ($P<0.0001$; $F(6, 27) = 13.32$). *:$p<0.05$ (fentanyl vs norfentanyl); ****:$p<0.0001$ (fentanyl vs norfentanyl); ++: $p<0.01$ (fentanyl vs 4-ANPP); +++:$p<0.0001$ (fentanyl vs norfentanyl).

Figure 5.4 cont.: c) Average concentration of morphine and its metabolite, morphine-3-β-D-glucuronide, in liver. Significant difference in analyte concentration ($P<0.001$; $F(1, 6) = 64.17$), significant effect of time ($P = 0.0012$; $F(3, 18) = 8.233$), and significant interaction of time and analyte concentration ($P = 0.0067$; $F(3, 18) = 5.620$). *:$p<0.05$ (morphine vs morphine-3-β-D-glucuronide); ****: $p<0.0001$ (morphine vs morphine-3-β-D-glucuronide). Data expressed as mean ± SD and analyzed by 2-way repeated-measures ANOVA, with Šídák's post hoc for multiple comparisons as needed. n = 4/group

No significant differences were observed between fentanyl and normalized morphine in lung at any of the four time points studied (**Figure 5.5a**). However, average fentanyl AUC was 33028 ng/g*min, while average morphine AUC (with original concentrations) was 2392610 ng/g*min ($p=0.0002$). Fentanyl and morphine both exhibited a t_{max} of 15 min. Due to a lack of 4-ANPP data at 5 and 240 min, statistical analysis was unable to be performed on potential differences between fentanyl and its metabolites, although detected quantities of fentanyl appear noticeably higher than norfentanyl and 4-ANPP at all available time points (**Figure 5.5b**). Concentration of morphine was significantly greater than morphine-3-β-D-glucuronide at 15 min ($p<0.0001$) (**Figure 5.5c**).

a)

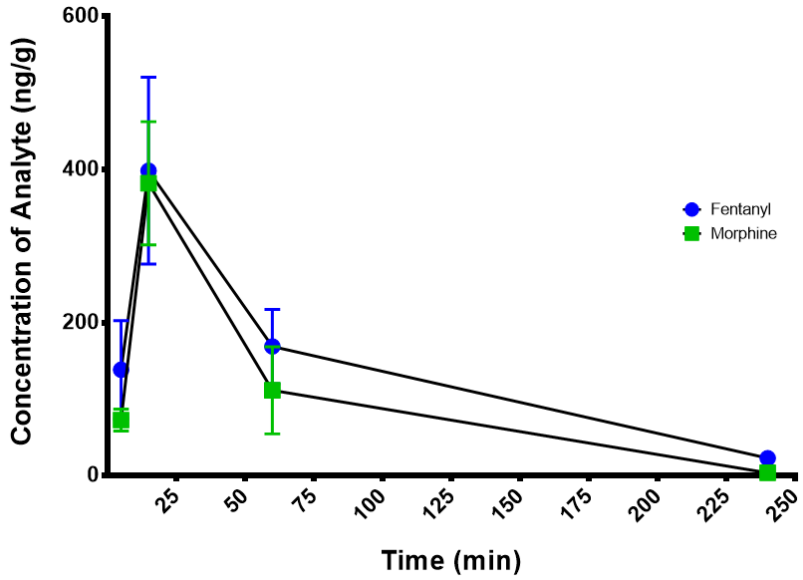

b)

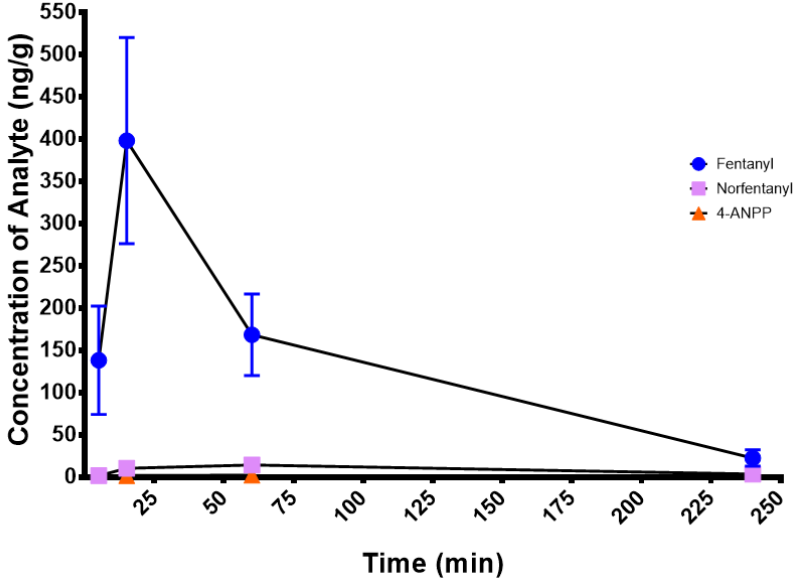

c)

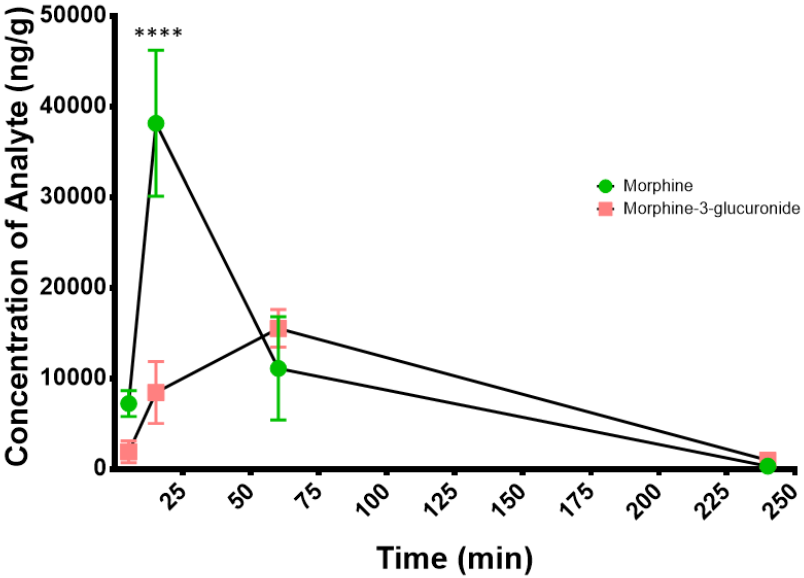

Figure 5.5: Concentration of Fentanyl, Morphine, and Select Metabolites in Lung from 5-240 Min in Mice.
a) Average concentration of fentanyl and morphine in lung in mice injected with either 0.3 mg/kg fentanyl sc or 30 mg/kg morphine sc. Morphine averages normalized by hundredfold division to account for the difference in dosage. Significant effect of treatment ($P=0.0280$; $F(1, 6) = 8.307$) and significant effect of time ($P<0.0001$; $F(3, 18) = 43.97$), but no significant interaction of time and treatment ($P = 0.8429$; $F(3, 18) = 0.2747$). Fentanyl AUC: 33028 ng/g*min; morphine AUC (original data): 2392610 ng/g*min ($p=0.0002$) b) Average concentration of fentanyl and its metabolites, norfentanyl and 4-ANPP, in lung. c) Average concentration of morphine and its metabolite, morphine-3-β-D-glucuronide, in lung. Significant difference in analyte concentration ($P = 0.0004$; $F(1, 6) = 48.05$), significant effect of time ($P<0.0001$; $F(3, 18) = 49.64$), and significant interaction of time and analyte concentration ($P<0.0001$; $F(3, 18) = 28.79$). ****: $p<0.0001$ (morphine vs morphine-3-β-D-glucuronide). Data expressed as mean ± SD and analyzed by 2-way repeated-measures ANOVA, with Šídák's post hoc for multiple comparisons as needed. n = 4/group

In heart, fentanyl was measured at significantly higher concentrations than normalized morphine at 5 min ($p<0.0001$), 15 min ($p<0.0001$), and 60 min ($p<0.05$) (**Figure 5.6a**). Average fentanyl AUC was 18806 ng/g*min, while average morphine AUC (with original concentrations) was 85531 ng/g*min ($p=0.0038$). Fentanyl exhibited a t_{max} of 15 min, while morphine displayed a t_{max} of 5 min. Due to a lack of 4-ANPP data at 60 min and 240 min, statistical analysis was unable to be performed on potential differences between fentanyl and its metabolites; however, detected quantities of fentanyl appear noticeably higher than norfentanyl at 5 min, 15 min, and 60 min, and higher than 4-ANPP at 5 and 15 min (**Figure 5.6b**). Morphine levels were significantly lower than morphine-3-β-D-glucuronide at 60 min ($p<0.0001$) (**Figure 5.6c**).

a)

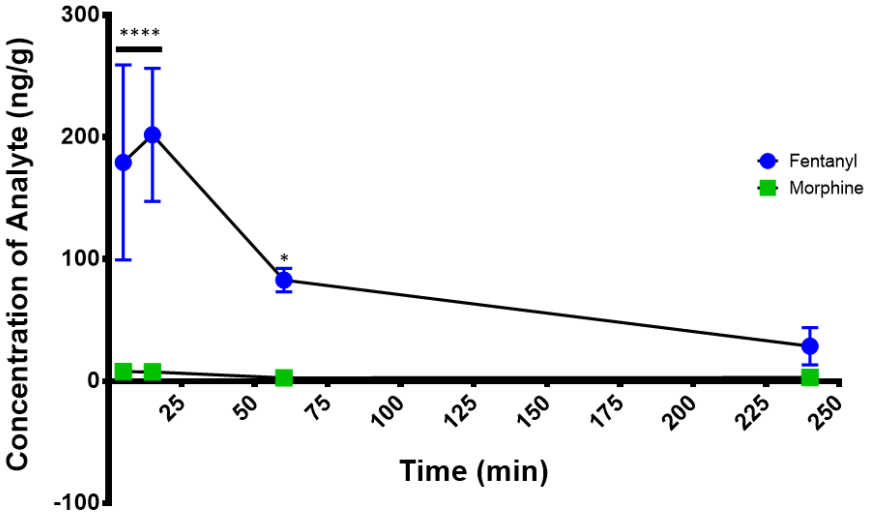

b)

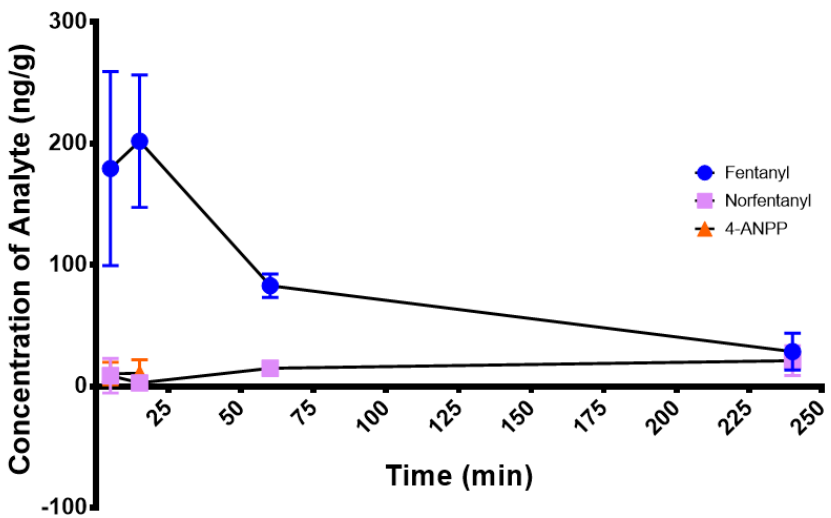

c)

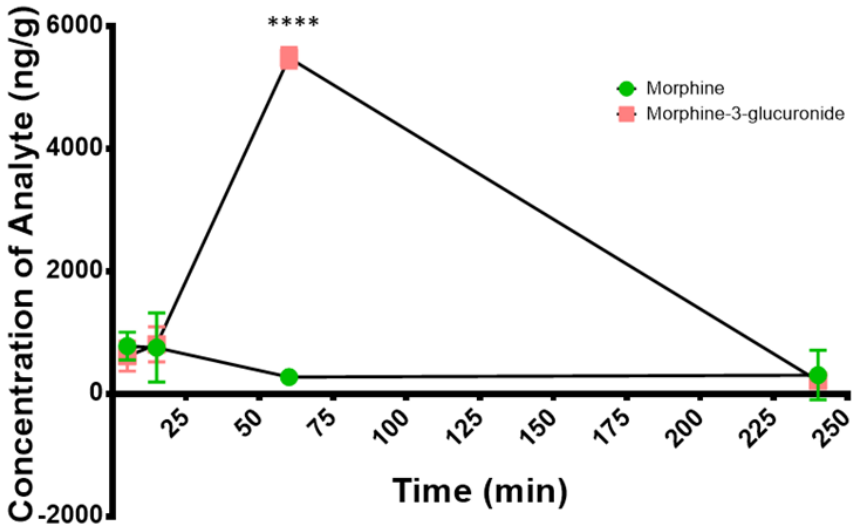

Figure 5.6: Concentration of Fentanyl, Morphine, and Select Metabolites in Heart from 5-240 Min in Mice. a) Average concentration of fentanyl and morphine in heart in mice injected with either 0.3 mg/kg fentanyl sc or 30 mg/kg morphine sc. Morphine averages normalized by hundredfold division to account for the difference in dosage. Significant effect of treatment ($P<0.0001$; $F(1, 6) = 401.3$), significant effect of time ($P = 0.0006$; $F(3, 18) = 9.222$), significant interaction of time and treatment ($P = 0.0012$; $F(3, 18) = 8.125$). *: $p<0.05$ (fentanyl vs morphine), ****: $p<0.0001$ (fentanyl vs morphine). Fentanyl AUC: 18806 ng/g*min; morphine AUC (original data): 85531 ng/g*min ($p=0.1283$) b) Average concentration of fentanyl and its metabolites, norfentanyl and 4-ANPP, in heart. c) Average concentration of morphine and its metabolite, morphine-3-β-D-glucuronide, in heart. Significant difference in analyte concentration ($P<0.0001$; $F(1, 6) = 153.9$), significant effect of time ($P<0.0001$; $F(3, 18) = 118.7$), and significant interaction of time and treatment ($P<0.0001$; $F(3, 18) = 150.6$). ****: $p<0.0001$ (morphine vs morphine-3-β-D-glucuronide) Data expressed as mean ± SD and analyzed by 2-way repeated-measures ANOVA, with Šídák's post hoc for multiple comparisons as needed. n = 4/group

Repeated-measures ANOVA revealed no significant differences between fentanyl and normalized morphine in kidney at any of the time points studied. (**Figure 5.7a**). Average fentanyl AUC was 51484 ng/g*min, while average morphine AUC (with original concentrations) was 8503320 ng/g*min ($p=0.0018$). Fentanyl exhibited a t_{max} of 15 min, while morphine exhibited a t_{max} of 60 min. Fentanyl was measured at significantly higher levels than its metabolites norfentanyl and 4-ANPP at 5 min ($p<0.0001$, 15 min ($p<0.0001$), and 60 min ($p<0.0001$) (**Figure 5.7b**). Repeated-measures ANOVA revealed no significant differences between morphine and morphine-3-β-D-glucuronide concentration at any time point (**Figure 5.7c**).

a)

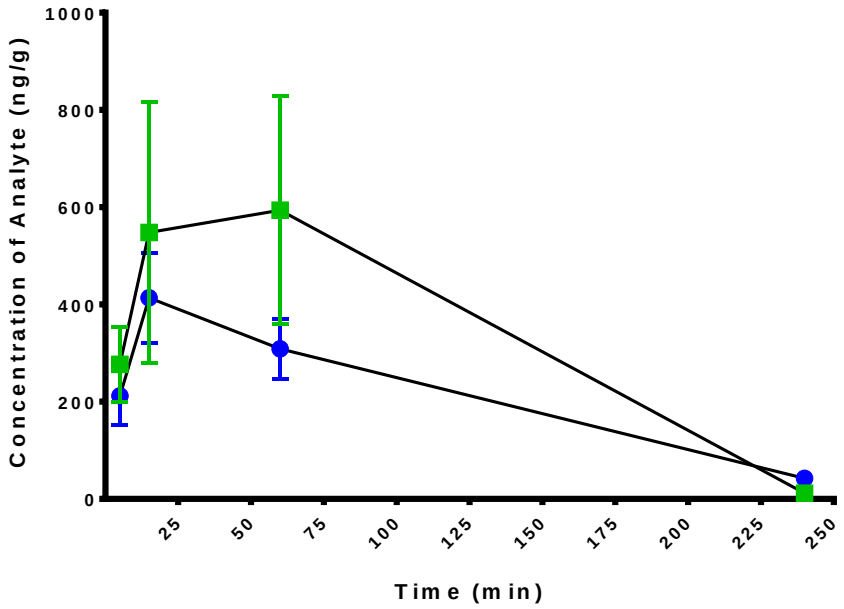

b)

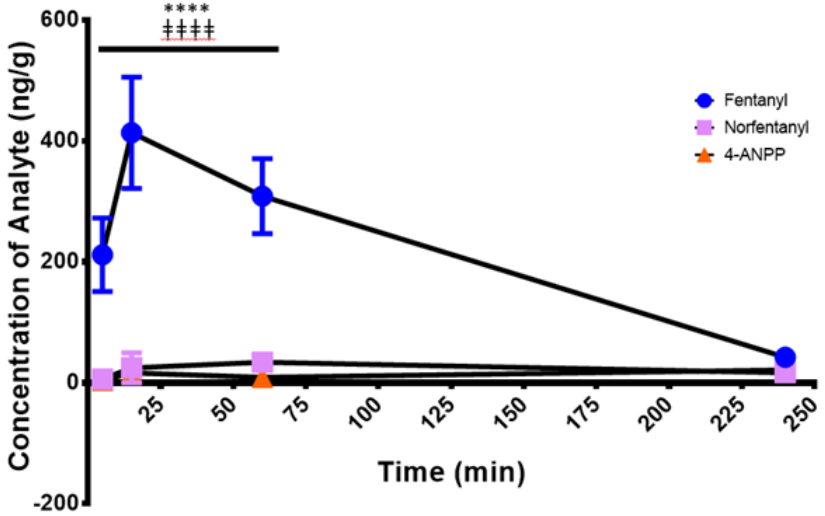

c)

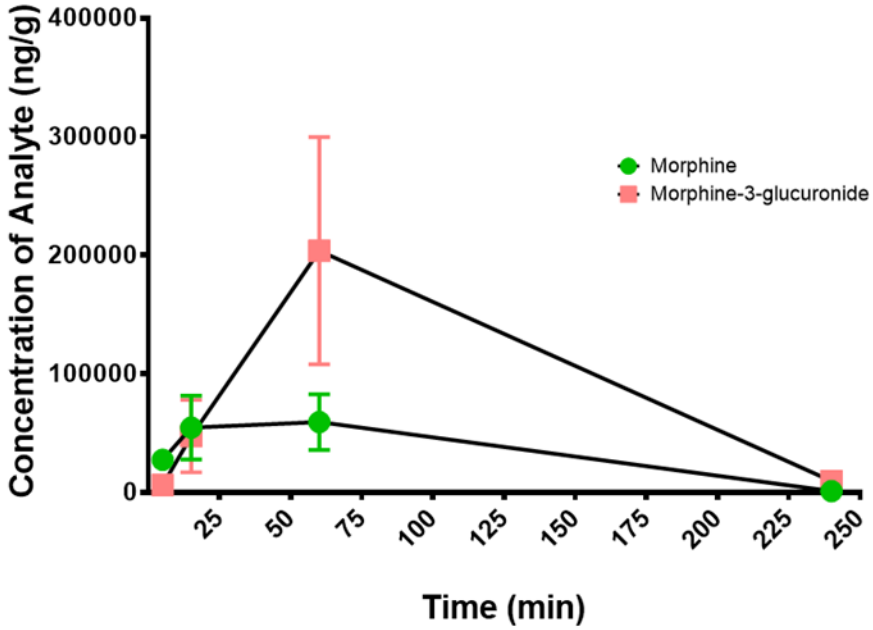

Figure 5.7: Concentration of Fentanyl, Morphine, and Select Metabolites in Kidney from 5-240 Min in Mice. a) Average concentration of fentanyl and morphine in kidney in mice injected with either 0.3 mg/kg fentanyl sc or 30 mg/kg morphine sc. Morphine averages normalized by hundredfold division to account for the difference in dosage. No significant effect of treatment ($P = 0.1153$; $F(1, 6) = 3.388$) or significant interaction of time and treatment ($P = 0.1005$; $F(3, 18) = 2.411$), but significant effect of time ($P<0.0001$; $F(3, 18) = 24.21$). Fentanyl AUC: 51484 ng/g*min; morphine AUC (original data): 8503320 ng/g*min ($p=0.0018$) b) Average concentration of fentanyl and its metabolites, norfentanyl and 4-ANPP, in kidney. Significant difference in analyte concentration ($P<0.0001$; $F(2, 9) = 344.6$), significant effect of time ($P<0.0001$; $F(3, 27) = 20.92$), and significant interaction of time and analyte concentration ($P<0.0001$; $F(6, 27) = 19.45$). ****: $p<0.0001$ (fentanyl vs norfentanyl); ####: $p<0.0001$ (fentanyl vs 4-ANPP) c) Average concentration of morphine and its metabolite, morphine-3-β-D-glcuronide, in kidney. No significant difference in analyte concentration ($P = 0.0627$; $F(1, 6) = 5.204$), but significant effect of time ($P<0.0001$; $F(3, 18) = 18.34$) and significant interaction of time and analyte concentration ($P<0.01$; $F(3, 18) = 8.284$). Data expressed as mean ± SD and analyzed by 2-way repeated-measures ANOVA, with Šídák's post hoc for multiple comparisons as needed. n = 4/group

In spleen, repeated-measures ANOVA revealed no significant differences between fentanyl and normalized morphine at any timepoint (**Figure 5.8a**). However, average fentanyl AUC was 39463 ng/g*min, while average morphine AUC (with original concentrations) was 3556074 ng/g*min ($p=0.0002$). Fentanyl exhibited a t_{max} of 60 min, while morphine's t_{max} occurred at 15 min. Due to a lack of norfentanyl data at 5 and 240 min, statistical analysis could not be performed to compare fentanyl and norfentanyl concentrations, but fentanyl levels appear to be higher relative to norfentanyl at 15 min and 60 min (**Figure 5.8b**). No 4-ANPP was detected at any time point. Due to a lack of morphine-3-β-D-glucuronide data at 240 min, statistical analysis comparing morphine and morphine-3-β-D-glucuronide levels could not be performed. However, morphine concentration appears noticeably greater than morphine-3-β-D-glucuronide at 5 min, 15 min, and 60 min (**Figure 5.8c**).

a)

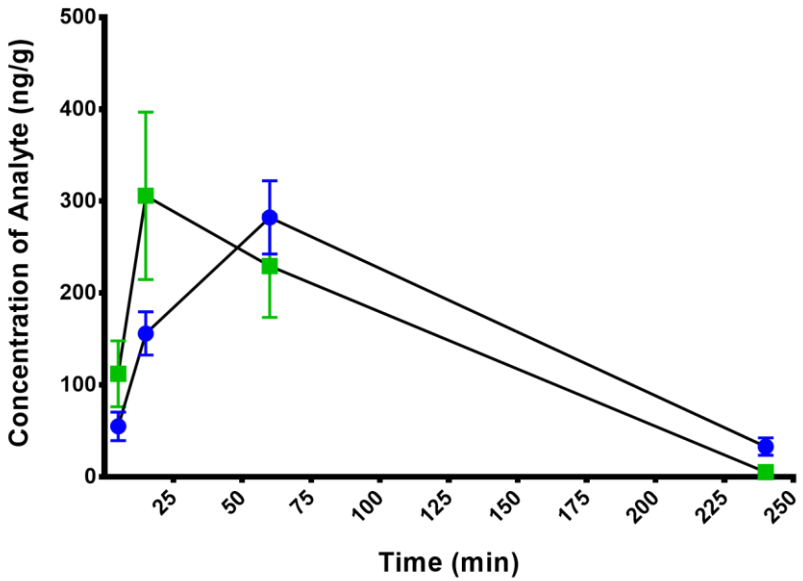

b)

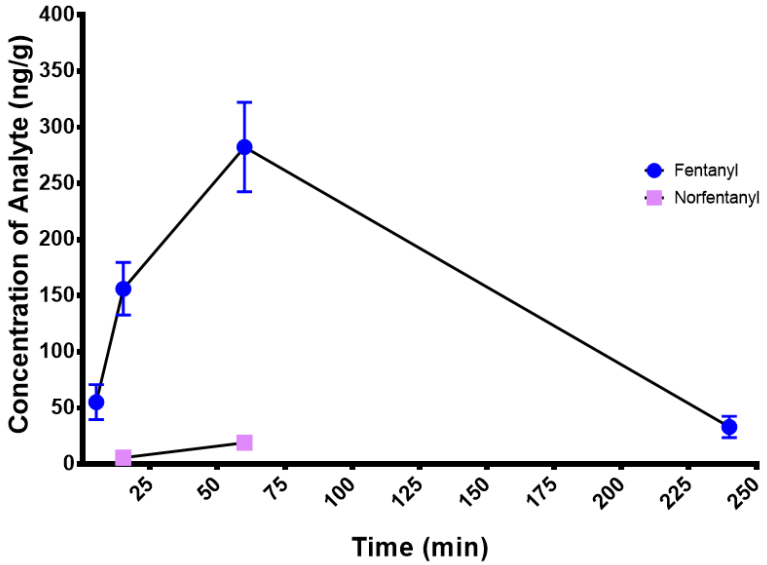

c)

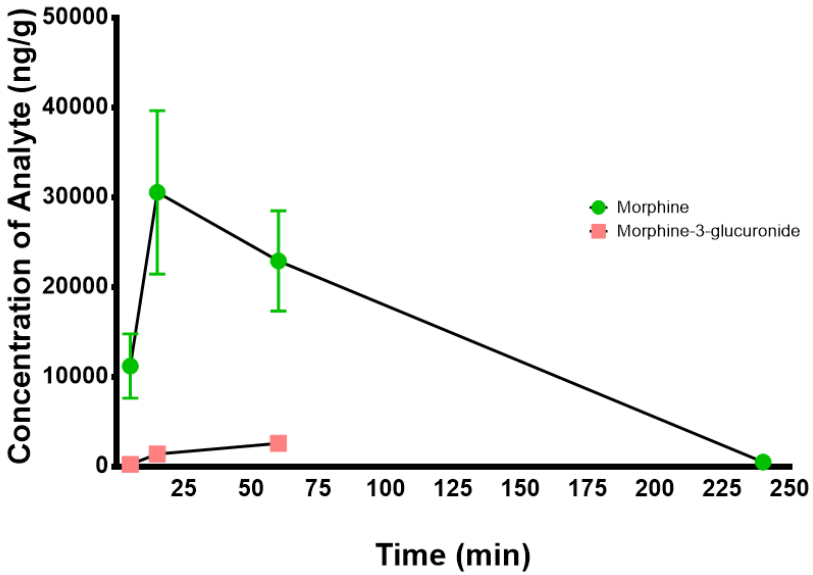

Figure 5.8: Concentration of Fentanyl, Morphine, and Select Metabolites in Spleen from 5-240 Min in Mice. a) Average concentration of fentanyl and morphine in spleen in mice injected with either 0.3 mg/kg fentanyl sc or 30 mg/kg morphine sc. Morphine averages normalized by hundredfold division to account for the difference in dosage. No significant effect of treatment ($P = 0.1814$; $F(1, 6) = 2.285$), but significant effect of time ($P<0.0001$; $F(3, 18) = 76.57$) and significant interaction of time and treatment ($P=0.0001$; $F(3, 18) = 12.32$). Fentanyl AUC: 39463 ng/g*min; morphine AUC (original data): 3556074 ng/g*min ($p=0.0002$) b) Average concentration of fentanyl and its metabolite, norfentanyl, in spleen. c) Average concentration of morphine and its metabolite, morphine-3-β-D-glucuronide, in spleen. Data expressed as mean ± SD and analyzed by 2-way repeated-measures ANOVA, with Šídák's post hoc as needed. n = 4/group

There were no significant differences between fentanyl and normalized morphine concentrations in small intestine (**Figure 5.9a**). However, average fentanyl AUC was 15115 ng/g*min, while average morphine AUC (with original concentrations) was 2064465 ng/g*min ($p=0.0010$). For both opioids, t_{max} occurred at 60 min. Due to the lack of norfentanyl data at 5 min, 15 min, and 240 min, statistical analysis comparing fentanyl and norfentanyl concentrations could not be performed, but fentanyl appears greater than norfentanyl at 60 min (**Figure 5.9b**). No 4-ANPP was detected at any time point. Repeated-measures ANOVA revealed no significant differences between morphine and morphine-3-β-D-glucuronide at any time point (**Figure 5.9c**).

a)

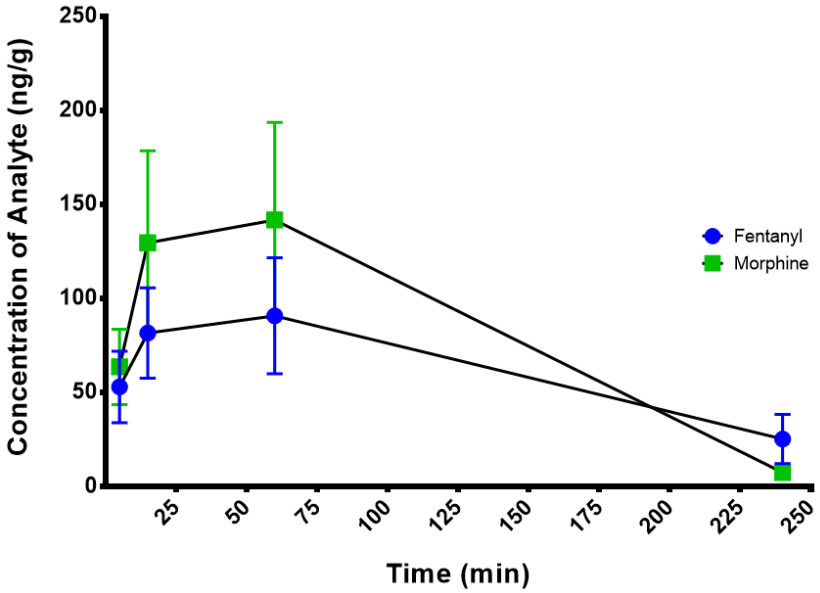

b)

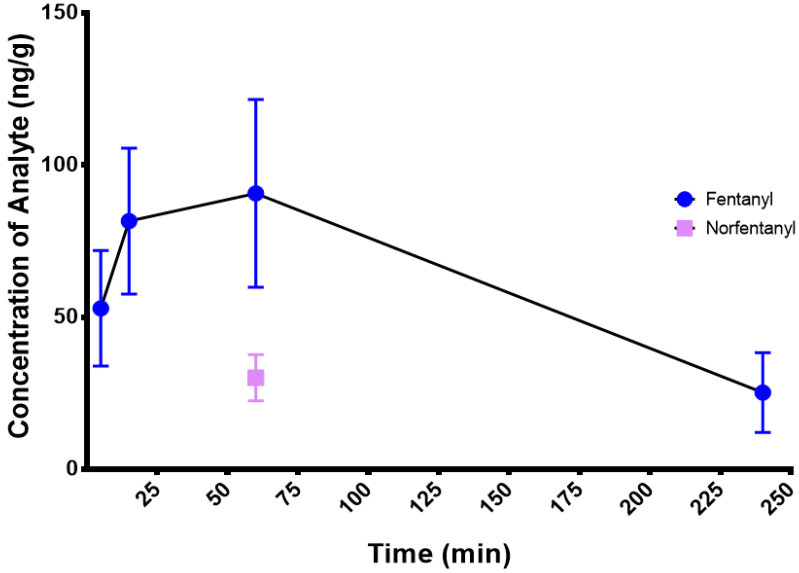

c)

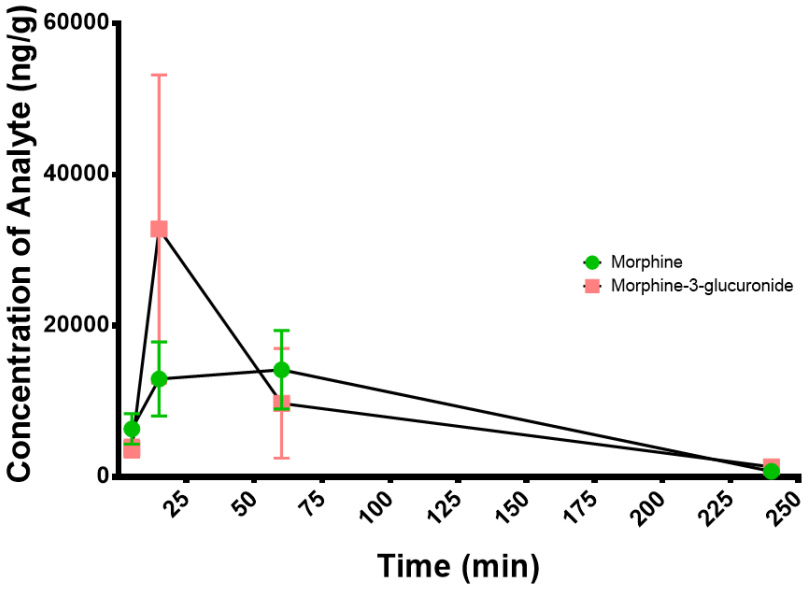

Figure 5.9: Concentration of Fentanyl, Morphine, and Select Metabolites in Small Intestine from 5-240 Min in Mice. a) Average concentration of fentanyl and morphine in small intestine mice injected with either 0.3 mg/kg fentanyl sc or 30 mg/kg morphine sc. Morphine averages normalized by hundredfold division to account for the difference in dosage. No significant effect of treatment ($P = 0.1261$; $F(1, 6) = 3.154$) or significant interaction of time and treatment ($P = 0.0805$; $F(3, 18) = 2.644$), but significant effect of time ($P<0.0001$; $F(3, 18) = 20.81$). Fentanyl AUC: 15115 ng/g*min; morphine AUC (original data): 2064465 ng/g*min ($p=0.0010$) b) Average concentration of fentanyl and its metabolites, norfentanyl, in small intestine. c) Average concentration of morphine and its metabolite, morphine-3-β-D-glucuronide, in small intestine. No significant difference in analyte concentration ($P = 0.3344$; $F(1, 6) = 1.101$), but significant effect of time ($P = 0.0001$; $F(3, 18) = 12.13$) and significant interaction between time and analyte concentration ($P = 0.0212$; $F(3, 18) = 4.151$). Data expressed as mean ± SD and analyzed by 2-way repeated-measures ANOVA, with Šídák's post hoc for multiple comparisons as needed. n = 4/group

No significant difference was found between fentanyl and normalized morphine concentration in large intestine (**Figure 5.10a**). Average fentanyl AUC was 13798 ng/g*min, while average morphine AUC (with original concentrations) was 3842585 ng/g*min (p=0.0114). Fentanyl exhibited a t_{max} of 60 min, while morphine displayed a t_{max} of 240 min. Due to a lack of norfentanyl data at 5, 15, and 60 min, statistical analysis could not be performed to compare fentanyl and norfentanyl concentrations, but norfentanyl concentration appears slightly higher relative to fentanyl (**Figure 5.10b**). No 4-ANPP was detected at any time point. No morphine-3-β-D-glucuronide was detected at any time point.

a)

b)

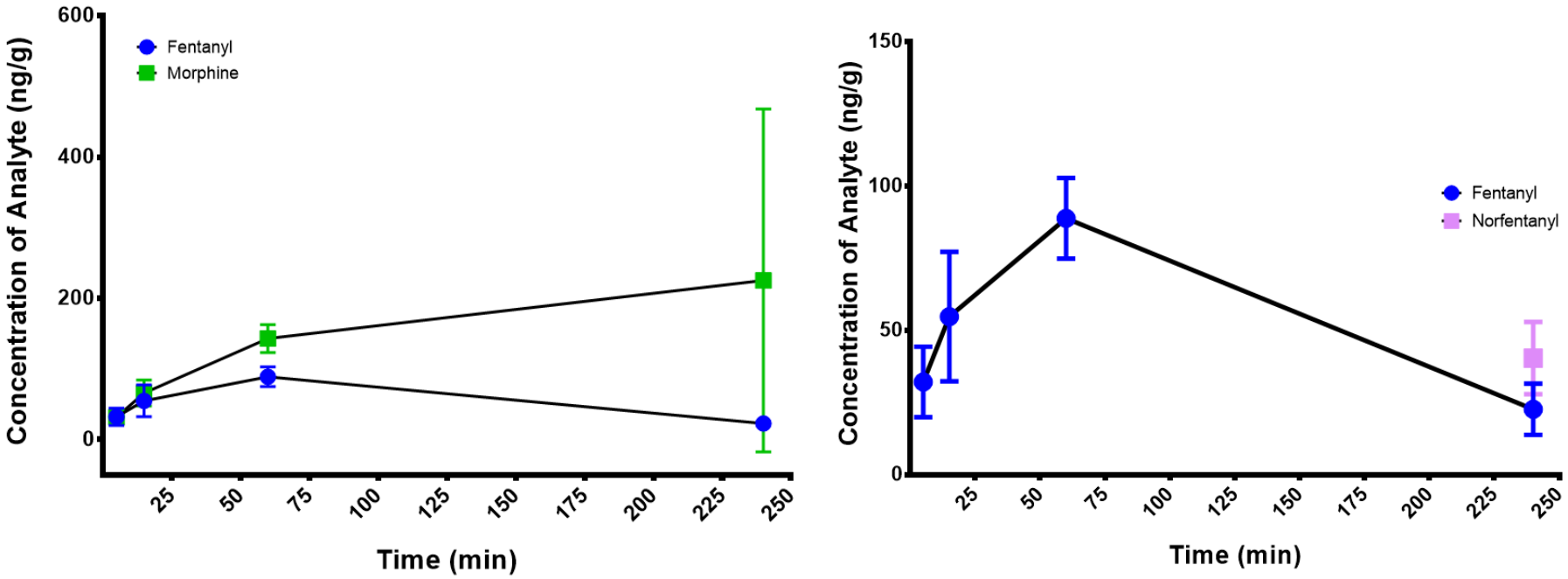

Figure 5.10: Concentration of Fentanyl, Morphine, and Select Metabolites in Large Intestine from 5-240 Min in Mice. a) Average concentration of fentanyl and morphine in large intestine in mice injected with either 0.3 mg/kg fentanyl sc or 30 mg/kg morphine sc. Morphine averages normalized by hundredfold division to account for the difference in dosage. No significant effect of treatment ($P = 0.0729$; $F(1, 6) = 4.717$), effect of time ($P = 0.1400$; $F(3, 18) = 2.071$), or interaction of time and treatment ($P = 0.1113$; $F(3, 18) = 2.305$). Fentanyl AUC: 13798 ng/g*min; morphine AUC (original data): 3842585 ng/g*min ($p=0.0114$) b) Average concentration of fentanyl and its metabolite, norfentanyl, in large intestine. Data expressed as mean ± SD and analyzed by 2-way repeated-measures ANOVA, with Šídák's post hoc for multiple comparisons as needed. n = 4/group

In stomach, normalized morphine concentration exceeded fentanyl at 15 min ($p<0.001$) and at 60 min ($p<0.0001$) (**Figure 5.11a**). However, average fentanyl AUC was 19369 ng/g*min, while average morphine AUC (with original concentrations) was 3040544 ng/g*min ($p<0.0001$). Both opioids displayed a t_{max} of 60 min. Due to a lack of norfentanyl data at 5, 15, and 240 minutes, statistical analysis comparing fentanyl and norfentanyl concentrations could not be performed, but fentanyl levels appear higher at 60 min (**Figure 5.11b**). No 4-ANPP was detected at any time point. Morphine was detected at greater quantities than morphine-3-β-D-glucuronide at 15 min ($p<0.0001$) and 60 min ($p<0.0001$) (**Figure 5.11c**).

a)

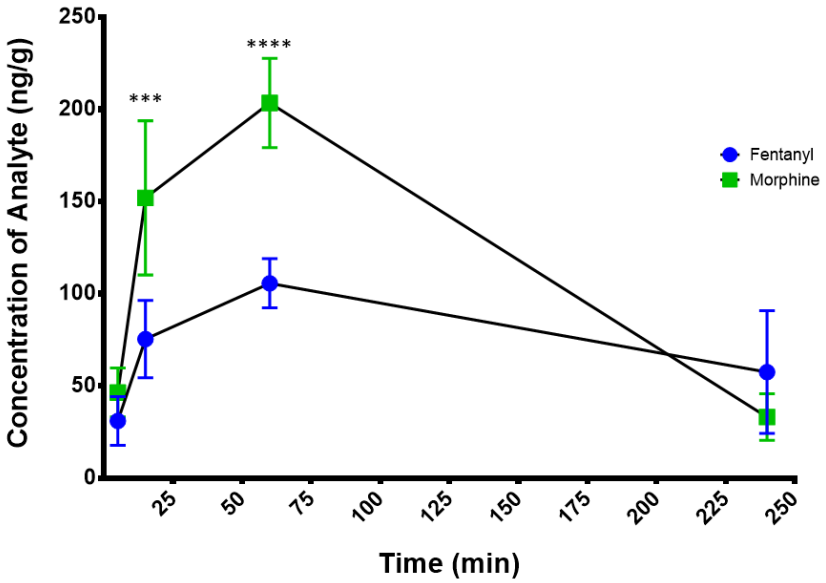

b)

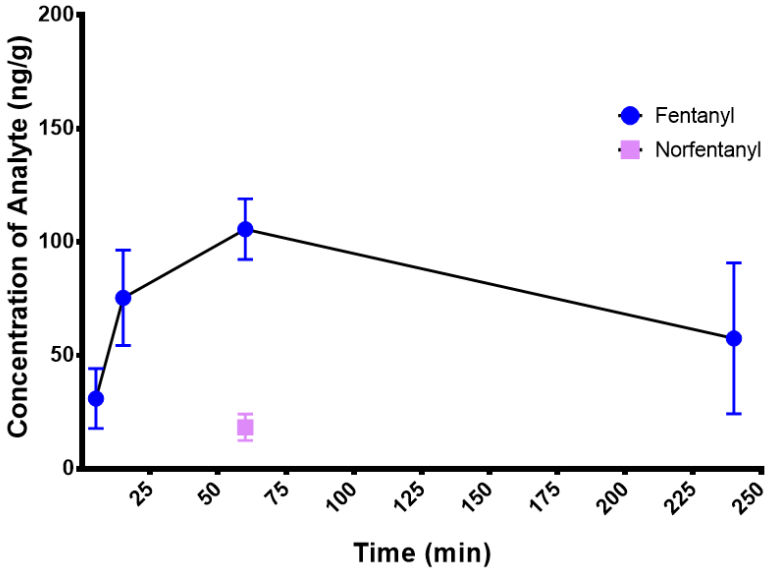

c)

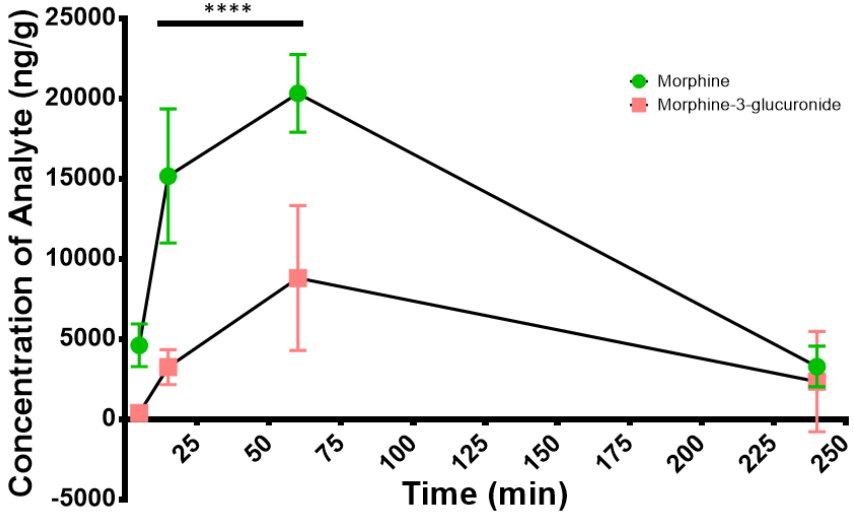

Figure 5.11: Concentration of Fentanyl, Morphine, and Select Metabolites in Stomach from 5-240 Min in Mice. a) Average concentration of fentanyl and morphine in stomach in mice injected with either 0.3 mg/kg fentanyl sc or 30 mg/kg morphine sc. Morphine averages normalized by hundredfold division to account for the difference in dosage. Significant effect of treatment ($P = 0.0059$; $F(1, 6) = 17.33$), significant effect of time ($P<0.0001$; $F(3, 18) = 49.87$), and significant interaction of time and treatment ($P = 0.0001$; $F(3, 18) = 12.58$). ***: $p<0.001$ (fentanyl vs morphine); ****: $p<0.0001$ (fentanyl vs morphine). Fentanyl AUC: 19369 ng/g*min; morphine AUC (original data): 3040544 ng/g*min ($p<0.0001$) b) Average concentration of fentanyl and its metabolite, norfentanyl, in stomach. c) Average concentration of morphine and its metabolite, morphine-3-β-D-glucuronide, in stomach. Significant difference in analyte concentration ($P=0.0004$; $F(1, 6) = 48.91$), significant effect of time ($P<0.0001$; $F(3, 18) = 38.40$), and significant interaction of time and analyte concentration ($P=0.0009$; $F(3, 18) = 8.576$). ****:$p<0.0001$ (morphine vs morphine-3-β-D-glucuronide). Data expressed as mean ± SD and analyzed by 2-way repeated-measures ANOVA, with Šídák's post hoc for multiple comparisons as needed. n = 4/group

Statistical analysis comparing fentanyl and morphine in muscle could not be performed due to lack of morphine data at 5 min and 240 min, but fentanyl concentration appears higher at 15 min, while normalized morphine concentration appears higher at 60 min (**Figure 5.12a**). Average fentanyl AUC was 1467 ng/g*min, while average morphine AUC (with original concentrations) was 519773 ng/g*min (p=0.1903). Fentanyl displayed a t_{max} of 15 min, while morphine exhibited a t_{max} of 60 min. Due to a lack of norfentanyl data at 5 min, 15 min, and 240 min, statistical analysis comparing fentanyl and norfentanyl could not be performed, but norfentanyl concentration appears higher at 60 min (**Figure 5.12b**). No 4-ANPP was detected at any timepoint. Due to the aforementioned lack of morphine data at 5 min and 240 min, statistical analysis comparing levels of morphine and morphine-3-β-D-glucuronide could not be performed, but measured concentrations appear similar at time points for which data was available (**Figure 5.12c**).

a)

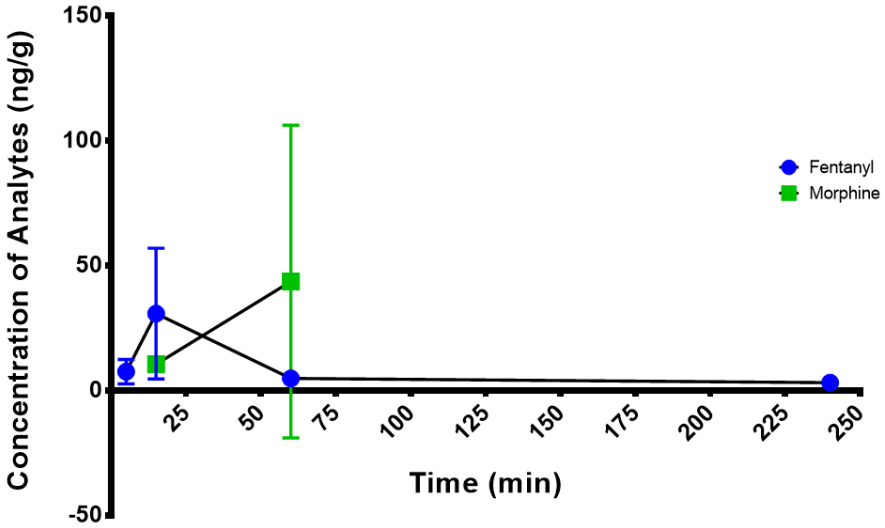

c)

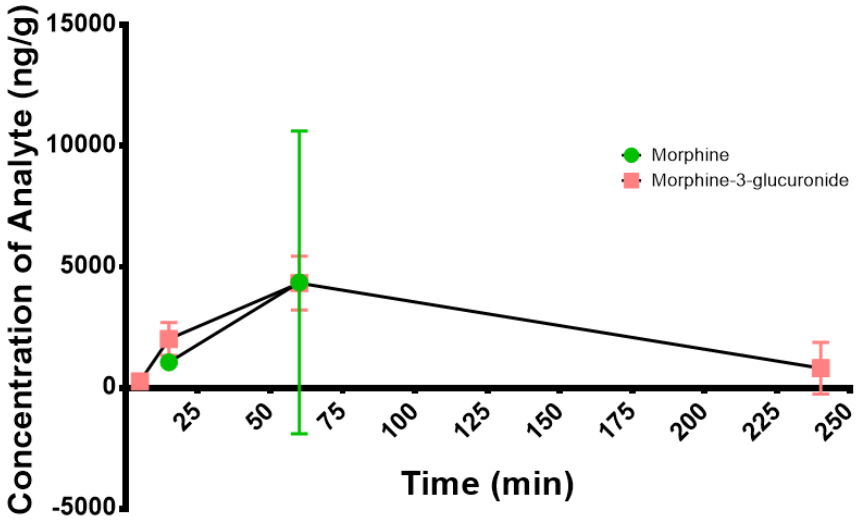

b)

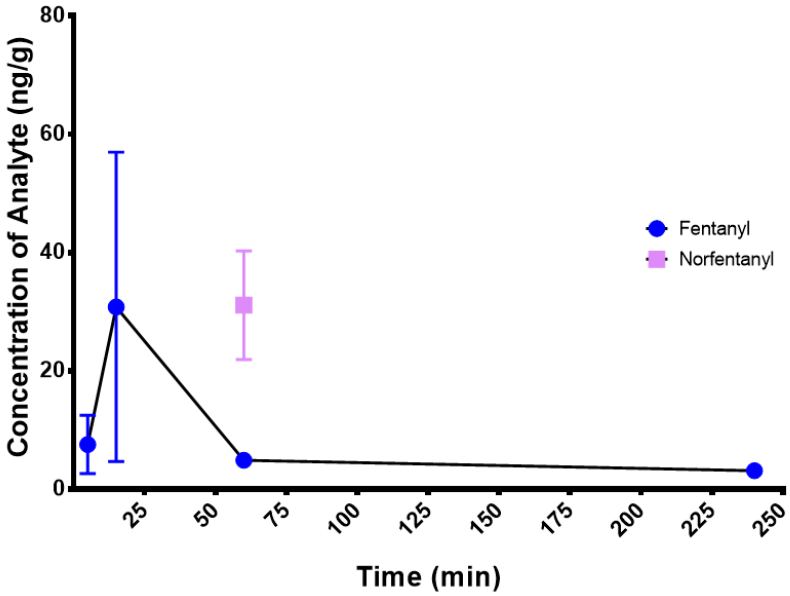

Figure 5.12: Concentration of Fentanyl, Morphine, and Select Metabolites in Muscle from 5-240 Min in Mice. a) Average concentration of fentanyl and morphine in muscle in mice injected with either 0.3 mg/kg fentanyl sc or 30 mg/kg morphine sc. Morphine averages normalized by hundredfold division to account for the difference in dosage. Fentanyl AUC: 1467 ng/g*min ; morphine AUC (original data): 93818 ng/g*min (p=0.1903) b) Average concentration of fentanyl and its metabolite, norfentanyl, in muscle. c) Average concentration of morphine and its metabolite, morphine-3-β-D-glucuronide, in muscle. Data expressed as mean ± SD and analyzed by 2-way repeated-measures ANOVA, with Šídák's post hoc for multiple comparisons as needed. n = 4/group

Fentanyl concentration in fat exceeded normalized morphine concentration at 15 min ($p<0.05$), 60 min ($p<0.0001$), and 240 min ($p<0.0001$) (**Figure 5.13a**). Average fentanyl AUC was 28097 ng/g*min, while average morphine AUC (with original concentrations) was 328093 ng/g*min ($p=0.0159$). Both opioids exhibited a t_{max} of 60 min. Due to a lack of norfentanyl data at 5 min and 15 min, statistical comparisons of fentanyl and norfentanyl levels could not be performed. However, fentanyl concentration appeared higher at 60 min and 240 min relative to its metabolite (**Figure 5.13b**). 4-ANPP was not detected at any time point. No significant differences were observed between morphine and morphine-3-β-D-glucuronide at any time point (**Figure 5.13c**).

a)

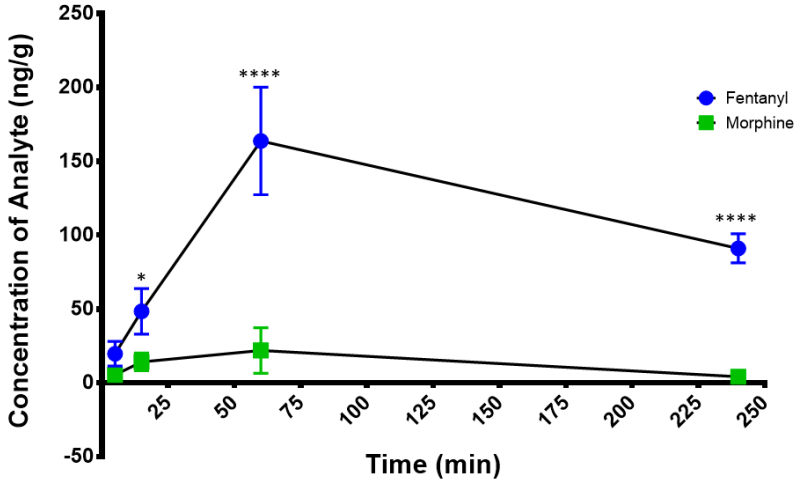

b)

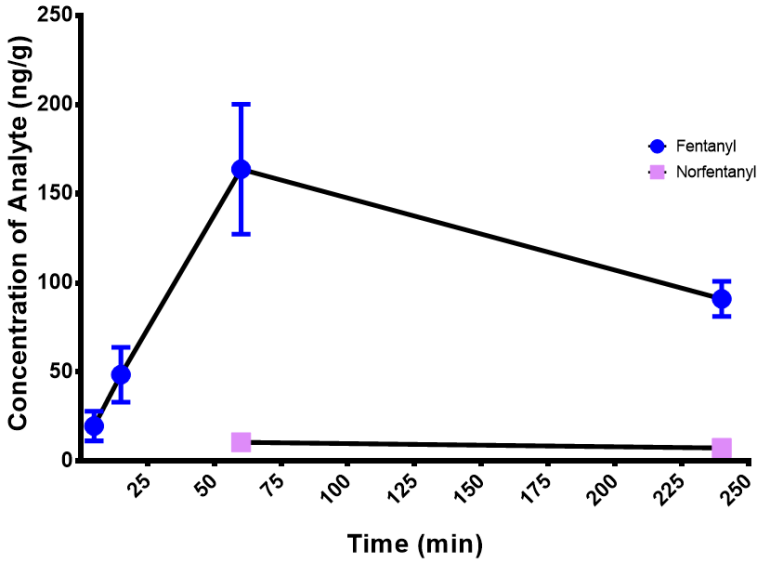

c)

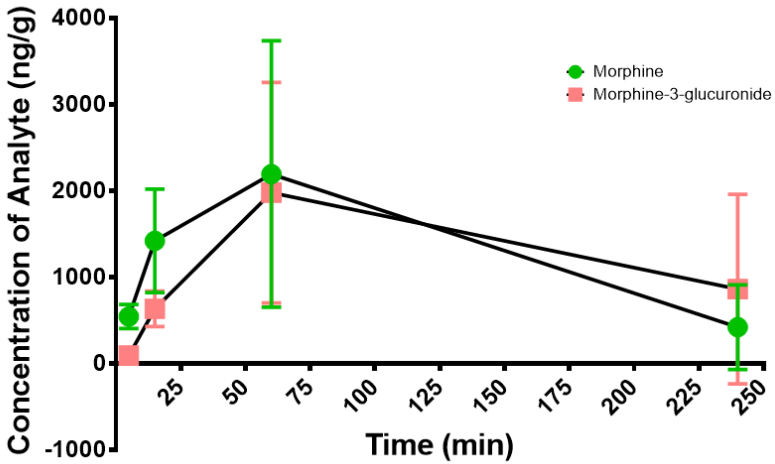

Figure 5.13: Concentration of Fentanyl, Morphine, and Select Metabolites in Fat from 5-240 Min in Mice. a) Average concentration of fentanyl and morphine in fat in mice injected with either 0.3 mg/kg fentanyl sc or 30 mg/kg morphine sc. Morphine averages normalized by hundredfold division to account for the difference in dosage. Significant effect of treatment ($P<0.0001$; $F(1, 6) = 201.2$), significant effect of time ($P<0.0001$; $F(3, 18) = 34.31$), and significant interaction of time and treatment ($P<0.0001$; $F(3, 18) = 23.86$). *: $p<0.05$ (fentanyl vs morphine); ****: $p<0.0001$ (fentanyl vs morphine). Fentanyl AUC: 28097 ng/g*min; morphine AUC (original data): 328093 ng/g*min ($p=0.0159$). b) Average concentration of fentanyl and its metabolite, norfentanyl, in fat.
c) Average concentration of morphine and its metabolite, morphine-3-β-D-glucuronide, in fat. No significant differences in analyte concentration ($P = 0.4752$; $F (1, 6) = 0.5799$) or significant interaction of time and analyte concentration ($P = 0.5157$; $F(3, 18) = 0.7889$, but significant effect of time ($P = 0.0027$; $F(3, 18) = 6.911$). (Data expressed as mean ± SD and analyzed by 2-way repeated-measures ANOVA, with Šídák's post hoc for multiple comparisons as needed. n = 4/group

In skin, morphine was measured at significantly higher levels than fentanyl at 5 min ($p<0.001$) and 15 min ($p<0.01$) (**Figure 5.14a**). Average fentanyl AUC was 16246 ng/g*min, while average morphine AUC (with original concentrations) was 4434730 ng/g*min ($p=0.0017$). Fentanyl exhibited a t_{max} of 60 min, while morphine displayed a t_{max} of 5 min. No norfentanyl or 4-ANPP were detected at any time point. Morphine concentration was greater than morphine-3-β-D-glucuronide at 5 min ($p<0.001$) and 15 min ($p<0.01$) (**Figure 5.14b**).

a)

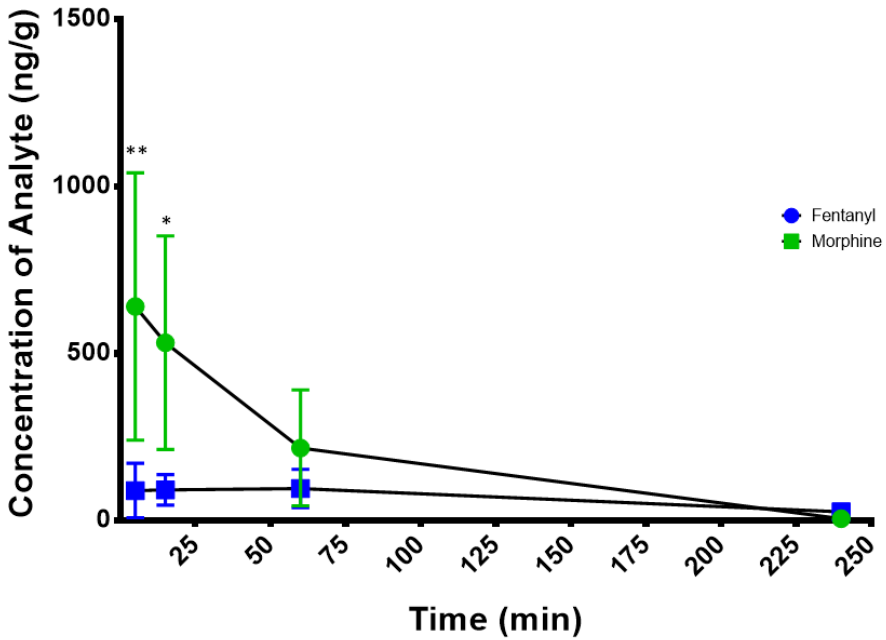

b)

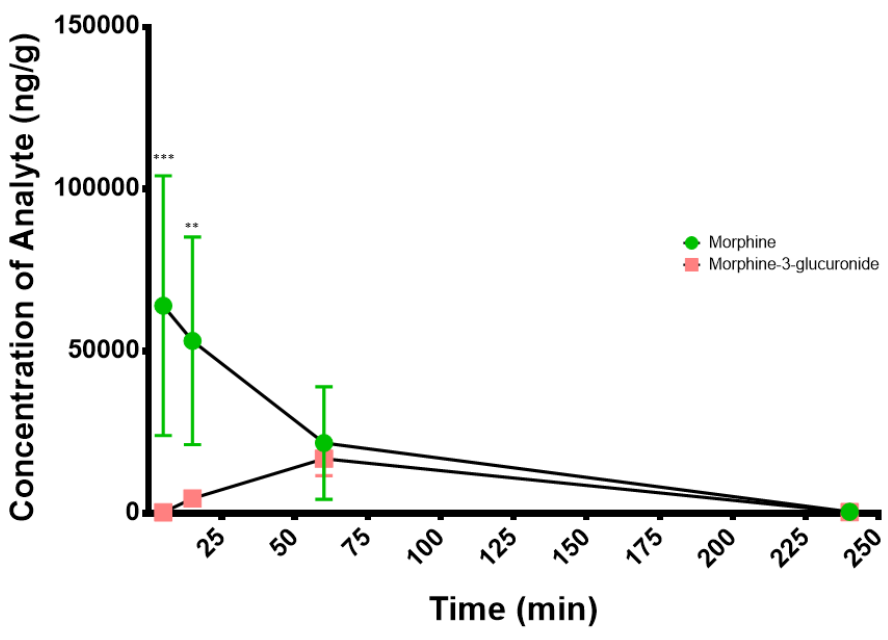

Figure 5.14: Concentration of Fentanyl, Morphine, and Select Metabolites in Skin from 5-240 Min in Mice. a) Average concentration of fentanyl and morphine in skin in mice injected with either 0.3 mg/kg fentanyl sc or 30 mg/kg morphine sc. Morphine averages normalized by hundredfold division to account for the difference in dosage. Significant effect of treatment (P=0.0052; F(1, 6) = 18.26), significant effect of time (P = 0.0105; F(3, 18) = 5.029), and significant interaction of time and treatment (P = 0.0343; F(3, 18) = 3.585). *: p<0.05 (fentanyl vs morphine); **:p<0.01 (fentanyl vs morphine). Fentanyl AUMC: 1240734 ng/g*min^2; morphine AUMC (original data): 182243325 ng/g*min^2 (p=0.0151)b) Average concentration of morphine and its metabolite, morphine-3-β-D-glucuronide, in skin. Significant differences in analyte concentration (P = 0.0037; F (1, 6) = 21.14), significant effect of time (P = 0.0197; F (3, 18) = 4.240), and significant interaction of time and analyte concentration (P=0.0091; F (3, 18) = 5.220). **: p<0.01 (morphine vs morphine-3-β-D-glucuronide); ***: p<0.001 (morphine vs morphine-3-β-D-glucuronide). Data expressed as mean ± SD and analyzed by 2-way repeated-measures ANOVA, with Šídák's post hoc for multiple comparisons as

5.3.2. Biodistribution of Fentanyl, Morphine, and Their Metabolites at 60 min Following a Repeated Injection Schedule.

Mice received repeated injections of either 0.3 mg/kg fentanyl sc or 30 mg/kg morphine sc (once daily/4 days). On the fifth experimental day (24 hr after the fourth injection), mice received a final injection of either saline, 0.3 mg/kg fentanyl (if given repeated fentanyl injections), or 30 mg/kg morphine (if given repeated morphine injections) sc and were sacrificed 60 min later. Mice receiving acute saline before sacrifice were used to test whether fentanyl or morphine had accumulated over the course of the repeated injection schedule, while mice receiving fentanyl or morphine prior to sacrifice were used to test how biodistribution of these opioids was influenced by a previous history of opioid exposure. Tissues were harvested as described above, and whole blood, brain, lung, and fat samples subjected to bioanalytical analysis. This subset of tissues was selected due to their varying roles in distribution (blood), respiration (brain and lung) and storage (fat).

For comparison with fentanyl, average morphine concentrations were normalized to account for the hundred-fold difference in dose between 0.3 mg/kg fentanyl and 30 mg/kg morphine. For comparisons between morphine and its metabolite, morphine-3-β-D-glucuronide, average morphine concentration was calculated from raw data. Morphine-6-β-D-glucuronide was not detected in any tissue samples at any time point in morphine-treated mice.

None of the target opioid analytes were detected in mice that received repeated fentanyl or repeated morphine injections followed by an acute saline injection 60 min prior to sacrifice. Therefore, further mention of "repeated treatment" may be understood to refer to the treatment groups that received a total of five injections of fentanyl or morphine (once daily every 24 hr) and were sacrificed 60 min after the last injection.

In whole blood, morphine in repeatedly-treated mice was measured at significantly higher concentrations at 60 min compared to mice repeatedly treated with fentanyl ($P = 0.0162$) (**Figure 5.15a**). However, fentanyl was measured at significantly higher concentrations than its metabolite, norfentanyl ($P<0.0001$), in whole blood at this time point (**Figure 5.15b**), while morphine-3-β-D-glucuronide was measured at significantly higher levels than morphine ($P=0.0179$) (**Figure 5.15c**). No 4-ANPP was detected in the blood of fentanyl-treated mice.

a)

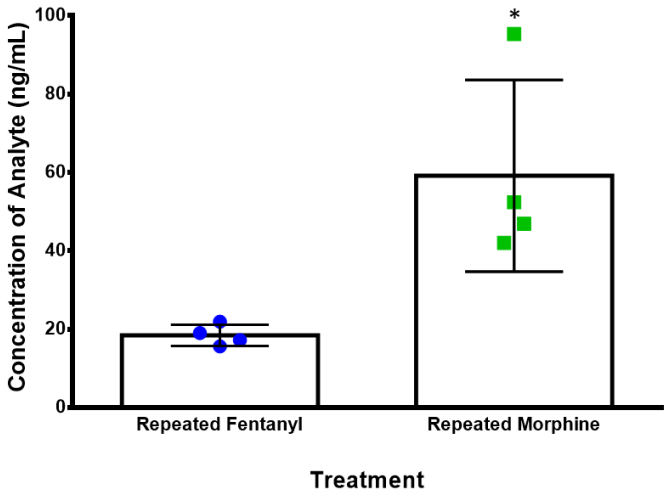

b)

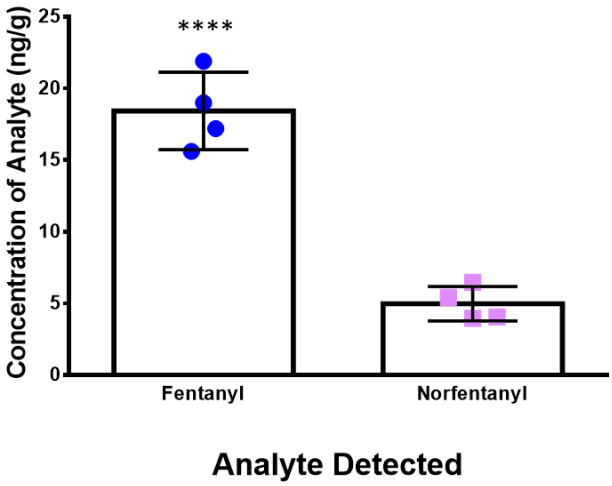

c)

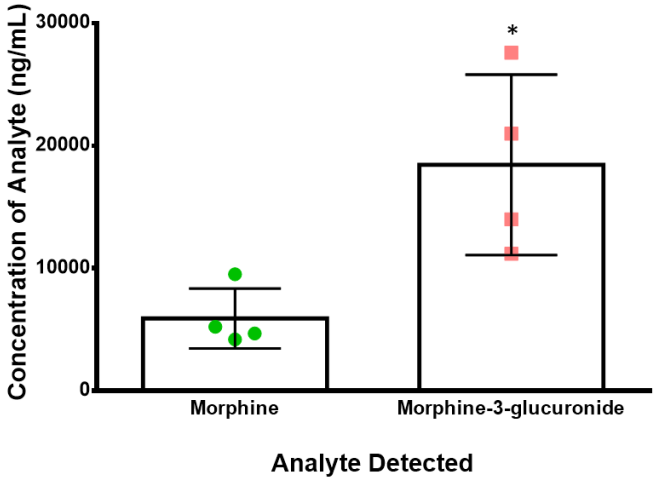

Figure 5.15: Concentration of Fentanyl, Morphine, and Select Metabolites Found in Whole Blood at 60 Min in Mice Repeatedly Injected with Either 0.3 mg/kg Fentanyl sc or 30 mg/kg Morphine sc (Once Daily for 5 Days). a) Average concentration of fentanyl or morphine in whole blood 60 min after last injection. Morphine averages normalized by hundredfold division to account for the difference in dosage. Significant difference in analyte concentration ($P = 0.0162$). b) Average concentration of fentanyl and its metabolite, norfentanyl, in whole blood 60 min after last fentanyl injection. Significant difference in analyte concentration ($P<0.0001$). c) Average concentration of morphine and its metabolite, morphine-3-β-D-glucuronide, in whole blood 60 min after last morphine injection. Significant difference in analyte concentration ($P = 0.0179$). Data expressed as mean ± SD and analyzed by unpaired 2-tailed T-test. n = 4/group

In brain, fentanyl concentration at 60 min in repeatedly-treated mice was significantly higher than morphine concentration in repeatedly-treated mice ($P = 0.0002$) (**Figure 5.16a**). Norfentanyl and 4-ANPP were not detected in the brains of fentanyl-treated mice, while morphine was measured at significantly higher concentrations than morphine-3-β-D-glucuronide ($P = 0.0046$) (**Figure 5.16b**).

a)

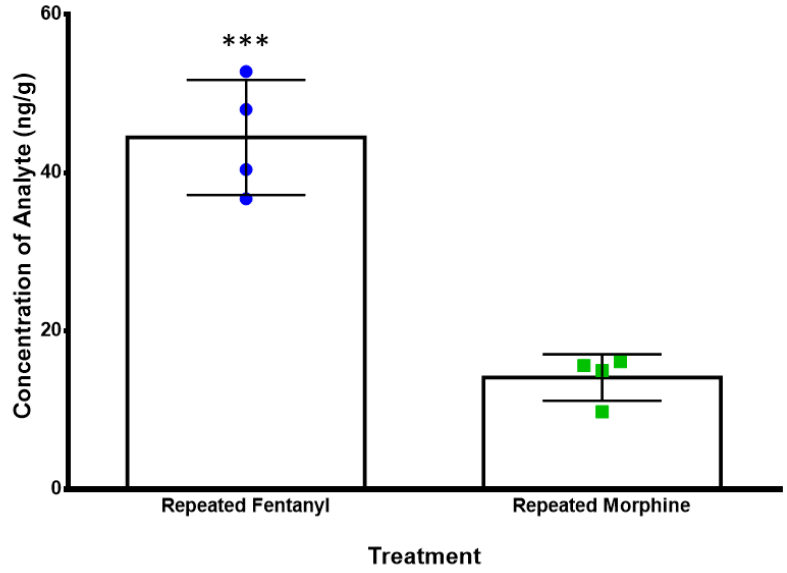

b)

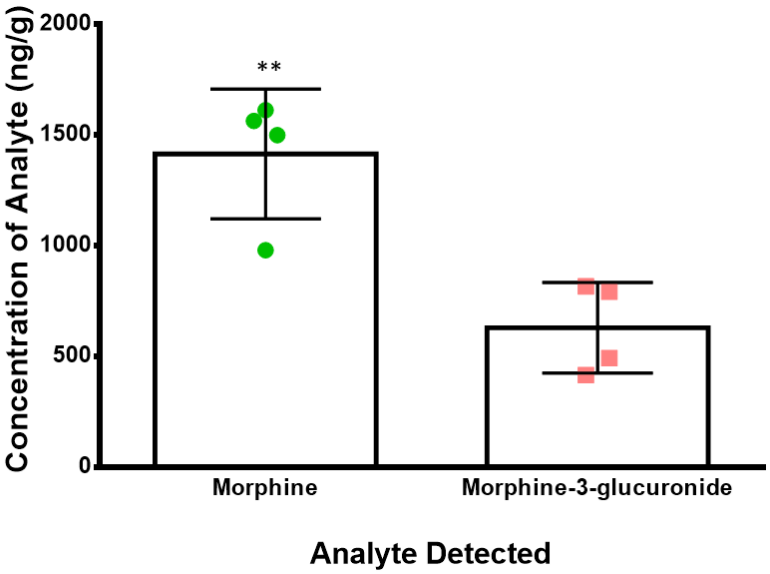

Figure 5.16: Concentration of Fentanyl, Morphine, and Select Metabolites Found in Whole Brain at 60 Min in Mice Repeatedly Injected with Either 0.3 mg/kg Fentanyl sc or 30 mg/kg Morphine sc (Once Daily for 5 Days). a) Average concentration of fentanyl or morphine in brain 60 min after last injection. Morphine averages normalized by hundredfold division to account for the difference in dosage. Significant difference in concentration ($P = 0.0002$). b) Average concentration of morphine and its metabolite, morphine-3-β-D-glucuronide, in brain 60 min after last morphine injection. Significant difference in concentration ($P = 0.0046$). Data expressed as mean ± SD and analyzed by unpaired 2-tailed T-test. n = 4/group

In lung, no significant differences were observed between concentrations of fentanyl and morphine ($P = 0.2611$) (**Figure 5.17a**) or between morphine and morphine-3-β-D-glucuronide ($P = 0.5560$) at 60 min in repeatedly-treated mice (**Figure 5.17c**). However, fentanyl was detected at significantly higher concentrations than its metabolites, norfentanyl ($p<0.0001$) and 4-ANPP ($p<0.0001$), at this time point (**Figure 5.17b**).

a)

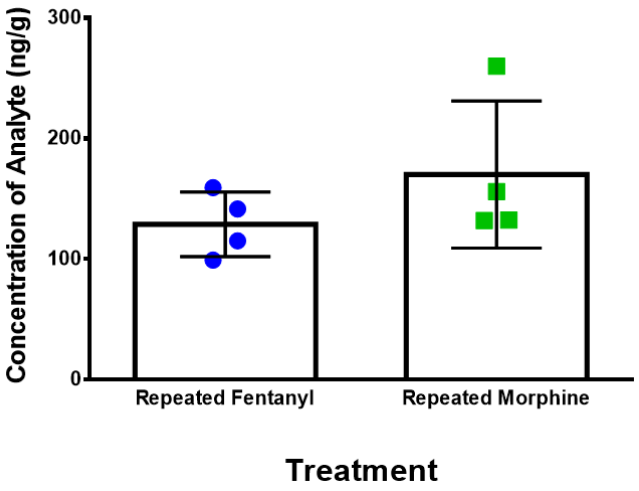

b)

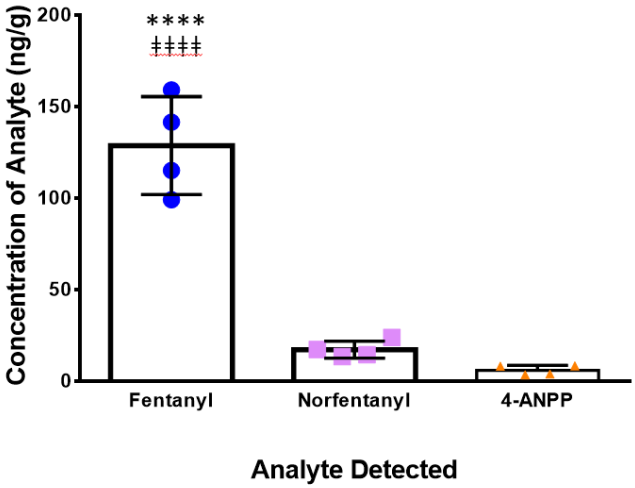

c)

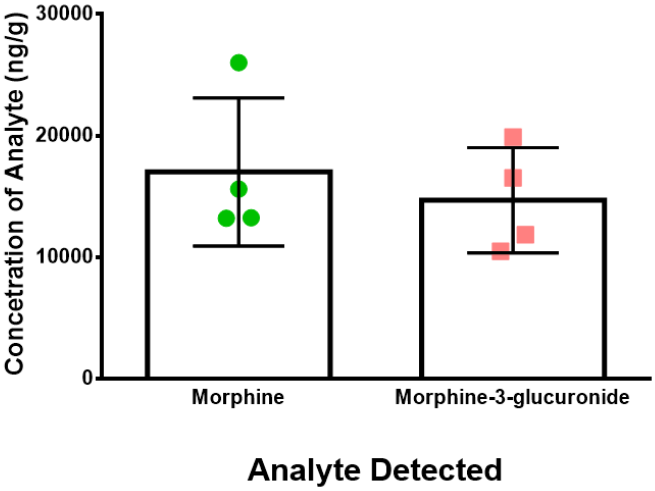

Figure 5.17: Concentration of Fentanyl, Morphine, and Select Metabolites Found in Lung at 60 Min in Mice Repeatedly Injected with Either 0.3 mg/kg Fentanyl sc or 30 mg/kg Morphine sc (Once Daily for 5 Days). a) Average concentration of fentanyl or morphine in lung 60 min after last injection. Morphine averages normalized by hundredfold division to account for the difference in dosage. No significant difference in concentration ($P = 0.2611$). b) Average concentration of fentanyl and its metabolites, norfentanyl and 4-ANPP, in lung 60 min after last fentanyl injection. Significant difference in concentration ($P<0.0001$; $F(2, 9) = 13.54$). ****: $p<0.0001$ (fentanyl vs norfentanyl); ++++: $p<0.0001$ (fentanyl vs 4-ANPP) c) Average concentration of morphine and its metabolite, morphine-3-β-D-glucuronide, in lung 60 min after last morphine injection. No significant difference in concentration ($P = 0.5560$). Data expressed as mean ± SD and analyzed by unpaired 2-tailed T-test or one-way ANOVA as appropriate. n = 4/group

In fat, fentanyl was measured at significantly higher concentrations than morphine at 60 min in repeatedly-treated mice ($P = 0.0210$) (**Figure 5.18a**). Norfentanyl and 4-ANPP were not detected in fat in repeatedly-treated mice. No significant differences were observed between morphine and morphine-3-β-D-glucuronide in fat at this time point ($P = 0.4864$) (**Figure 5.18b**).

a)

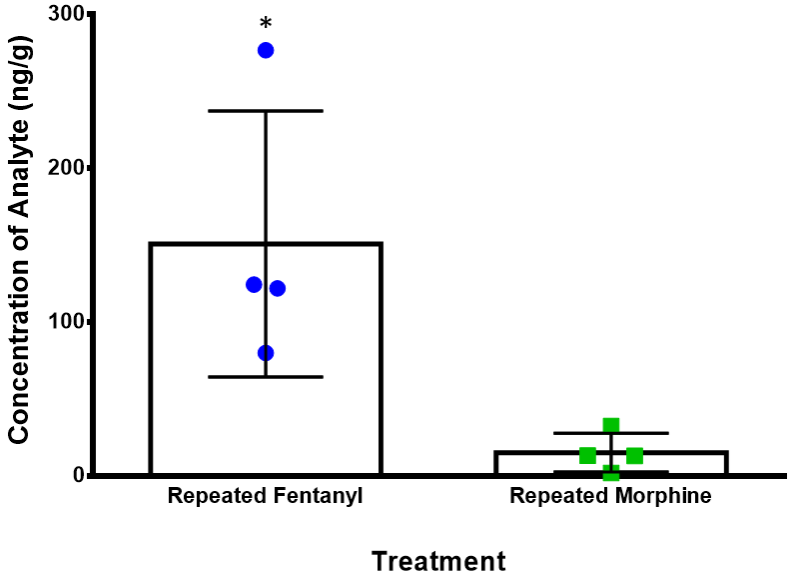

b)

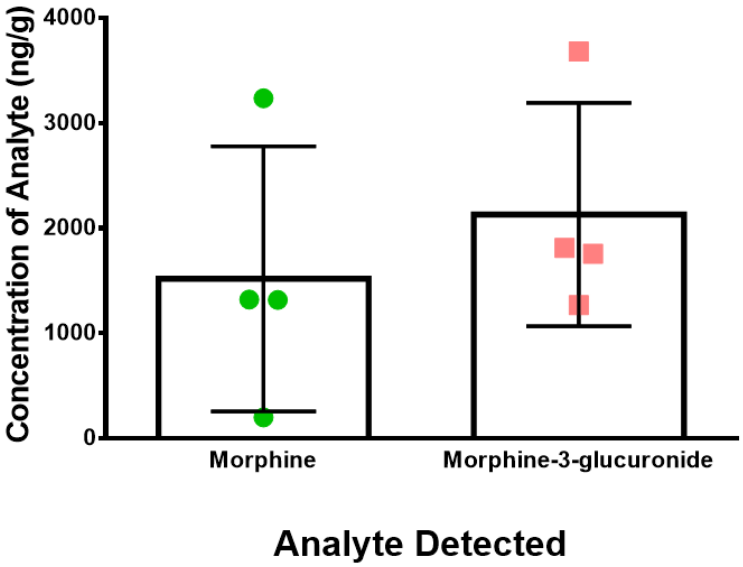

Figure 5.18: Concentration of Fentanyl, Morphine, and Select Metabolites Found in Fat at 60 Min in Mice Repeatedly Injected with Either 0.3 mg/kg Fentanyl sc or 30 mg/kg Morphine sc (Once Daily for 5 Days). a) Average concentration of fentanyl or morphine in fat 60 min after last injection. Morphine averages normalized by hundredfold division to account for the difference in dosage. Significant difference in concentration ($P = 0.0210$). b) Average concentration of morphine and its metabolite, morphine-3-β-D-glucuronide, in fat 60 min after last morphine injection. No significant difference in concentration ($P = 0.4864$). Data expressed as mean ± SD and analyzed by unpaired 2-tailed T-test. n = 4/group

5.3.3. Comparison of Fentanyl and Morphine Biodistribution at 60 Min in Opioid-Naïve and Opioid-Experienced Mice

To examine potential differences in opioid biodistribution between drug-naïve mice given a single acute injection of 0.3 mg/kg fentanyl or 30 mg/kg morphine and mice with a history of repeated fentanyl or morphine injection, opioid analyte concentrations at 60 min in whole blood, brain, lung, and fat samples from these two cohorts were compared.

In whole blood, no significant differences in fentanyl concentration ($P = 0.5550$) (**Figure 5.19a**), norfentanyl concentration ($P = 0.2007$) (**Figure 5.19b**), morphine concentration ($P = 0.8003$) (**Figure 5.19c**), or morphine-3-β-D-glucuronide concentration ($P = 0.7172$) (**Figure 5.19d**) were observed at 60 min between mice receiving acute or repeated injections. Since 4-ANPP was not detected in whole blood in the repeated fentanyl group, relative levels of this metabolite could not be compared between cohorts.

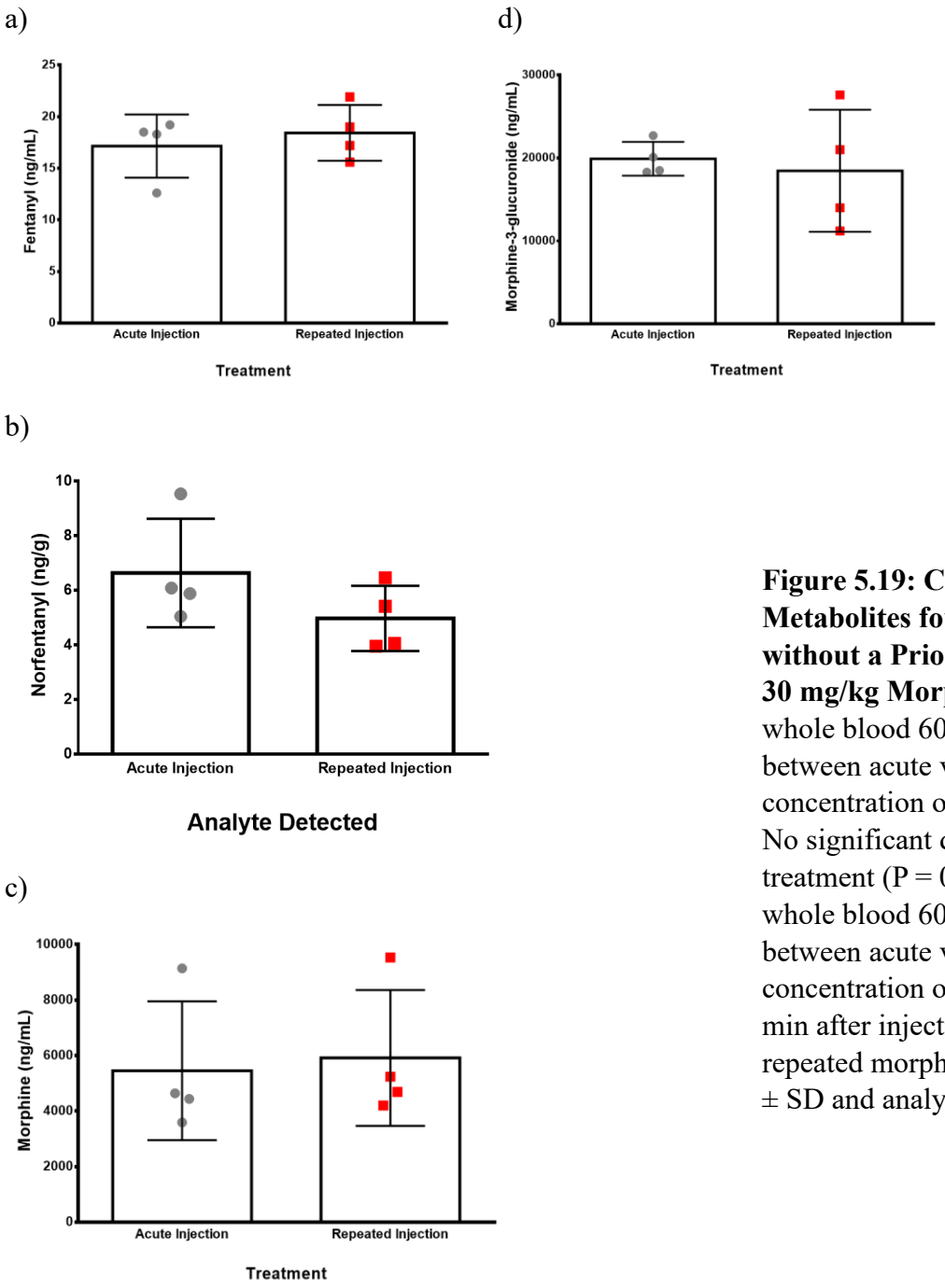

Figure 5.19: Concentration of Fentanyl, Morphine, and Select Metabolites found in Whole Blood at 60 Min in Mice with or without a Prior History of Exposure to 0.3 mg/kg Fentanyl sc or 30 mg/kg Morphine sc. a) Average concentration of fentanyl in whole blood 60 min after injection. No significant difference between acute vs repeated treatment (P = 0.5550). b) Average concentration of norfentanyl in whole blood 60 min after injection. No significant difference between acute vs repeated fentanyl treatment (P = 0.2007). c) Average concentration of morphine in whole blood 60 min after injection. No significant difference between acute vs repeated treatment (P = 0.8003). d) Average concentration of morphine-3-β-D-glucuronide in whole blood 60 min after injection. No significant difference between acute vs repeated morphine treatment (P = 0.7172). Data expressed as mean ± SD and analyzed by unpaired 2-tailed T-test. n = 4/group

In brain, fentanyl concentration at 60 min was significantly higher in acutely-treated mice compared with their repeatedly-treated counterparts ($P = 0.0367$) (**Figure 5.20a**). However, concentrations of morphine ($P = 0.1475$) (**Figure 5.20b**) and morphine-3-β-D-glucuronide ($P = 0.0795$) (**Figure 5.20c**) measured in brain did not significantly differ at this time point between mice receiving acute or repeated injections. Comparisons of norfentanyl and 4-ANPP concentrations in brain at 60 min between acutely- and repeatedly-treated animals could not be made due to a lack of data for these metabolites in repeatedly-exposed mice.

a)

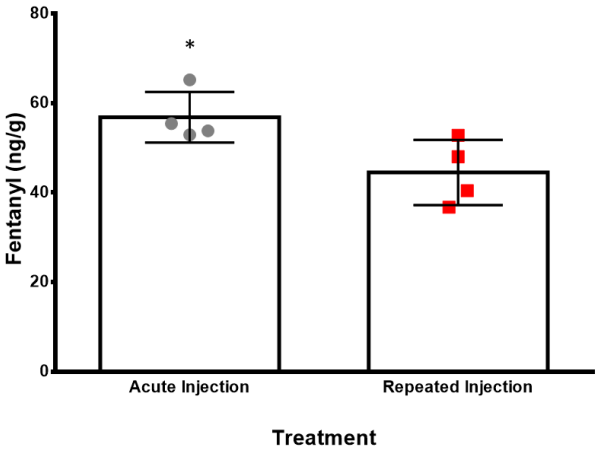

b)

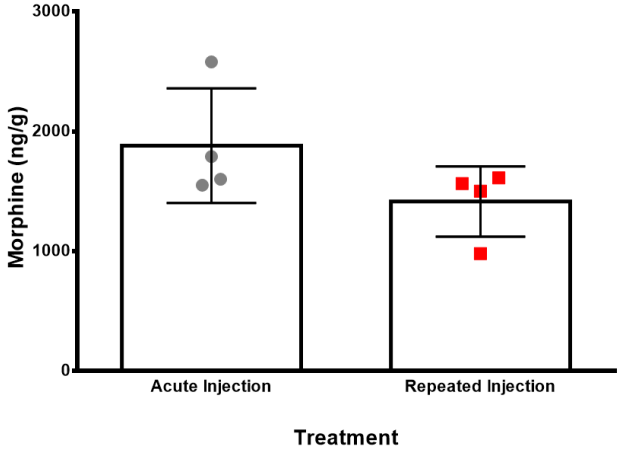

c)

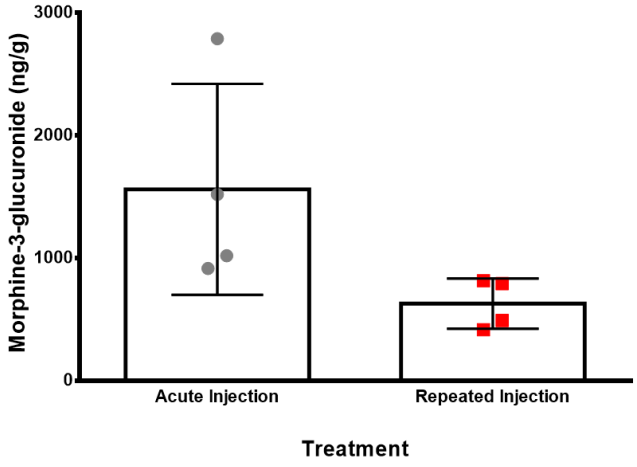

Figure 5.20: Concentration of Fentanyl, Morphine, and Select Metabolites found in Whole Brain at 60 Min in Mice with or without a Prior History of Exposure to 0.3 mg/kg Fentanyl sc or 30 mg/kg Morphine sc. a) Average concentration of fentanyl in brain 60 min after injection. Significant difference between acute vs repeated treatment (P = 0.0367). b) Average concentration of morphine in brain 60 min after injection. No significant difference between acute vs repeated treatment (P = 0.1475). c) Average concentration of morphine-3-β-D-glucuronide in brain 60 min after injection. No significant difference between acute vs repeated morphine treatment (P = 0.0795). Data expressed as mean ± SD and analyzed by unpaired 2-tailed T-test. n = 4/group

In lung, no significant differences in fentanyl concentration (P = 0.1984) (**Figure 5.21a**), norfentanyl concentration (P = 0.4880) (**Figure 5.21b**), 4-ANPP concentration (P = 0.1628) (**Figure 5.21c**), morphine concentration (P = 0.2095) (**Figure 5.21d**), or morphine-3-β-D-glucuronide concentration (P = 0.7232) (**Figure 5.21e**) were observed at 60 min between mice receiving acute or repeated injections.

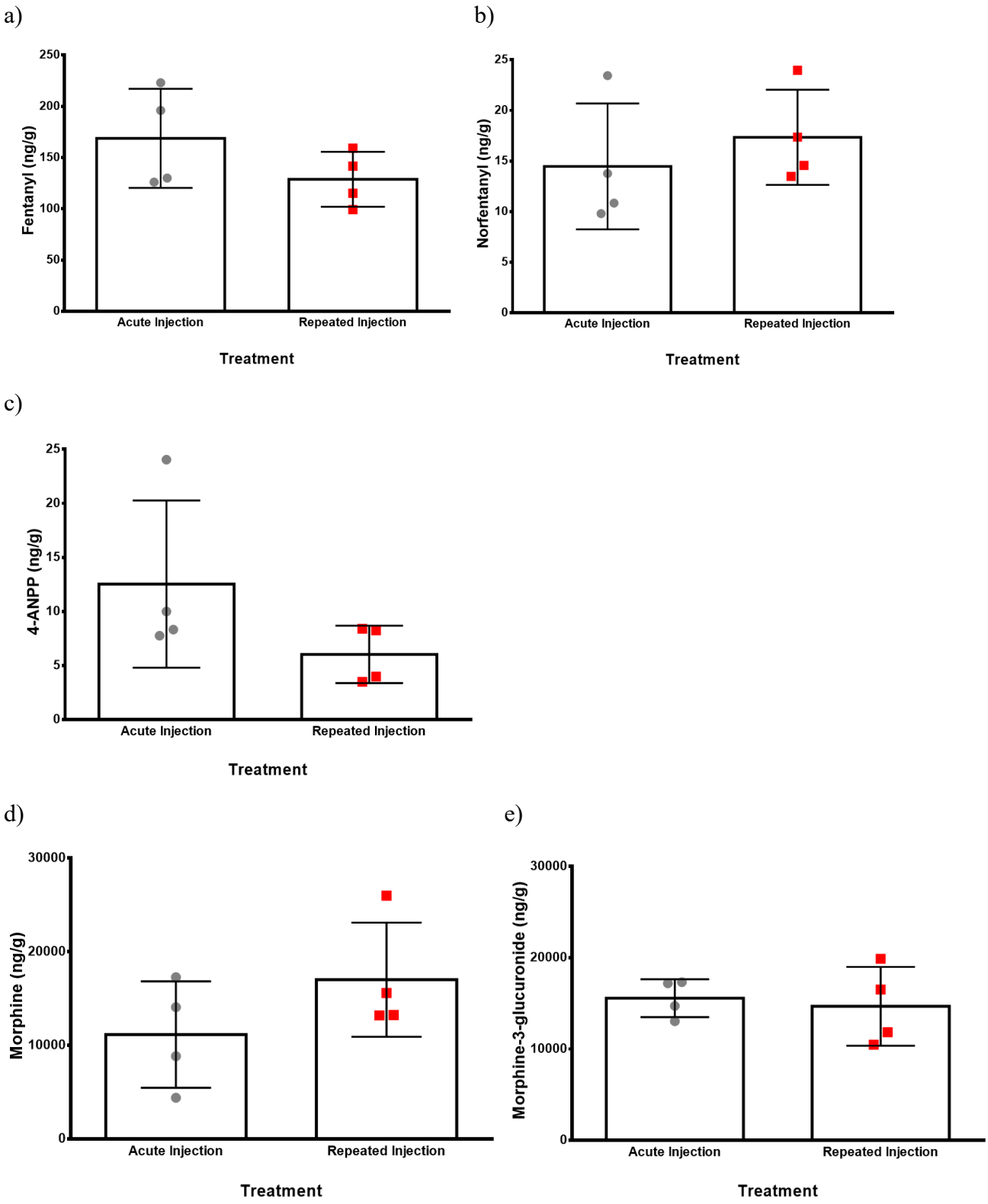

Figure 5.21: Concentration of Fentanyl, Morphine, and Select Metabolites found in Lung at 60 Min in Mice with or without a Prior History of Exposure to 0.3 mg/kg Fentanyl sc or 30 mg/kg Morphine sc. a) Average concentration of fentanyl in lung 60 min after injection. No significant difference between acute vs repeated treatment (P = 0.1984). b) Average concentration of norfentanyl in lung 60 min after injection. No significant difference between acute vs repeated fentanyl treatment (P = 0.4880).

Figure 5.21 cont. c) Average concentration of 4-ANPP in lung 60 min after injection. No significant difference between acute vs repeated fentanyl treatment (P = 0.1628). d) Average concentration of morphine in lung 60 min after injection. No significant difference between acute vs repeated treatment (P = 0.2095). e) Average concentration of morphine-3-β-D-glucuronide in lung 60 min after injection. No significant difference between acute vs repeated treatment (P = 0.7232). Data expressed as mean ± SD and analyzed by unpaired 2-tailed T-test. n = 4/group

In fat, no significant differences in fentanyl concentration (P = 0.7917) (**Figure 5.22a**), morphine concentration (P = 0.5219) (**Figure 5.22b**), or morphine-3-β-D-glucuronide concentration (P=0.8636) (**Figure 5.22c**) were observed at 60 min in mice receiving acute or repeated injections. Comparisons of norfentanyl and 4-ANPP concentrations in fat at 60 min between acutely- and repeatedly-treated animals could not be made due to a lack of data for these metabolites in repeatedly-exposed mice.

a)

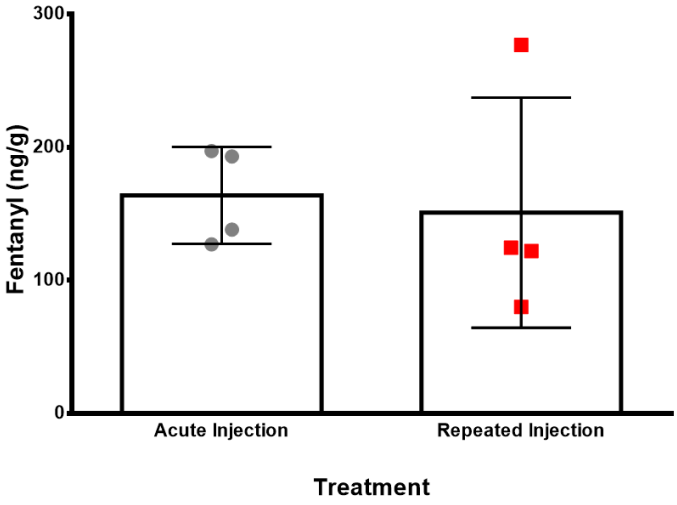

b)

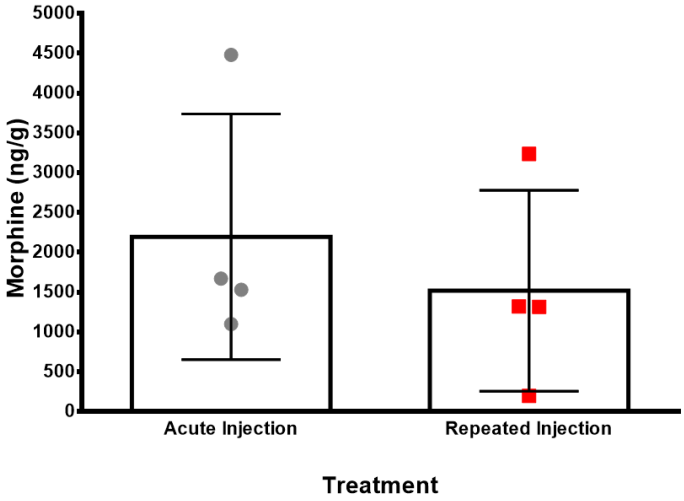

c)

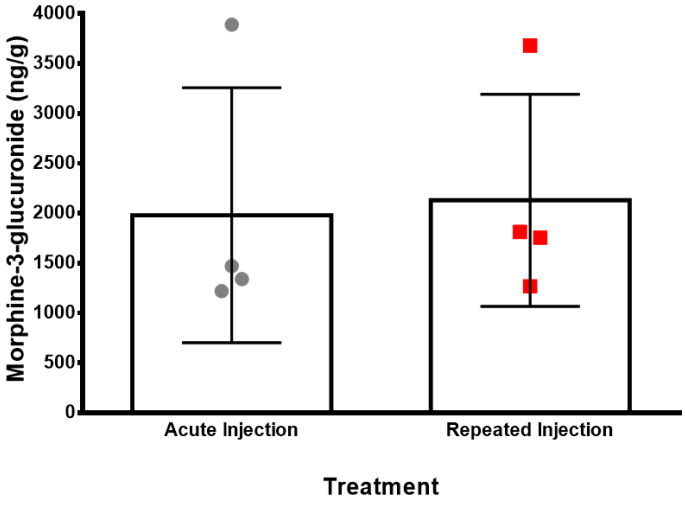

Figure 5.22: Concentration of Fentanyl, Morphine, and Select Metabolites found in Fat at 60 Min in Mice with or without a Prior History of Exposure to 0.3 mg/kg Fentanyl sc or 30 mg/kg Morphine sc. a) Average concentration of fentanyl in fat 60 min after injection. No significant difference between acute vs repeated treatment (P = 0.7917). b) Average concentration of morphine in fat 60 min after injection. No significant difference between acute vs repeated treatment (P = 0.5219). c) Average concentration of morphine-3-β-D-glucuronide in fat 60 min after injection. No significant difference between acute vs repeated morphine treatment (P = 0.8636). Data expressed as mean ± SD and analyzed by unpaired 2-tailed T-test. n = 4/group

As summarized in **Table 5.9** below, fentanyl concentration in whole blood, lung, and fat at 60 min did not differ significantly between acutely- and repeatedly-treated mice. However, fentanyl concentration in brain at 60 min was higher in acutely-treated mice than in their opioid-experienced counterparts (P = 0.0367).

Table 5.9: Comparison of Fentanyl Concentration at 60 Min in Whole Blood, Brain, Fat, and Tissue After Acute vs Repeated Treatment (0.3 mg/kg Fentanyl sc). Unpaired 2-tailed T-test. n = 4/group

Tissue	Acute vs Repeated Injection
Whole Blood	No significant difference in fentanyl concentration (P = 0.5550)
Brain	Greater fentanyl concentration after acute injection (P = 0.0367)
Lung	No significant difference in fentanyl concentration (P = 0.1984)
Fat	No significant difference in fentanyl concentration (P = 0.7917)

Meanwhile, **Table 5.10** demonstrates that morphine concentration in whole blood, brain, lung, and fat at 60 min did not differ significantly between acutely- vs repeatedly-treated mice.

Table 5.10: Comparison of Morphine Concentration at 60 Min in Whole Blood, Brain, Fat, and Tissue After Acute vs Repeated Treatment (30 mg/kg Morphine sc). Unpaired 2-tailed T-test. n = 4/group

Tissue	Acute vs Repeated Injection
Whole Blood	No significant difference in morphine concentration (P = 0.8003)
Brain	No significant difference in morphine concentration (P = 0.1475)
Lung	No significant difference in morphine concentration (P = 0.2095)
Fat	No significant difference in morphine concentration (P = 0.5219)

As shown in **Table 5.11**, while there was no significant difference between fentanyl and normalized morphine concentration in whole blood or brain at 60 min in acutely-treated mice,

morphine concentration was greater than fentanyl at 60 min in whole blood from repeatedly-treated animals (P = 0.0162), while fentanyl concentrations in brain were greater than morphine at 60 min in repeatedly-treated mice (P = 0.0002). However, neither acutely-treated nor repeatedly-treated mice demonstrated a significant difference between fentanyl and morphine in lung at 60 min. In contrast, fentanyl concentration in fat exceeded morphine at 60 min in both acutely- and repeatedly-treated mice.

Table 5.11: Comparisons of Fentanyl and Morphine Concentration in Blood, Brain, Lung, and Fat 60 Min After Acute or Repeated Treatment. Morphine averages normalized by hundredfold division to account for the difference in dosage. 2-way repeated-measures ANOVA with Šídák's post hoc (acute injection) or unpaired 2-tailed T-test (repeated injection). n = 4/group

Tissue	Acute Injection	Repeated Injection
Whole Blood	No significant difference between fentanyl and morphine concentration	morphine > fentanyl (P = 0.0162)
Brain	No significant difference between fentanyl and morphine concentration	fentanyl > morphine (P = 0.0002)
Lung	No significant difference between fentanyl and morphine concentration	No significant difference between fentanyl and morphine concentration
Fat	fentanyl > morphine (p<0.0001)	fentanyl > morphine (P = 0.0210)

Table 5.12 illustrates differences in concentration between fentanyl and its metabolites under acute or repeated treatment schedules. Although concentrations of fentanyl and norfentanyl did not significantly differ in whole blood at 60 min in acutely-treated mice, fentanyl was present at significantly higher concentrations than this metabolite in repeatedly-treated mice. Conversely, fentanyl concentrations at 60 min in brain were greater than norfentanyl in acutely-treated animals, but no norfentanyl was detected at this time point in repeatedly-treated mice. Similarly, fentanyl concentration appeared to be higher than norfentanyl in fat at 60 min in acutely-treated

animals, but no norfentanyl was detected in fat sample collected from repeatedly-treated animals at this time point. Fentanyl concentration at 60 min in lung appeared to be greater than norfentanyl in both acutely- and repeatedly-treated mice. While 4-ANPP was not detected in blood or brain at 60 min in repeatedly-treated mice, it was detected in acutely-treated mice, albeit at significantly lower concentrations than fentanyl. Fentanyl appeared to be present at greater concentrations than 4-ANPP at 60 min in lung in both acutely- and repeatedly-treated mice. 4-ANPP was not detected in fat at 60 min in either acutely- or repeatedly-treated mice.

Table 5.12: Comparison of Fentanyl and Its Metabolites, Norfentanyl and 4-ANPP, in Whole Blood, Brain, Lung, and Fat 60 Min After Acute or Repeated Treatment (0.3 mg/kg Fentanyl sc). 2-way repeated-measures ANOVA with Šídák's post hoc (acute injection) or unpaired 2-tailed T-test (repeated injection). n = 4/group

Tissue	Acute Injection	Repeated Injection
Whole Blood	No significant difference between Fentanyl and Norfentanyl Fentanyl > 4-ANPP ($p<0.05$)	Fentanyl > Norfentanyl ($p<0.0001$) No 4-ANPP detected
Brain	Fentanyl > Norfentanyl ($p<0.01$) Fentanyl > 4-ANPP ($p<0.05$)	No Norfentanyl detected No 4-ANPP detected
Lung	Unable to run full analysis (no 4-ANPP at 5 & 240 min), but fentanyl appears greater than norfentanyl & 4-ANPP	Fentanyl > Norfentanyl ($p<0.0001$) Fentanyl > 4-ANPP ($p<0.0001$)
Fat	Unable to run full analysis (no norfentanyl at 5 & 15 min), but fentanyl appears greater than norfentanyl No 4-ANPP detected	No Norfentanyl detected No 4-ANPP detected

Meanwhile, **Table 5.13** displays differences in concentration between morphine and morphine-3-β-D-glucuronide under acute or repeated treatment schedules. While ANOVA did not indicate a significant difference between morphine and morphine-3-β-D-glucuronide at 60 min in whole blood in acutely-treated animals, Šídák's post hoc suggested that morphine-3-β-D-

glucuronide concentration was significantly higher than morphine, and T-tests in repeatedly-treated animals also showed that morphine-3-β-D-glucuronide concentration exceeded morphine. In brain, there was no significant difference between morphine and morphine-3-β-D-glucuronide concentration at 60 min in acutely-treated animals, but morphine was significantly higher than morphine-3-β-D-glucuronide in repeatedly-treated mice. In lung and fat, morphine and morphine-3-β-D-glucuronide did not differ significantly in either acutely- or repeatedly-treated mice.

Table 5.13: Comparison of Morphine and Its Metabolite, Morphine-3-β-D-Glucuronide, in Whole Blood, Brain, Lung, and Fat 60 Min After Acute or Repeated Treatment (30 mg/kg Morphine sc). 2-way repeated-measures ANOVA with Šídák's post hoc (acute injection) or unpaired 2-tailed T-test (repeated injection). n = 4/group

Tissue	Acute Injection	Repeated Injection
Whole Blood	No significant difference between Morphine and Morphine-3-β-D-glucuronide	Morphine-3-β-D-glucuronide > Morphine (P=0.0179)
Brain	No significant difference between Morphine and Morphine-3-β-D-glucuronide	Morphine > Morphine-3-β-D-glucuronide (P=0.0046)
Lung	No significant difference between Morphine and Morphine-3-β-D-glucuronide	No significant difference between Morphine and Morphine-3-β-D-glucuronide
Fat	No significant difference between Morphine and Morphine-3-β-D-glucuronide	No significant difference between Morphine and Morphine-3-β-D-glucuronide

5.3.3. Thermal Nociception Following Repeated Opioid Injection

To determine whether the treatment regimen in repeated opioid biodistribution study constituted a model of tolerance, mice received 0.3. mg/kg fentanyl or 30 mg/kg morphine sc once every 24 hr for 5 days. Two control groups receiving repeated saline (once every 24 hr for 4 days) followed by acute 0.3 mg/kg fentanyl or 30 mg/kg morphine sc on the fifth experimental day were also included. For the basis of comparison with repeated opioid biodistribution study,

in which tissue samples were harvested 60 min after administration of drug, thermal nociception was evaluated 60 min after injection on the fifth day by means of the warm water tail withdrawal assay.

Figure 5.23 demonstrates that 0.3 mg/kg fentanyl and 30 mg/kg morphine induced maximal antinociception regardless of whether mice had a history of repeated saline, repeated fentanyl, or repeated morphine. Therefore, this repeated injection schedule does not generate antinociceptive tolerance to the doses tested.

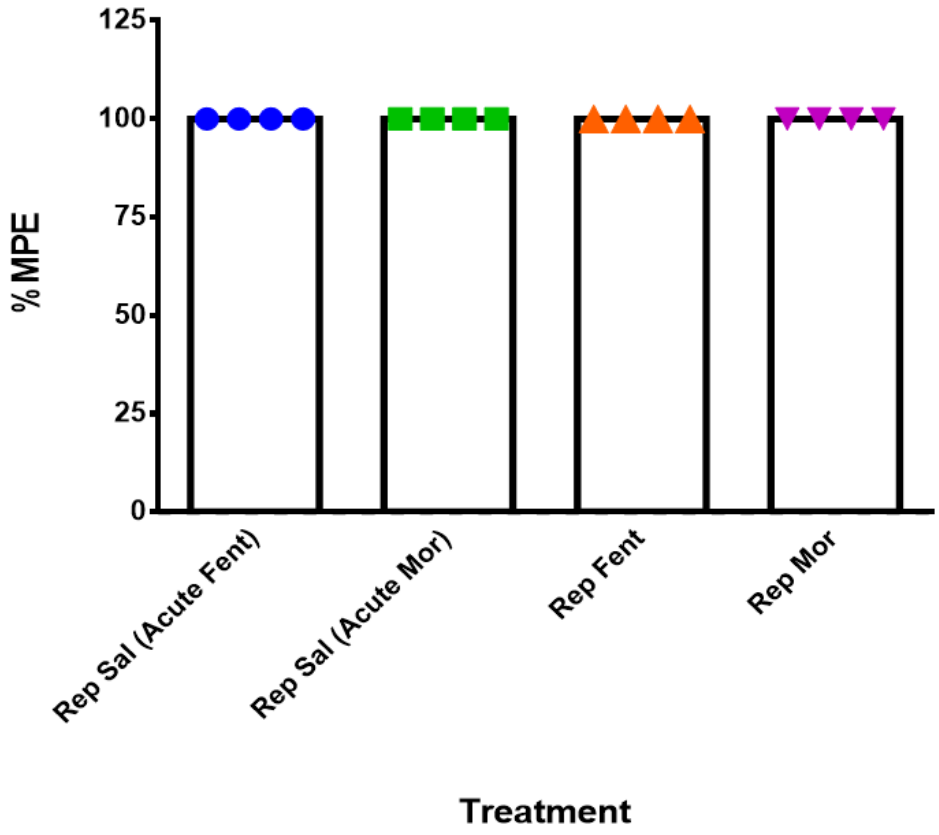

Figure 5.23: Thermal Antinociception (As Measured by Warm-Water Tail Withdrawal) in Opioid-Experienced Mice. Mice with a history of repeated saline, repeated fentanyl, or repeated morphine exposure tested 60 min after injection with 0.3 mg/kg fentanyl sc (Repeated Saline [Acute Fentanyl] and Repeated Fentanyl groups) or 30 mg/kg morphine sc (Repeated Saline [Acute Morphine] and Repeated Morphine groups). Tail withdrawal latency expressed as percent maximum possible effect (%MPE). Mice displayed 100% MPE regardless of pretreatment history. n = 4/group

CHAPTER 6: DISCUSSION

6.1. Fentanyl and Morphine Dose Response in Respiratory Depression.

In a recent study using the same mouse strain and sex (male Swiss Webster) and route of administration (sc injection) as the above respiratory depression pilot experiments, doses of 0.1 mg/kg fentanyl or higher (up to 10 mg/kg) significantly decreased minute volume starting 5 min after administration in a dose-dependent manner (Elder et al. 2023). Maximal respiratory depression tended to occur between 10–15 min after injection, and 0.3 mg/kg fentanyl was determined to be the lowest dose that consistently induced respiratory depression by 20 min after injection and sustained respiratory depression for at least 30 min (Elder et al. 2023). Similarly, in the present studies, 0.1 mg/kg fentanyl was the lowest tested dose at which respiratory depression was observed, and doses that induced significant respiratory depression compared to saline did so within 5 min (0.1, 0.3, and 1 mg/kg). Pilot data likewise revealed maximal respiratory depression at 10 min following injection with 0.1, 0.3, or 1 mg/kg fentanyl, with 0.3 mg/kg being the lowest dose that sustained respiratory depression for over 30 min. Another study involving fentanyl-induced respiratory depression in male Swiss Webster mice across a range of doses showed significant decreases in minute volume at all doses tested (0.001–3.2 mg/kg) except for 0.001 mg/kg, which falls within the range of fentanyl doses used in the above pilot and is in keeping with observed changes in minute volume. This lends credibility to the dose-response data for fentanyl- and morphine-induced respiratory depression and the doses of fentanyl and morphine selected for biodistribution studies, thus strengthening the claim that the acute biodistribution data are applicable to fentanyl and morphine tissue distribution in murine models of opioid-induced respiratory depression.

Elder et al. (2023) reported that respiratory rate was the main source of decreases in minute volume, with only small decreases in tidal volume following injection with 0.1–1.0 mg/kg fentanyl. The current pilot studies are generally consistent with these results in that decreases in tidal volume at 0.3 and 1 mg/kg fentanyl were observed, although no significant changes compared to saline were observed in tidal volume following 0.1 mg/kg fentanyl, with respiratory rate chiefly responsible for decreases in minute volume. In contrast, despite using the same gas mixture as these and Elder et al.'s studies (5 % CO_2, 21 % O_2, and balance N_2), Varshneya et al. did not observe significant decreases in tidal volume (2022). This could point to potential variability in tidal volume changes at these doses of fentanyl; however, since the observed decreases in tidal volume of smaller magnitude than changes in minute volume, this minor discrepancy does not automatically call the above results into question.

Male CD-1 mice given a range of morphine doses (3–30 mg/kg ip) displayed dose-dependent respiratory depression, but no decrease in tidal volume was observed (Hill et al. 2016). Morphine-induced respiratory depression was detected at 5 min and persisted for 30 min (Hill et al. 2016). Similarly, Varshneya et al. observed significant decreases in minute volume and respiratory rate, but not tidal volume, at doses of 1–32 mg/kg morphine administered sc in male Swiss Webster mice (2022). These previous findings corroborate the minute volume and respiratory rate data from the morphine pilot study, in which observed dose-dependent induction of respiratory depression was also observed over a similar morphine dose range (1–30 mg/kg sc). Similarly to Hill et al., morphine-induced respiratory depression was observed at 5 min, which lasted for over 30 min at the highest tested doses (10 and 30 mg/kg morphine). Unlike these experiments, however, significant, dose-dependent depression of tidal volume was also observed. Although mouse strain (Swiss Webster) and route of drug administration (sc) differed from Hill

et al., and Varshneya et al. used a cumulative dosing injection schedule rather than single acute injections, Varshneya et al. used the same strain and injection route, and both studies, like the pilot, ran mice on a 5% CO_2 gas mixture. Therefore, it is not entirely clear why changes in tidal volume occurred. However, the morphine-induced tidal volume decreases were somewhat smaller in magnitude than morphine-induced depression of minute volume and respiratory rate (see **Figures 4.6-4.8**). Consequently, and considering the agreement of the minute volume data from our dose-response studies with the previous literature, this does not substantially undermine the utility of chosen fentanyl and morphine doses for studying biodistribution of these opioids at doses relevant to respiratory depression.

Overall, the dose response of fentanyl- and morphine-induced respiratory depression in pilot studies seems to align with the established literature apart from minor discrepancies regarding tidal volume, thus supporting the choice of 0.3 mg/kg fentanyl and 30 mg/kg fentanyl as comparable doses for use in biodistribution comparison studies.

6.2. Comparison of Fentanyl- and Morphine-Induced Respiratory Depression and Biodistribution.

The post-injection times at which blood and tissue samples were collected from fentanyl- and morphine-treated mice (5, 15, 60, and 240 min) partially overlapped with the time course of our whole-body plethysmography dose-response studies, in which respiratory parameters were measured for 70 min after injection with opioid agonist. Therefore, it was deemed of interest to determine whether observed differences between fentanyl and morphine concentrations in blood and 12 tissue types over time coincided with statistical differences in fentanyl- and morphine-induced depression of MVb, f, or TVb in acutely-treated mice.

5 min after injection with 0.3 mg/kg fentanyl or 30 mg/kg morphine sc, magnitude of fentanyl-induced depression of MVb was significantly greater ($p<0.01$) than changes in MVb caused by morphine, although no significant differences in f or TVb under the two treatments were observed at this time point. 15 min after injection with 0.3 mg/kg fentanyl or 30 mg/kg morphine, no statistically significant differences between the magnitude of fentanyl- and morphine-induced changes in MVb, f, or TVb were observed. 60 min after injection with 0.3 mg/kg fentanyl or 30 mg/kg morphine, magnitude of morphine-induced depression of TVb was significantly greater relative to fentanyl ($p<0.001$), although there were no significant differences in MVb or f from fentanyl- and morphine-treated mice at this time point. Since respiration following injection with opioid agonist was not recorded past 70 min, it cannot be stated with certainty what differences, if any, might exist between respiratory depression induced by 0.3 mg/kg fentanyl and 30 mg/kg morphine at this time point.

Naturally, due to the 100-fold larger dose of morphine used, concentration of morphine in in blood and tissue tended to be greater than that observed for fentanyl (see **Table 5.5** and **5.6**). However, based on AUC tissue:blood ratios for the acute biodistribution time period, fentanyl distributed out of blood into tissue to a greater extent than morphine in brain, liver, lung, heart, kidney, spleen, small intestine, stomach, and fat, while no differences in tissue:blood ratio were observed for skin and large intestine, or muscle (though muscle results must be interpreted with caution due to lack of morphine data at 5 and 240 min). In general, these differences between fentanyl and morphine concentration in blood and tissue did not directly correspond to the pattern of statistically significant differences in fentanyl and morphine respiratory depressant effects. For example, although depression of MVb at 5 min was significantly greater in fentanyl-treated mice compared to morphine-treated mice, AUC values for *morphine* were significantly

greater than fentanyl in sample types such as brain and lung. The data thus indicate that observed differences in respiratory depression under 0.3 mg/kg fentanyl and 30 mg/kg morphine, though statistically significant, did not confound biodistribution studies, which supports the justification for treating these doses as equivalent.

6.3. Quantification of Fentanyl, Morphine, and Select Metabolites.

Though the bioanalytical method described above is far from the first to compare fentanyl and morphine, it presents a relative degree of novelty due to the fact that it quantifies these opioids and a few of their metabolites (norfentanyl/4-ANPP and morphine-3-β-D glucuronide, respectively) in thirteen matrices in the mouse: Whole blood, brain, liver, lung, heart, kidney, spleen, small intestine, large intestine, stomach, muscle, fat, and skin. In contrast, other analytical methods may be intended to compare fentanyl and morphine in human samples rather than preclinical models (Gaugler et al. 2018; Ferreira et al. 2020; Oiestad et al. 2011; Vandenbosch et al. 2022) or tailored to murine samples that only contain one of these two opioids, such as morphine (Guillot et al. 2007) or morphine plus its glucuronides (Zuccaro et al. 1997; Heydari et al. 2021; Gabel et al. 2023), often with limited sample types. For example, although Heydari et al. developed a UPLC-MS/MS method for quantifying morphine, morphine-3-β-D-glucuronide, and morphine-6-β-D-glucuronide in plasma and several tissues (brain, spleen, kidney, small intestine, and liver) in the mouse, their method does not include fentanyl, nor did they examine all of the tissues processed in the present experiments. Zuccaro et al.'s liquid chromatography-atmospheric pressure ion spray-mass spectrometry technique only measured morphine and its glucuronides in serum (1997), while Gabel et al.'s examination of morphine and its metabolites in mice through LC-MS/MS was limited to blood, brain, and lumbar spinal cord (2023). Furthermore, solid-phase extraction, which is included in the current

analytical method, presents certain advantages compared to liquid-liquid extractions (i.e. Øiestad et al.'s method for comparing morphine and fentanyl in human blood) because of the smaller sample volumes and production of less solvent waste (Ferreira et al. 2020). That being said, this method is not without its flaws: Compared to techniques like dried blood spot analysis, which can be run with only 15 µL of blood (Gaugler et al. 2018), the solid phase extraction protocol required much larger aliquots (100-µL) of homogenate for successful analysis.

6.4. Biodistribution of Fentanyl and Morphine After Acute Administration.

Some differences in tissue:blood concentration ratios of fentanyl and morphine appear consistent with what is known in the literature. For example, tissue:blood ratios (see **Tables 5.2** and **5.3**) for fentanyl concentration in brain at 5 and 15 minutes appear higher than those for morphine, which reflects fentanyl's rapid uptake into the central nervous system compared to other abused opioids like heroin (Hill et al. 2020). Furthermore, noticeably higher tissue:blood concentration ratios of fentanyl in fat at 60 and 240 min are consistent with fentanyl's greater lipophilicity relative to morphine (Kelly et al. 2021), while the gradual accumulation of fentanyl in fat has also been observed in other rodent models of fentanyl biodistribution (Hug and Murphy 1981; Schneider and Brune 1986). Moderately greater tissue:blood ratios of fentanyl compared to morphine in liver at 5 and 15 min could be indicative of fentanyl's rapid metabolism (Iula 2017), though the time course (C_{max} = 15 min, followed by a decline in concentration at 60 and 240 min) in this tissue is similar for both opioids.

That being said, the current data, including tissue:blood concentration ratios and tissue AUC:blood AUC ratios (see **Tables 5.7** and **5.8**), enhance knowledge of fentanyl and morphine biodistribution by providing comparisons of relative fentanyl and morphine disposition throughout the body. For example, AUC tissue:blood ratios for fentanyl, which encompass drug

distribution over the 240-minute period studied, were significantly greater than those for morphine in brain, liver, lung, heart, kidney, spleen, small intestine, stomach, and fat. This implies greater accumulation of fentanyl into these tissues out of the blood compared to morphine, which, in turn, suggests potential for deleterious fentanyl effects not only in organs directly involved in respiration, such as the lungs, but on cardiac function, removal of metabolic waste/filtration of blood (kidney and spleen), and gastrointestinal activity (stomach and small intestine). Furthermore, fentanyl accumulation in fat, implied by increasing tissue:blood ratios as well as higher AUC tissue:blood ratios compared to morphine, points to sequestration of this drug in adipose tissue after administration. This could entail release of fentanyl from fat in the hours after initial use. However, since fentanyl concentration in fat was already starting to decline at 240 minutes, and no fentanyl was detected in fat from mice sacrificed ~24 hrs after receiving their last repeated injection of 0.3 mg/kg fentanyl (see **Section 5.3.2**), such storage might not necessarily persist long-term. Gradual release from fat would also pose less of an immediate health risk than the predominately centrally-mediated respiratory depression that can occur within minutes after fentanyl use (Kuczyńska 2018). It is important to note, however, that the dose of fentanyl used in the present study was well below the lethal range demonstrated in mice (Gardocki et al. 1964; Newman et al. 2024). Upon receiving an LD10 dose of fentanyl (110 mg/kg sc), SKH1 mice demonstrated reduced cardiac glucose uptake 40 min and 6 hrs later, which clearly illustrates fentanyl's potential to modify the heart's normal functioning. Moreover, the myocardium expresses α_{1A} and α_{1B} adrenergic receptors (Jensen et al. 2009), for which fentanyl, but not morphine, has been shown to have an affinity (Torralva et al. 2020), highlighting one potential way in which the greater fentanyl AUC tissue:blood and tissue:blood

concentration ratios observed in heart in the present studies could translate to ramifications for cardiac health effects of fentanyl vs morphine.

Despite the striking differences between acute fentanyl and morphine biodistribution, these disparities were not universal. Specifically, no significant differences were observed between AUC tissue:blood ratios for large intestine or skin, which could suggest similarities in certain aspects of gastrointestinal function. In addition, while tissue:blood concentration ratios for liver, lung, heart, and kidney at 5 and 15 minutes appear higher than those for morphine, indicating more rapid sequestration of fentanyl into these tissues out of the blood, tissue:blood concentration ratios also demonstrated accumulation of both fentanyl and morphine in tissue over the 4-hr period, with concentrations of both these opioids in in spleen, small intestine, large intestine, and stomach steadily increasing relative to concentration in blood, albeit to different extents. Fentanyl and morphine also exhibited the same t_{max} in certain sample types, including blood, liver, lung, small intestine, stomach, and fat, showing similar time courses in certain tissues even with their differences in distribution.

Presence of fentanyl and morphine metabolites in several tissues seems to be consistent with prior knowledge of their metabolism. Specifically, norfentanyl was measured at significantly higher concentrations than fentanyl in liver at 60 min and was also present at earlier timepoints (4-ANPP was detected as well, but at lower concentrations than fentanyl), while morphine-3-β-D-glucuronide was quantified at significantly higher concentrations than morphine at 5, 15, and 60 min. This highlights the vital role of the liver in biotransformation of both fentanyl and morphine (Gabel et al. 2023; Iula 2017). Fentanyl was detected at significantly higher concentrations than metabolite in blood, brain, and kidney; although full ANOVA could not be run on metabolite data from lung, heart, spleen, small intestine, stomach, and fat,

metabolite concentrations were also notably smaller in those tissues. In muscle, a higher concentration of norfentanyl relative to fentanyl was measured at 60 min, while a slightly greater concentration of norfentanyl relative to fentanyl was detected in large intestine at 240 min, though differences could not be statistically analyzed due to lack of norfentanyl data at other time points. Norfentanyl was detected from at least one time point in whole blood, brain, liver, lung, heart, kidney, spleen, small intestine, large intestine, stomach, muscle, and fat, while 4-ANPP was detected from at least one time point in whole blood, brain, liver, lung, heart, and kidney. The low concentrations of these metabolites in organs other than liver further indicate that the liver is a principal site of fentanyl metabolism (Iula 2017). Conversely, morphine-3-β-d-glucuronide concentration, though not significantly greater than morphine, was observed to be present at similar levels to its parent compound in brain, kidney, and small intestine, as well as lung, muscle, fat, and whole blood. The metabolite was observed at significantly higher levels in heart at 60 min. UDP-glucuronosyltransferases, the family of enzymes chiefly responsible for morphine glucuronidation, are expressed in brain, kidney, and intestine as well as liver, which may account for the morphine-3-β-d-glucuronide concentrations observed in our data (Gabel et al. 2023). Presence of morphine-3-β-d-glucuronide in heart, lung, muscle, and fat, especially at 60 and 240 min, could potentially be explained by the increasing amounts of morphine-3-β-d-glucuronide in whole blood.

In brief, acute fentanyl and morphine biodistribution differed in both the central nervous system and the periphery. Though the liver was the primary site of metabolism for both opioids, fentanyl metabolites norfentanyl and 4-ANPP tended to be minimally present in most other tissues, while morphine-3-β-d-glucuronide also appeared at appreciable concentrations in tissues known to express UDP-glucuronosyltransferases, such as brain and kidney. It is also possible

that the difference in dose made biotransformation of morphine more readily detectable, since the dose of morphine (30 mg/kg) was 100-fold higher than the dose of fentanyl (0.3 mg/kg). As a whole, the aim to compare acute biodistribution of fentanyl and morphine in diverse murine matrices was accomplished, and the data support the hypotheses that fentanyl would demonstrate more rapid uptake in central tissues and greater accumulation in adipose tissue compared to morphine.

6.5. Acute Biodistribution of Fentanyl in Rodent Models.

Although several experiments on fentanyl biodistribution across various organs have been conducted in rats, the present findings augment such work by providing information on both fentanyl and morphine disposition in mice, another common model for studying opioid abuse. This accomplishes a dual purpose of contributing to the mouse literature on fentanyl distribution while enabling comparison with morphine, a traditional opiate. For example, after receiving 0.15-0.30 μg/min●kg fentanyl iv for 6 hr, followed by sacrifice immediately afterwards, Male Charles River F344 rats displayed higher concentrations of the opioid in fat (~115 ng/g) compared to kidney (~15-24 ng/g), liver (~16-17 ng/g), and muscle (~12-14 ng/g) (Björkman and Stanski 1988). This study followed a different time course (6 hr vs 240 min) and route of administration (iv vs sc) than the current acute study, as well as a different dose of fentanyl. However, a similar tendency for fentanyl concentration in fat to exceed that in kidney, liver, and muscle at the last time point studied (240 min) was observed, although average fentanyl concentration in kidney (42.3 ng/g) also appeared higher than that in liver (2.07 ng/g) and muscle (4.88 ng/g). Meanwhile, morphine concentration at 240 min in this subgroup of tissues was greatest in kidney (1190.5 ng/g), followed by fat (422 ng/g) and liver (172.3 ng/g) and was not detected in muscle. This highlights the observed tendency of fentanyl to accumulate

in adipose tissue to a greater extent than morphine following administration, although both opioids were continuing to undergo processing in the kidney at the last time point included.

In another study, male F1 hybrid rats received 13 μg/kg/hr fentanyl iv for 6 hr, after which 13 tissues (brain, heart, lungs, stomach, small intestine, large intestine, liver, pancreas, spleen, kidneys, testes, muscle, and fat) were harvested, and steady-state tissue/blood partition coefficients were determined (Björkman et al. 1990). Once again, fentanyl dose, route of administration, and time of sacrifice differed from the present acute biodistribution studies, and some of the tissues analyzed in Björkman et al.'s experiments (pancreas, testes) were not collected in the ones described above. Moreover, fentanyl concentration in samples (ng/g for solid tissue and ng/mL in blood) was quantified as opposed to calculating tissue/blood partition coefficients. However, after determining simple tissue to blood ratios of fentanyl from the data at the last time point (240 min), fat had one of the highest tissue:blood fentanyl concentration ratios (see **Table 5.2**). While Björkman et al. observed a high tissue/blood partition coefficient in fat for fentanyl, their partition coefficient for spleen was similarly high compared to the other tissues, whereas the ratio of tissue:blood fentanyl concentration in spleen was noticeably less than that for fat at 240 min (14 vs 37) in the present studies. Björkman et al also noted that fentanyl steady-state tissue/blood partition coefficients for lung, stomach, and kidneys, though lower than those for fat and spleen, were higher compared to brain, heart, small and large intestines, liver, and muscle. Although the tissue:blood fentanyl concentration ratio in mouse lung in the present studies was similar to those for heart, intestine, etc., tissue:blood concentration ratios for stomach and kidney did in fact tend to be higher than those for brain, heart, muscle, liver, etc. In contrast, morphine tissue:blood concentration ratios at 240 min were highest for large intestine, stomach, and kidney, followed by lower ratios for small intestine, spleen, brain, lung, heart, fat, and liver

(**see Table 5.3**). Fentanyl tissue:blood ratio for fat at this time point (37) was noticeably higher than that for morphine (5.0), as was fentanyl tissue:blood ratio for heart (12 vs 3.7 for morphine), suggesting greater sequestration of fentanyl in fat and certain central tissues. However, brain tissue:blood ratios (3.6 for fentanyl vs 5.3 for morphine) were similar at 240 min, highlighting that the prominent differences between fentanyl and morphine distribution to brain occur early after administration. Interestingly, morphine tissue:blood ratio in large intestine was much greater (268) than that for fentanyl (9.3) 240 min, pointing to differences in excretion at this time point.

In male Sprague-Dawley rats receiving 5 min of iv infusion with 5.25 μg/kg/min fentanyl, concentration of the opioid (ng/ml) in plasma, brain, and lung peaked at ~5 min (Elkiweri et al. 2009). Meanwhile, whole blood, brain, and lung samples in mice in the present studies exhibited fentanyl C_{max} at 15 min (although fentanyl concentration in blood at 5 and 15 min was almost identical). Differing modes of drug administration (5-min iv infusion vs single acute sc injection) might account for this discrepancy, though it could point to a need to assess additional time points between 5 and 15 minutes to better pinpoint time of peak fentanyl concentration. Meanwhile, morphine C_{max} was observed at 15 min in blood and lung but 60 min in brain, emphasizing that time course of fentanyl and morphine distribution differs in certain central tissues but displays similarities in other tissues.

In a fentanyl time course study in male Sprague-Dawley rats, animals received 50 μg/kg (tritium-labelled) fentanyl iv followed by sacrifice at 1.5, 5, 15, 30, 60, 120, or 240 min, a similar range to the current acute biodistribution study, albeit with different dosing and route of administration (Hug and Murphy 1981). Fentanyl uptake in lung, heart, and brain in these rats achieved maximal concentration at or before 1.5 min, and fentanyl elimination from these tissues

followed a similar time course to plasma. In contrast, fentanyl concentration peaked at 15 min in lung, heart, and brain samples in mice in the current experiments, although this is not surprising given the difference in routes of administration (iv vs sc), while morphine concentration peaked at 15 min in lung but 5 min in heart and 60 min in brain, indicating a more diverse time course among these tissues that contrasted with fentanyl results. However, the broad pattern of fentanyl distribution in whole blood, brain, heart, and lung in the current cohort (C_{max} observed at 15 min, followed by a sharp decline at 60 and 240 min) is similar across the different sample types. Meanwhile, morphine distribution exhibits this pattern of C_{max} observed at 15 min, followed by a sharp decline at 60 and 240 min in whole blood and lung, while heart morphine C_{max} was observed at 5 min and declined thereafter, and brain morphine concentration gradually increased to C_{max} at 60 min before tapering off, thus illustrating a disparity in cardiac and whole brain accumulation of morphine compared to fentanyl. Hug and Murphy also noted that fentanyl uptake into and elimination from fat and muscle occurred at a slower rate compared to the aforementioned tissues, and that fentanyl concentration was greater in both muscle (2-4x) and fat (30x) compared to plasma. While observed fentanyl C_{max} in muscle (15 min) was the same as that for brain, lung, and heart, and fentanyl concentration in muscle in the current studies was generally lower than in whole blood, a slower time course for fentanyl accumulation in fat was observed compared to tissues such as brain, liver, heart, and kidney, as well as markedly higher fentanyl concentrations in fat compared to blood at 60 and 240 min. On the other hand, observed morphine C_{max} in muscle in the present studies was the same as that for brain but later than that for heart and lung, while morphine concentrations in muscle (when detected) were lower than in blood. Morphine time course for accumulation in fat (C_{max} of 60 min) was similar to tissues such as brain and kidney but slower than heart and liver, with lower morphine concentrations in fat

than blood at 60 min but higher morphine concentrations in fat than blood at 240 min. This underscores morphine's lesser tendency to accumulate in fat due to being more hydrophilic than fentanyl. Interestingly, Hug and Murphy only observed the presence of a single fentanyl metabolite, despropionyl fentanyl (4-ANPP), in liver and kidney, while norfentanyl was detected in blood, brain, liver, lung, heart, kidney, spleen, small intestine, large intestine, stomach, muscle, and fat and 4-ANPP in blood, brain, liver, lung, heart, and kidney during at least one of the four time points in the current acute biodistribution studies. This could be due to differences in bioanalytical methods, although norfentanyl and 4-ANPP did appear to be present at higher concentrations in liver than in other murine tissues. Morphine's metabolite, morphine-3-β-D-glucuronide, was detected in blood, brain, liver, lung, heart, and kidney. Notably, whereas norfentanyl and 4-ANPP were often detected at seemingly lower concentrations than fentanyl (i.e. brain, lung, heart, kidney), there were time points where morphine-3-β-D-glucuronide concentration appeared higher than morphine (i.e. heart, kidney), though not approaching statistical significance. This illustrates potential metabolic differences between fentanyl and morphine in various tissue types.

In another study by Schneider and Brune (1986), female Wistar rats were injected iv over a 9-min period with ^{3}H-phenethyl-fentayl (5.96 μg of fentanyl per 100 g of body weight) or ^{14}C-anilino-fentanyl (6 μg of fentanyl per 100 g of body weight) and distribution of fentanyl and several of its metabolites (including norfentanyl and 4-ANPP) was assessed up to 270 min after injection. Fentanyl's phenethyl side chain and aniline region were labeled to aid in tracking metabolism. The data indicated that fentanyl C_{max} was reached earlier in brain (immediately after infusion) than in other organs, and that organs involved more prominently in metabolic processes, such as liver and kidney, were generally found to have greater presence of fentanyl

metabolites relative to brain. Appreciable amounts of fentanyl metabolites were also observed in small intestine and stomach. Tissues with an abundant blood supply that did not have a direct role in metabolism or excretion, such as heart, lung, and skeletal muscle, displayed an early peak in fentanyl concentration followed by metabolites, while these compounds took longer (90 min after infusion) to reach C_{max} in fat. Presumably due to the differences in injection route (iv in Schneider and Brune vs sc in the present studies), fentanyl C_{max} was reached at different times in the present studies; for example, fentanyl C_{max} was observed in brain at 15 min rather than immediately after infusion. However, the general pattern of distribution for fentanyl and its metabolites was similar in certain respects. For example, 60 min after injection, norfentanyl was present at greater quantities in liver and kidney than in brain, heart, or lung. In further keeping with this study, norfentanyl was detected at later time points (60 and 240 min) in fat, and fentanyl C_{max} was not reached in fat samples until 60 min after injection. Also, heart, lung, and muscle achieved fentanyl C_{max} at 15 min, while C_{max} for stomach, small intestine, and large intestine did not accumulate until 60 min. In contrast to Schneider and Brune (1986), however, only one metabolite, norfentanyl, was observed at a single time point (60 min) in these tissues. With regards to morphine, the metabolite morphine-3-β-D-glucuronide was present at greater concentrations in kidney and lung at 60 min compared to liver, heart, or brain, illustrating differences in distribution of metabolites between fentanyl and morphine. Unlike norfentanyl, morphine-3-β-D-glucuronide was present at all time points studied in fat, although, like fentanyl, morphine achieved C_{max} in fat 60 min after injection. Morphine also exhibited the same C_{max} as fentanyl in lung (15 min), stomach (60 min), and small intestine (60 min), indicating similar distribution timelines in peripheral tissues despite differences in morphine's C_{max} in heart (5 min) and muscle (60 min) compared to fentanyl.

Autoradiography studies of fentanyl biodistribution in rats, while not in perfect agreement with the above results, also appear to share certain commonalities, though the present data provide a broader perspective through comparisons of fentanyl concentration with morphine and shedding light on biodistribution in murine tissue. For example, in female Wistar rats injected with either ^{3}H-phenethyl-fentayl iv, 5.96 μg/100 g body weight or ^{14}C-anilino-fentanyl iv, 6 μg/100 g body weight, autoradiography revealed that fentanyl was most prominent in the central nervous system, heart, and lungs immediately after iv infusion (^{3}H-phenethyl-fentayl) (Schneider and Brune 1985). After 10 min, fentanyl had redistributed to kidney, stomach, and liver, although this redistribution, as well as redistribution to the small intestine and skeletal muscle, was more pronounced at 30 min (^{3}H-phenethyl-fentayl), and, by 90 min, most ^{3}H-phenethyl-fentayl was found in small intestine and kidney. At the latest post-injection time point, 270 min, fentanyl was primarily found in large intestine/colon, although trace amounts remained in stomach and kidney (Schneider and Brune 1985). Likewise, ^{14}C-anilino-fentanyl was present at high concentrations in the central nervous system, lungs, and heart immediately after infusion, in addition to the kidneys and liver. For the most part, ^{14}C-anilino-fentanyl redistribution was similar to ^{3}H-phenethyl-fentayl aside from slightly delayed accumulation in the kidney (which did not reach maximal concentration until 90 min) and lower concentrations in brain 10 minutes after the original iv injection. In the current studies, fentanyl concentration peaked at 15 min in whole blood, brain, liver, lung, heart, kidney, and muscle and at 60 min in spleen, small intestine, large intestine, stomach, fat, and skin. The pattern of fentanyl distribution observed was similar in certain respects to Schneider and Brune, i.e. initial high concentrations in brain, lung, and heart followed by distribution to stomach and small and large intestine at later time points. However, fentanyl reached C_{max} in liver and kidney sooner after injection (15 min) than ^{3}H-

phenethyl-fentayl or ^{14}C-anilino-fentanyl in Scheider and Brune's study, as did observed fentanyl C_{max} in muscle (15 min). Such differences in timing are presumably due to the different routes of drug administration used (sc vs iv). Meanwhile, morphine concentration in the current studies peaked at 5 min in heart and skin, 15 min in whole blood, liver, lung, and spleen, at 60 min in brain, muscle, kidney, small intestine, stomach, and fat, and at 240 min in large intestine. Initial high concentrations of morphine in lung and later distribution to stomach and small intestine are similar to the time course for fentanyl, although time course for peak concentration in other organs like kidney and large intestine appeared delayed compared to fentanyl. Meanwhile, in a whole-body radiography study comparing distribution of fentanyl and dihydromorphine (a semisynthetic opioid derived from morphine) in male and female mice, fentanyl was observed to be present at larger quantities in the central nervous system and intestinal contents (Appelgren et al. 1973). Though significant differences between fentanyl and normalized morphine concentrations in small or large intestine were not observed, fentanyl concentrations were significantly higher in brain at 5 and 15 min relative to normalized morphine.

The above protocol offers a few advantages compared to the above fentanyl biodistribution studies in rats. First, a thorough assessment of acute fentanyl biodistribution in mice, another widely-used preclinical model for studying opioid use, was conducted. Moreover, the analytical method enabled us to measure morphine alongside fentanyl, a feature not present in the analytical techniques from these previous experiments. These distribution studies also often featured iv administration of fentanyl over a protracted time period, which bears a closer resemblance to fentanyl administration during anesthesia (Stanley 2014). In contrast, the sc route of administration use in the present experiments is more in keeping with that used for respiratory depression studies (Elder et al. 2023; Varshneya et al. 2022) and may share similarities with

intranasal administration, one route of recreational or pathological fentanyl use (Abdulrahim et al. 2018), which increases the relevance of the current study. Unlike experiments that involved autoradiography (Schneider and Brune 1985), the method does not require use of radiolabeled compounds; instead, mass spectrometry can be used to reliably detect fentanyl, morphine, and their metabolites.

6.6. Acute Biodistribution of Morphine in Rodent Models.

Previous literature also lends a measure of support to the findings on morphine biodistribution, although, once again, the current data contributes additional insights due to the quantification of fentanyl along with morphine following acute administration.

In male Swiss Webster mice given 10 mg/kg morphine sc and sacrificed 60 min later, the highest concentrations of morphine (ng/g in solid tissue and ng/mL in serum) were observed in kidney, followed by lung and spleen, liver, serum, and brain (though concentrations varied slightly based on region since harvested brains were dissected into sections) (Bhargava and Bian 1998). Another study in which male Swiss Webster mice were sacrificed 60 min after receiving 10 mg/kg morphine sc reported similar relative concentrations of morphine (ng/g), with the greatest amounts present in kidney, approximately equal concentrations in lung and spleen, and the lowest concentrations in liver (Bian and Bhargava 1998). Since a 3-fold higher dose was used in the present studies, samples from these tissues contained higher absolute morphine concentrations 60 min after injection. However, examining relative morphine concentration among this subset of tissue types, morphine was also observed to be highest in kidney and lowest in liver, although morphine was higher in spleen than in lung (order from highest to lowest morphine concentration: kidney > spleen > lung > whole blood > whole brain > liver). In comparison, fentanyl concentrations at 60 min (ordered from highest to lowest) ranked kidney >

spleen > lung > whole brain > whole blood > liver, which suggests similar patterns of tissue distribution for fentanyl and morphine in this subset of tissues 60 min after administration. In addition to using a lower concentration of morphine than in the current studies, Bhargava and Bian quantified morphine concentration by radioimmunoassay rather than LC-MS/MS, which could account for these discrepancies.

Meanwhile, in male C57BL/6 mice administered 15 mg/kg morphine ip, morphine concentration (nmol/mg) steadily declined in liver from 10-60 min post-injection, while morphine-3-β-D-glucuronide concentration, though also decreasing from 10-60 min, remained higher than morphine at these time points (Chen et al. 2019). In plasma, morphine concentration (nM) steadily declined up to 60 min after injection, while morphine-3-β-D-glucuronide plasma concentration peaked at 20 min and appeared to be higher than morphine at this time point. In the current studies, morphine concentration (ng/mL) peaked in whole blood and liver at 15 min before tapering off at 60 min and beyond, while morphine-3-β-D-glucuronide concentration peaked at 60 min in whole blood and liver. This resulted in a significantly greater morphine-3-β-D-glucuronide concentration relative to morphine in liver at 60 min; in whole blood, even though the difference between morphine and its metabolite was not statistically significant, the numeric average for morphine-3-β-D-glucuronide concentration appeared higher. Thus, even with different dosing and route of administration, Chen et al. and the present experiments both demonstrate that decreases in morphine concentration coincide with increases in morphine-3-β-D-glucuronide due to glucuronidation of the parent compound over time. In comparison, fentanyl concentration reached C_{max} at 15 min in whole blood and liver, while norfentanyl C_{max} was observed at 60 min in whole blood and liver and 4-ANPP C_{max} was observed at 5 min in whole blood and 60 min in liver. Similarly to morphine-3-β-D-glucuronide, norfentanyl concentration

was significantly higher than its parent compound in liver at 60 min, although there was no significant difference between fentanyl and 4-ANPP concentration at this time point. In contrast with the relative levels of morphine and morphine-3-β-D-glucuronide in whole blood, however, fentanyl concentration was significantly greater than 4-ANPP at 60 min and appeared somewhat higher than norfentanyl. In another study in which morphine tissue distribution was analyzed after ip administration, C57BL6/J mice received 1.45 mg/kg morphine and were sacrificed 30 min later (Zhu et al. 2018). Morphine concentration (ng/g) in kidney appeared to be higher than morphine concentration in liver and plasma. At the nearest time point in the present studies, 15 min, similarly heightened concentration (ng/g) of morphine in kidney compared to whole blood and liver was observed, despite the sizable difference in dose. Concentration of fentanyl in kidney was also noticeably higher than in whole blood and liver at 15 min in fentanyl-treated mice. This indicates that, for both fentanyl and morphine, the parent compound was exiting the blood for distribution into tissue, undergoing metabolism in liver (hence the relatively low concentration), and undergoing appreciable filtration through the kidneys 15 min after administration.

In wild-type FVB/NRj mice administered 90 μmol/kg morphine by oral gavage and sacrificed 120 min later, relative concentrations of morphine (ng/mL), greatest to least, were kidney > small intestine > spleen > liver > brain, and relative concentrations of morphine-3-β-D-glucuronide were kidney > small intestine > liver > spleen > brain, with morphine-3-β-D-glucuronide concentrations in liver, kidney, and small intestine far exceeding those for morphine (Heydari et al. 2021). Though this exact time point was not included in the current studies, morphine data from those same tissues at 240 min indicated relative concentrations of morphine (ng/g), greatest to least, were kidney > small intestine > spleen > brain > liver, while relative

concentrations of morphine-3-β-D-glucuronide were kidney > small intestine > liver > brain (not detected in spleen). As a whole, observed distribution of morphine and morphine-3-β-D-glucuronide in this subset of tissues is similar to Heydari et al.'s findings, as are the somewhat larger morphine-3-β-D-glucuronide concentrations in liver, kidney, and small intestine than morphine, although these differences were not statistically significant (likely due to declining levels of metabolite). Concentrations of fentanyl and its metabolites were also quantitated in these tissues at 240 min. Specifically, relative concentrations of fentanyl (ng/g), greatest to least, were kidney > spleen > small intestine > brain > liver, relative concentrations of norfentanyl (ng/g) were kidney > brain > liver (metabolite was not detected in spleen or small intestine at this time point), and relative concentrations of 4-ANPP were kidney > brain > liver (metabolite was not detected in spleen or small intestine at this time point. Thus, patterns of fentanyl and morphine distribution within this subset of tissues appear similar at this time point. Although morphine-3-β-D-glucuronide was detected in kidney, small intestine, liver, and brain at 240 min, norfentanyl and 4-ANPP were not detected in small intestine, while none of these metabolites were detected in spleen. Brain concentrations of norfentanyl and 4-ANPP were higher than liver concentration at 240 min, while the reverse was true for morphine-3-β-D glucuronide, pointing to potential metabolic differences.

The acute biodistribution studies build upon the prior literature by comparing morphine concentration with the synthetic opioid fentanyl, and doing so in a wider range of murine tissue matrices (13 total) than those analyzed by certain previous groups. As stated in **Section 6.5**, the LC-MS/MS method is advantageous compared to techniques such as radioimmunoassay (Bian and Bhargava 1998) since it does not require radioactive isotopes to quantify our target analytes.

6.7. Biodistribution of Fentanyl, Morphine, and Select Metabolites after Repeated Opioid Exposure.

In the subset of samples analyzed (whole blood, brain, lung, and fat) in mice repeatedly exposed to 0.3 mg/kg fentanyl or 30 mg/kg morphine, the data indicate that repeated exposure to fentanyl or morphine is not sufficient to meaningfully change metabolism or distribution of these opioids, nor do these opioids accumulate in the tissues studied following the injection schedule used above. Specifically, fentanyl concentration in whole blood, lung, and fat at 60 min did not significantly differ between opioid-naïve and opioid-experienced mice, although fentanyl concentration in brain was slightly higher in opioid-naïve mice at 60 min. Morphine concentration in whole blood, lung, and fat at 60 min did not differ between opioid-naïve and opioid-experienced mice, nor, when detected, did concentrations of fentanyl and morphine metabolites. Therefore, the data do not support the hypothesis that fentanyl concentration in fat would be greater in mice receiving repeated fentanyl compared to mice receiving acute fentanyl. The results also disprove the hypothesis that differences in fat concentration between opioid-experienced and opioid-naïve mice would be greater in the fentanyl-treated mice compared to morphine-treated mice because, regardless of the opioid administered, significant differences were not observed in fat between acutely-treated and repeatedly-treated mice. This, in turn, implies that fentanyl is not sequestered in long-term storage in murine adipose tissue under the treatment schedule used.

Within the opioid-experienced cohort, normalized morphine concentration in whole blood was significantly higher than in fentanyl at 60 min; in contrast, morphine and fentanyl concentration in whole blood did not significantly differ at 60 min opioid-naïve mice, although normalized concentration of morphine still appeared somewhat higher than fentanyl in naïve

animals. In opioid-experienced mice, fentanyl concentration in brain was significantly greater than normalized morphine concentration at 60 min, while fentanyl and morphine concentration in brain in opioid-naïve mice did not differ significantly at this time point. However, fentanyl concentration still appeared slightly higher than morphine in naïve animals at this time point. In opioid-experienced mice, fentanyl and normalized morphine concentration did not significantly differ in lung at 60 min, nor were fentanyl and normalized morphine concentration significantly different in opioid-naïve mice. In opioid experienced mice, fentanyl concentration was greater than normalized morphine concentration in fat at 60 min, and fentanyl concentration in fat was also greater than morphine at this time point in opioid-naïve mice. This supports the hypothesis that fentanyl concentration in fat in repeatedly-treated mice would exceed morphine concentration in fat in repeatedly-treated mice. Be that as it may, the results as a whole do not provide compelling evidence for meaningful alterations to fentanyl or morphine biodistribution after repeated daily injections, which disproves the hypothesis that repeated exposure would affect tissue distribution of these opioids. However, the remaining harvested tissue samples will need to be analyzed to fully confirm this statement.

In opioid-experienced mice repeatedly treated with fentanyl, fentanyl concentration was significantly greater than norfentanyl in whole blood at 60 min, which was also observed in opioid-naïve mice that received acute fentanyl. In opioid-experienced mice, fentanyl concentration in lung was significantly higher than norfentanyl and 4-ANPP at 60 min; although data from lung could not be analyzed in opioid-naïve mice receiving fentanyl due to lack of 4-ANPP data at 5 and 240 min, concentration of fentanyl also appeared higher than its metabolites at this time point. Neither norfentanyl nor 4-ANPP was observed in brain at 60 min in opioid-experienced mice, despite both metabolites appearing at this time point in the brains of opioid-

naïve mice receiving acute fentanyl. Similarly, neither norfentanyl nor 4-ANPP was detected in opioid-experienced animals in fat at 60 min, although norfentanyl was observed at this time point in acutely-treated animals receiving fentanyl. In contrast, the morphine metabolite morphine-3-β-D glucuronide was observed at 60 min in whole brain, brain, lung, and fat in both acutely- and repeatedly-treated mice. Since norfentanyl and 4-ANPP tended to be present in only slight amounts in tissues other than liver in our acute biodistribution study, it is not necessarily surprising that they were not detected in all samples from opioid-experienced mice. This is particularly the case for fat since phase I metabolites like norfentanyl and 4-ANPP tend to be more polar than their parent compounds (Iula 2017), which might make these compounds less likely to accumulate in fat. Therefore, the data show that there are no robust differences in fentanyl metabolism in repeatedly-treated mice.

In opioid-experienced mice repeatedly treated with morphine, morphine-3-β-D-glucuronide concentration was significantly higher in whole-blood at 60 min. This poses a contrast to opioid-experienced mice that received fentanyl, in which concentration of the parent compound, fentanyl, in whole blood at 60 min was significantly higher than its detected metabolite, norfentanyl. Although morphine and its metabolite did not differ significantly at this time point in acutely-treated opioid-naïve mice, morphine-3-β-D-glucuronide concentration appeared noticeably greater at 60 min relative to morphine. In opioid-experienced mice repeatedly treated with morphine, morphine concentration was significantly greater than morphine-3-β-D glucuronide at 60 min, while morphine and morphine-3-β-D glucuronide concentration did not significantly differ in acutely-treated opioid-naïve mice, although morphine concentration still appeared slightly higher than its glucuronide at this time point. In opioid-experienced mice repeatedly treated with morphine, no significant differences were observed

between morphine and morphine-3-β-D glucuronide concentration in lung at 60 min; the same was true for lung samples from opioid-naïve mice. In opioid-experienced mice repeatedly treated with morphine, no significant differences were observed between morphine and morphine-3-β-D glucuronide concentration in fat at 60 min; the same was true for fat samples from opioid-naïve mice. Therefore, the data show that there are no major differences in morphine metabolism in repeatedly-treated mice compared to opioid-naïve mice.

Taken as a whole, the data from opioid-experienced mice (mice that received either 4-5 repeated daily injections of 0.3 mg/kg fentanyl or 4-5 repeated daily injections of 30 mg/kg morphine prior to sacrifice 60 min after the last injection) do no point to any significant changes in metabolism or storage of fentanyl and morphine. That being said, since only one post-injection time point was selected, potential analyte concentration changes over time in these repeatedly-treated mice could not be confirmed.

The repeated fentanyl and morphine injection schedule was intended to establish a history of exposure to opioids, not to model opioid tolerance. However, the lack of antinociceptive tolerance under this injection schedule was confirmed by testing repeatedly-injected mice in the warm-water tail withdrawal assay and determining that they did not differ from drug-naïve controls. Typically, multiple daily injections (Bilsky et al. 1996; Hill et al. 2016), or implantation of osmotic minipumps (Chan et al. 1997; Duttaroy et al. 1995) or subcutaneous pellets (Terman et al. 2004) are required to induce tolerance to fentanyl and/or morphine in mice.

6.8. Clinical Context.

The above studies have contributed a novel bioanalytical method for quantifying fentanyl and morphine in several murine tissues that was used to generate a detailed profile of acute fentanyl and morphine biodistribution in a preclinical mouse model. While drug elimination

occurs more quickly in rodents than in higher-order species (Hug and Murphy 1981), and lethal dose of fentanyl has been observed to be much higher in mice (Gardocki and Yelnosky 1964; Newman et al. 2024) than in humans (DEA), fentanyl demonstrates dramatically greater potency relative to morphine in both species (CDC 2023; Varshneya et al. 2022). Thus, mice remain a valuable model for examining the mechanisms that contribute to fentanyl's heightened potency and toxicity. For example, as mentioned in **Section 6.4**, AUC tissue:blood ratio for fentanyl in heart was significantly greater than that for morphine. Considering the impact of an LD10 of fentanyl on cardiac glucose uptake in other mouse models (Newman et al. 2024) and the fact that fentanyl could have nonspecific effects on the heart, i.e. via α_{1A} and α_{1B} receptors in myocardium (Jensen et al. 2009; Torralva et al. 2020), such data point to potential concerns about the cardiovascular ramifications of fentanyl abuse. Moreover, the present acute biodistribution studies also highlighted greater AUC tissue:blood ratio for fentanyl in lung compared to morphine. Depending on the route of administration, a limited number of case studies indicate risk of diffuse alveolar hemorrhage (Ruzycki et al. 2016) or pulmonary alveolar proteinosis (Chapman et al. 2012) after fentanyl use, emphasizing the potential for noxious pulmonary effects associated with this synthetic opioid. By adding to the current body of knowledge of fentanyl disposition in mice at doses known to cause respiratory depression, as well as elucidating the similarities and differences in fentanyl disposition compared to traditional opiates such as morphine, this research has played a role in investigating potential causes of fentanyl's unique lethality, a problem which is key to addressing the ongoing public health threat posed by the opioid crisis.

6.9. Future Directions

While these studies provide greater insight into the comparative biodistribution of fentanyl and morphine in a preclinical mouse model, they also open avenues for further investigation. Both respiratory depression and biodistribution studies exclusively used male mice. Thus, it remains an open question whether there are sex differences in tissue distribution of fentanyl and morphine in mice, especially since, according to prior literature, sex differences may occur in mice's response to fentanyl and morphine across various assays. For example, following morphine withdrawal, distinct alterations in GABAergic signaling in the bed nucleus of the stria terminalis were observed in males versus females (Luster et al. 2020), and C57BL/6J mice have been shown to exhibit sex-related differences in morphine withdrawal-associated behavior (Bravo et al. 2020). Prolonged (24-hour) exposure to morphine promoted vascular abnormalities in arteries from female, but not male, mice (Cheon et al. 2021), while Kest et al. reported sex differences in the effects of acute and chronic morphine on thermoregulation (Kest, Adler, and Hopkins 2000), as well as acute withdrawal (Kest et al. 2001) from and analgesic tolerance to morphine (Kest, Palmese, and Hopkins 2000). Moreover, female ICR mice displayed greater sensitivity to the effects of repeated morphine treatment on anxiety-like behaviors, locomotion, and social behaviors relative to males (Zhan et al. 2015). In addition, sex differences in expression of certain UGTs, the enzymes largely responsible for morphine metabolism, have been observed in mouse brain and liver (Buckley & Klaassen 2007). Sex differences have also been noted in fentanyl consumption and preference, as well as expression of Rho GTPases in the nucleus accumbens, in C57BL/6 mice placed on a fentanyl drinking schedule after being subjected to psychosocial stress (Franco et al. 2022). Mutant *Hnrnph1* mice (gene encoding an RNA-binding protein involved in post-transcriptional regulation of MOR

gene *Oprm1*) displayed sex-specific differences in fentanyl reinforcement and locomotor sensitization (Bryant et al. 2021), and mice with a genetic deletion of circadian protein NPAS2 demonstrated sex differences in fentanyl-induced hypersensitivity, dependence, and analgesic tolerance (Puig et al. 2022). Therefore, it would be of interest to replicate the current studies in female mice to determine if sex influences fentanyl and/or morphine biodistribution.

The data suggest a need for other directions of future study, as well. Since the repeated opioid biodistribution experiments were designed to test fentanyl and morphine distribution following a history of opioid exposure rather than establishment of tolerance, it remains to be determined whether chronic fentanyl or morphine treatment that induces tolerance would affect patterns of biodistribution in the murine model described herein. Moreover, while use of single doses of fentanyl (0.3 mg/kg) and morphine (30 mg/kg) was suitable for the goal of comparing biodistribution of the two opioid agonists at behaviorally equivalent doses, replicating the current studies with a wider range of doses could elucidate potential dose-response of fentanyl and morphine tissue distribution. Lastly, incorporation of additional time points into the acute biodistribution studies, both early after injection (i.e. between 5-15 min) and at later times than those covered in the present experiments (i.e. 6 hr, 12 hr) could aid in more accurately calculating parameters such as drug clearance and build upon the knowledge generated in these investigations.

6.10. Conclusion.

In summary, the initial aim to develop a novel bioanalytical method for quantifying fentanyl, norfentanyl, 4-ANPP, morphine, and morphine-3-β-D-glucuronide in 13 biological matrices (whole blood, brain, lung, heart, kidney, spleen, small intestine, large intestine, stomach, muscle, fat, and skin) in mice was achieved. Thus, the method was successfully utilized in

biodistribution studies of acute and repeated fentanyl and morphine. Acute biodistribution (5, 15, 60, and 240 min after injection) of doses of fentanyl (0.3 mg/kg sc) and morphine (30 mg/kg sc) producing comparable effects in respiratory depression was analyzed across these tissues in male Swiss Webster mice. Based on tissue:blood ratios of AUC data, fentanyl accumulation out of blood into tissue significantly exceed that of morphine in brain, liver, lung, heart, kidney, spleen, small intestine, stomach, and fat. However, no differences in AUC tissue:blood ratios were observed in large intestine or skin. The data thus underscore the potential for deleterious fentanyl effects in several organs, both those involved in respiratory depression and those not directly involved in respiratory depression, relative to classical opioids. Time course of drug distribution (i.e. time at which C_{max} was reached) between the two opioids varied based on tissue, i.e. peak morphine concentration accumulated later than fentanyl in brain but at the same time as fentanyl in tissues such as lung, stomach, and small intestine. The results support the hypothesis that the more lipophilic opioid, fentanyl, would accumulate to a greater extent in fat, though rapidity of fentanyl distribution depends on tissue type, and fentanyl and morphine biodistribution appear similar in certain organs. These findings point to appreciable temporary storage of fentanyl in fat relative to morphine, although fentanyl fat concentration had already declined at 240 min compared to peak concentration at 60 min, raising the possibility of fentanyl being released from adipose tissue at later time points after initial administration. Depending on dosage received, such a scenario could result in re-exposure to fentanyl over time as excess drug was released from fat stores, though not necessarily at lethal levels.

In mice given repeated daily injections (once/24 hrs) of 0.3 mg/kg fentanyl sc or 30 mg/kg morphine sc, opioid biodistribution in drug-experienced animals did not typically differ from biodistribution in opioid-naïve mice, nor did repeated daily injections of fentanyl or

morphine result in accumulation of these drugs in the samples studied (blood, brain, fat, and lung). Therefore, the data do not support the hypothesis that fentanyl would accumulate over time in adipose tissue of repeatedly-exposed mice.

Future directions for this area of study could include replications of the above experiments in female mice to investigate sex differences, studying the biodistribution effects of chronic fentanyl and morphine treatment schedules known to produce tolerance, or incorporating additional doses and time points.

REFERENCES

Abdulrahim, D. and Bowden-Jones, O. (2018). The misuse of synthetic opioids: harms and clinical management of fentanyl, fentanyl analogues and other novel synthetic opioids. On behalf of the NEPTUNE Group (Ed.). London: NEPTUNE.

Abrams, J. T., Horrow, J. C., Bennett, J. A., Van Riper, D. F., & Storella, R. J. (1996). Upper airway closure: a primary source of difficult ventilation with sufentanil induction of anesthesia. *Anesth Analg, 83*(3), 629-632. doi:10.1097/00000539-199609000-00034

Appelgren, L. E., & Terenius, L. (1973). Differences in the autoradiographic localization of labelled morphine-like analgesics in the mouse. *Acta Physiol Scand, 88*(2), 175-182. doi:10.1111/j.1748-1716.1973.tb05444.x

Baird, T. R., Akbarali, H. I., Dewey, W. L., Elder, H., Kang, M., Marsh, S. A., Peace, M. R., Poklis, J. L., Santos, E. J., & Negus, S. S. (2022). Opioid-like adverse effects of tianeptine in male rats and mice. *Psychopharmacology (Berl), 239*(7), 2187-2199. doi:10.1007/s00213-022-06093-w

Ban, B., Barrientos, R. C., Oertel, T., Komla, E., Whalen, C., Sopko, M., Yingjian, Y., Banerjee, P., Sulima, A., Jacobson, A. E., Rice, K. C., Matyas, G. R., & Yusibov, V. (2021). Novel chimeric monoclonal antibodies that block fentanyl effects and alter fentanyl biodistribution in mice. *MAbs, 13*(1), 1991552. doi:10.1080/19420862.2021.1991552

Barash, J. A., Ganetsky, M., Boyle, K. L., Raman, V., Toce, M. S., Kaplan, S., Lev, M. H., Worth, J. L., & DeMaria, A., Jr. (2018). Acute Amnestic Syndrome Associated with Fentanyl Overdose. *N Engl J Med, 378*(12), 1157-1158. doi:10.1056/NEJMc1716355

Bennett, J. A., Abrams, J. T., Van Riper, D. F., & Horrow, J. C. (1997). Difficult or impossible ventilation after sufentanil-induced anesthesia is caused primarily by vocal cord closure. *Anesthesiology, 87*(5), 1070-1074. doi:10.1097/00000542-199711000-00010

Benthuysen, J. L., Smith, N. T., Sanford, T. J., Head, N., & Dec-Silver, H. (1986). Physiology of alfentanil-induced rigidity. *Anesthesiology, 64*(4), 440-446. doi:10.1097/00000542-198604000-00005

Bentley, K. W. (1954). *The Chemistry of the Morphine Alkaloids (Monographs on the Chemistry of Natural Products)*. Oxford, UK: Clarendon Press.

Bhargava, H. N., & Bian, J. T. (1998). Effects of acute administration of L-arginine on morphine antinociception and morphine distribution in central and peripheral tissues of mice. *Pharmacol Biochem Behav, 61*(1), 29-33. doi:10.1016/s0091-3057(98)00067-7

Bian, J. T., & Bhargava, H. N. (1998). Effect of chronic administration of L-arginine, NG-nitro-L-arginine or their combination on morphine concentration in peripheral tissues and urine of the mouse. *Gen Pharmacol, 30*(5), 753-757. doi:10.1016/s0306-3623(97)00336-4

Bilsky, E. J., Inturrisi, C. E., Sadee, W., Hruby, V. J., & Porreca, F. (1996). Competitive and non-competitive NMDA antagonists block the development of antinociceptive tolerance to morphine, but not to selective mu or delta opioid agonists in mice. *Pain, 68*(2-3), 229-237. doi:10.1016/s0304-3959(96)03185-5

Björkman, S., & Stanski, D. R. (1988). Simultaneous determination of fentanyl and alfentanil in rat tissues by capillary column gas chromatography. *J Chromatogr, 433*, 95-104. doi:10.1016/s0378-4347(00)80588-5

Björkman, S., Stanski, D. R., Verotta, D., & Harashima, H. (1990). Comparative tissue concentration profiles of fentanyl and alfentanil in humans predicted from tissue/blood partition data obtained in rats. *Anesthesiology, 72*(5), 865-873. doi:10.1097/00000542-199005000-00017

Blakemore, P. R., & White, J. D. (2002). Morphine, the Proteus of organic molecules. *Chem Commun (Camb)*(11), 1159-1168. doi:10.1039/b111551k

Booth, J. V., Grossman, D., Moore, J., Lineberger, C., Reynolds, J. D., Reves, J. G., & Sheffield, D. (2002). Substance abuse among physicians: a survey of academic anesthesiology programs. *Anesth Analg, 95*(4), 1024-1030, table of contents. doi:10.1097/00000539-200210000-00043

Bravo, I. M., Luster, B. R., Flanigan, M. E., Perez, P. J., Cogan, E. S., Schmidt, K. T., & McElligott, Z. A. (2020). Divergent behavioral responses in protracted opioid withdrawal in male and female C57BL/6J mice. *Eur J Neurosci, 51*(3), 742-754. doi:10.1111/ejn.14580

Bremer, P. T., Kimishima, A., Schlosburg, J. E., Zhou, B., Collins, K. C., & Janda, K. D. (2016). Combatting Synthetic Designer Opioids: A Conjugate Vaccine Ablates Lethal Doses of Fentanyl Class Drugs. *Angew Chem Int Ed Engl, 55*(11), 3772-3775. doi:10.1002/anie.201511654

Brook, K., Bennett, J., & Desai, S. P. (2017). The Chemical History of Morphine: An 8000-year Journey, from Resin to de-novo Synthesis. *J Anesth Hist, 3*(2), 50-55. doi:10.1016/j.janh.2017.02.001

Bryant, C. D., Healy, A. F., Ruan, Q. T., Coehlo, M. A., Lustig, E., Yazdani, N., Luttik, K. P., Tran, T., Swancy, I., Brewin, L. W., Chen, M. M., & Szumlinski, K. K. (2021). Sex-dependent effects of an Hnrnph1 mutation on fentanyl addiction-relevant behaviors but not antinociception in mice. *Genes Brain Behav, 20*(3), e12711. doi:10.1111/gbb.12711

Buckley, D. B., & Klaassen, C. D. (2007). Tissue- and gender-specific mRNA expression of UDP-glucuronosyltransferases (UGTs) in mice. *Drug Metab Dispos, 35*(1), 121-127. doi:10.1124/dmd.106.012070

Butora, G. a. H., Tomas. (1998). The Story of Morphine Structure Elucidation: 100 Years of Deductive Reasoning. *Organic Synthesis: Theory and Applications, 4*(1-51).

Centers for Disease Control and Prevention. (2015). *Increases in Fentanyl Drug Confiscations and Fentanyl-related Overdose Fatalities*. Retrieved from https://emergency.cdc.gov/han/han00384.asp

Centers for Disease Control and Prevention. (2023, August 8, 2023). Fentanyl. Retrieved from https://www.cdc.gov/opioids/basics/fentanyl.html

Centers for Disease Control and Prevention. (2023, August 23, 2023). Opioid Overdose. Retrieved from https://www.cdc.gov/drugoverdose/deaths/opioid-overdose.html#synthetic

Chan, K. W., Duttory, A., & Yoburn, B. C. (1997). Magnitude of tolerance to fentanyl is independent of mu-opioid receptor density. *Eur J Pharmacol, 319*(2-3), 225-228. doi:10.1016/s0014-2999(96)00960-0

Chapman, E., Leipsic, J., Satkunam, N., & Churg, A. (2012). Pulmonary alveolar proteinosis as a reaction to fentanyl patch smoke. *Chest, 141*(5), 1321-1323. doi:10.1378/chest.11-1462

Chen, M., Guo, L., Dong, D., Yu, F., Zhang, T., & Wu, B. (2019). The nuclear receptor Shp regulates morphine withdrawal syndrome via modulation of Ugt2b expression in mice. *Biochem Pharmacol, 161*, 163-172. doi:10.1016/j.bcp.2019.01.019

Cheon, S., Tomcho, J. C., Edwards, J. M., Bearss, N. R., Waigi, E., Joe, B., McCarthy, C. G., & Wenceslau, C. F. (2021). Opioids Cause Sex-Specific Vascular Changes via Cofilin-Extracellular Signal-Regulated Kinase Signaling: Female Mice Present Higher Risk of Developing Morphine-Induced Vascular Dysfunction than Male Mice. *J Vasc Res, 58*(6), 392-402. doi:10.1159/000517555

Comstock, M. K., Carter, J. G., Moyers, J. R., & Stevens, W. C. (1981). Rigidity and hypercarbia associated with high dose fentanyl induction of anesthesia. *Anesth Analg, 60*(5), 362-363.

Crone, S. A., Viemari, J. C., Droho, S., Mrejeru, A., Ramirez, J. M., & Sharma, K. (2012). Irregular Breathing in Mice following Genetic Ablation of V2a Neurons. *J Neurosci, 32*(23), 7895-7906. doi:10.1523/JNEUROSCI.0445-12.2012

Criée, C. P., Sorichter, S., Smith, H. J., Kardos, P., Merget, R., Heise, D., Berdel, D., Köhler, D., Magnussen, H., Marek, W., Mitfessel, H., Rasche, K., Rolke, M., Worth, H., Jörres, R. A., & Working Group for Body Plethysmography of the German Society for Pneumology and Respiratory Care. (2011). Body plethysmography—its principles and clinical use. Respir Med, 105(7), 959-971. doi:10.1016/j.rmed.2011.02.006

Darke, S., & Duflou, J. (2016). The toxicology of heroin-related death: estimating survival times. *Addiction, 111*(9), 1607-1613. doi:10.1111/add.13429

Davenport-Hines, R. (2002). *The Pursuit of Oblivion: A Global History of Narcotics*. New York: Norton.

de Quincey, T. (1821). *Confessions of an English Opium Eater*

de Waal, P. W., Shi, J., You, E., Wang, X., Melcher, K., Jiang, Y., Xu, H. E., & Dickson, B. M. (2020). Molecular mechanisms of fentanyl mediated beta-arrestin biased signaling. *PLoS Comput Biol, 16*(4), e1007394. doi:10.1371/journal.pcbi.1007394

Dosen-Micovic, L., Ivanovic, M., & Micovic, V. (2006). Steric interactions and the activity of fentanyl analogs at the mu-opioid receptor. *Bioorg Med Chem, 14*(9), 2887-2895. doi:10.1016/j.bmc.2005.12.010

Duttaroy, A., & Yoburn, B. C. (1995). The effect of intrinsic efficacy on opioid tolerance. *Anesthesiology, 82*(5), 1226-1236. doi:10.1097/00000542-199505000-00018

Elder, H. J., Varshneya, N. B., Walentiny, D. M., & Beardsley, P. M. (2023). Amphetamines modulate fentanyl-depressed respiration in a bidirectional manner. *Drug Alcohol Depend, 243*, 109740. doi:10.1016/j.drugalcdep.2022.109740

Elkiweri, I. A., Zhang, Y. L., Christians, U., Ng, K. Y., Tissot van Patot, M. C., & Henthorn, T. K. (2009). Competitive substrates for P-glycoprotein and organic anion protein transporters differentially reduce blood organ transport of fentanyl and loperamide: pharmacokinetics and pharmacodynamics in Sprague-Dawley rats. *Anesth Analg, 108*(1), 149-159. doi:10.1213/ane.0b013e31818e0bd1

Ellis, C. R., Kruhlak, N. L., Kim, M. T., Hawkins, E. G., & Stavitskaya, L. (2018). Predicting opioid receptor binding affinity of pharmacologically unclassified designer substances using molecular docking. *PLoS One, 13*(5), e0197734. doi:10.1371/journal.pone.0197734

Ferreira, E., Corte Real, F., Pinho, E. M. T., & Margalho, C. (2020). A Novel Bioanalytical Method for the Determination of Opioids in Blood and Pericardial Fluid. *J Anal Toxicol, 44*(8), 754-768. doi:10.1093/jat/bkaa064

Florida State University. Functional Groups. Retrieved from https://www.chem.fsu.edu/chemlab/chm1046course/functional.html

Franco, D., Wulff, A. B., Lobo, M. K., & Fox, M. E. (2022). Chronic Physical and Vicarious Psychosocial Stress Alter Fentanyl Consumption and Nucleus Accumbens Rho GTPases in Male and Female C57BL/6 Mice. *Front Behav Neurosci, 16*, 821080. doi:10.3389/fnbeh.2022.821080

Gabel, F., Hovhannisyan, V., Andry, V., & Goumon, Y. (2023). Central metabolism as a potential origin of sex differences in morphine antinociception but not induction of antinociceptive tolerance in mice. *Br J Pharmacol, 180*(7), 843-861. doi:10.1111/bph.15792

Gardocki, J. F., & Yelnosky, J. (1964). A Study of Some of the Pharmacologic Actions of Fentanyl Citrate. *Toxicol Appl Pharmacol, 6*, 48-62. doi:10.1016/0041-008x(64)90021-3

Gaugler, S., Rykyl, J., Grill, M., and Cebolla, V. L. (2018). Fully automated drug screening of dried blood spots using online LC-MS/MS analysis. *Journal of Applied Bioanalysis, 4*(1), 7-15.

Giannakopoulou, C. E., Sotiriou, A., Dettoraki, M., Yang, M., Perlikos, F., Toumpanakis, D., Prezerakos, G., Koutsourelakis, I., Kastis, G. A., Vassilakopoulou, V., Mizi, E., Papalois, A., Greer, J. J., & Vassilakopoulos, T. (2019). Regulation of breathing pattern by IL-10. *Am J Physiol Regul Integr Comp Physiol, 317*(1), R190-R202. doi:10.1152/ajpregu.00065.2019

Glovak, Z. T., Baghdoyan, H. A., & Lydic, R. (2022). Fentanyl and neostigmine delivered to mouse prefrontal cortex differentially alter breathing. *Respir Physiol Neurobiol, 303*, 103924. doi:10.1016/j.resp.2022.103924

Grell, F. L., Koons, R. A., & Denson, J. S. (1970). Fentanyl in anesthesia: a report of 500 cases. *Anesth Analg, 49*(4), 523-532.

Griswold, M. K., Chai, P. R., Krotulski, A. J., Friscia, M., Chapman, B., Boyer, E. W., Logan, B. K., & Babu, K. M. (2018). Self-identification of nonpharmaceutical fentanyl exposure following heroin overdose. *Clin Toxicol (Phila), 56*(1), 37-42. doi:10.1080/15563650.2017.1339889

Grung, M., Skurtveit, S., Aasmundstad, T. A., Handal, M., Alkana, R. L., & Morland, J. (1998). Morphine-6-glucuronide-induced locomotor stimulation in mice: role of opioid receptors. *Pharmacol Toxicol, 82*(1), 3-10. doi:10.1111/j.1600-0773.1998.tb01390.x

Guillot, E., de Mazancourt, P., Durigon, M., & Alvarez, J. C. (2007). Morphine and 6-acetylmorphine concentrations in blood, brain, spinal cord, bone marrow and bone after lethal acute or chronic diacetylmorphine administration to mice. *Forensic Sci Int, 166*(2-3), 139-144. doi:10.1016/j.forsciint.2006.03.029

Gulland, J. R., and Robinson, R. (1925). The constitution of codeine and thebaine. *Mem. Proc. Manchester Lit. Phil. Soc., 69*, 79.

Handal, M., Grung, M., Skurtveit, S., Ripel, A., & Morland, J. (2002). Pharmacokinetic differences of morphine and morphine-glucuronides are reflected in locomotor activity. *Pharmacol Biochem Behav, 73*(4), 883-892. doi:10.1016/s0091-3057(02)00925-5

Harris, L. S., & Pierson, A. K. (1964). Some Narcotic Antagonists in the Benzomorphan Series. *J Pharmacol Exp Ther, 143*, 141-148.

Heydari, P., Martins, M. L. F., Rosing, H., Hillebrand, M. J. X., Gebretensae, A., Schinkel, A. H., & Beijnen, J. H. (2021). Development and validation of a UPLC-MS/MS method with a broad linear dynamic range for the quantification of morphine, morphine-3-glucuronide and morphine-6-glucuronide in mouse plasma and tissue homogenates. *J Chromatogr B Analyt Technol Biomed Life Sci, 1166*, 122403. doi:10.1016/j.jchromb.2020.122403

Hill, R., Lyndon, A., Withey, S., Roberts, J., Kershaw, Y., MacLachlan, J., Lingford-Hughes, A., Kelly, E., Bailey, C., Hickman, M., & Henderson, G. (2016). Ethanol Reversal of Tolerance to the Respiratory Depressant Effects of Morphine. *Neuropsychopharmacology, 41*(3), 762-773. doi:10.1038/npp.2015.201

Hill, R., Sanchez, J., Lemel, L., Antonijevic, M., Hosking, Y., Mistry, S. N., Kruegel, A. C., Javitch, J. A., Lane, J. R., & Canals, M. (2023). Assessment of the potential of novel and classical opioids to induce respiratory depression in mice. *Br J Pharmacol, 180*(24), 3160-3174. doi:10.1111/bph.16199

Hill, R., Santhakumar, R., Dewey, W., Kelly, E., & Henderson, G. (2020). Fentanyl depression of respiration: Comparison with heroin and morphine. *Br J Pharmacol, 177*(2), 254-266. doi:10.1111/bph.14860

Hodgson, B. (2001). *In the Arms of Morpheus: The Tragic History of Laudanum, Morphine, and Patent Medicines*. Buffalo, New York: Firefly Books.

Hug, C. C., Jr., & Murphy, M. R. (1981). Tissue redistribution of fentanyl and termination of its effects in rats. *Anesthesiology, 55*(4), 369-375. doi:10.1097/00000542-198110000-00006

International Council for Harmonisation of Technical Requirements for Pharmaceuticals for Human Use. (2022). Bioanalytical Method Validation and Study Sample Analysis. In (M10 ed.).

Ishikawa, K., Shibanoki, S., & McGaugh, J. L. (1983). Direct correlation between level of morphine and its biochemical effect on monoamine systems in mouse brain. Evidence for involvement of dopaminergic neurons in the pharmacological action of acute morphine. *Biochem Pharmacol, 32*(9), 1473-1478. doi:10.1016/0006-2952(83)90468-9

Iula, D. M. (2017). What Do We Know about the Metabolism of the New Fentanyl Derivatives? Retrieved from https://www.caymanchem.com/news/what-do-we-know-about-the-metabolism-of-the-new-fentanyl-derivative

Jannetto, P. J., Helander, A., Garg, U., Janis, G. C., Goldberger, B., & Ketha, H. (2019). The Fentanyl Epidemic and Evolution of Fentanyl Analogs in the United States and the European Union. *Clin Chem, 65*(2), 242-253. doi:10.1373/clinchem.2017.281626

Jensen, B. C., Swigart, P. M., De Marco, T., Hoopes, C., & Simpson, P. C. (2009). alpha1-Adrenergic receptor subtypes in nonfailing and failing human myocardium. *Circ Heart Fail, 2*(6), 654-663. doi:10.1161/CIRCHEARTFAILURE.108.846212

Jin, W. Q., Xu, H., & Chi, Z. Q. (1986). [Absorption, distribution and excretion of 3-methyl[carbonyl-14C] fentanyl in mice]. *Zhongguo Yao Li Xue Bao, 7*(5), 399-401.

Kalvass, J. C., Olson, E. R., Cassidy, M. P., Selley, D. E., & Pollack, G. M. (2007). Pharmacokinetics and pharmacodynamics of seven opioids in P-glycoprotein-competent mice: assessment of unbound brain EC50,u and correlation of in vitro, preclinical, and clinical data. *J Pharmacol Exp Ther, 323*(1), 346-355. doi:10.1124/jpet.107.119560

Kapoor, A., Martinez-Rosell, G., Provasi, D., de Fabritiis, G., & Filizola, M. (2017). Dynamic and Kinetic Elements of micro-Opioid Receptor Functional Selectivity. *Sci Rep, 7*(1), 11255. doi:10.1038/s41598-017-11483-8

Karinen, R., Andersen, J. M., Ripel, A., Hasvold, I., Hopen, A. B., Morland, J., & Christophersen, A. S. (2009). Determination of heroin and its main metabolites in small sample volumes of whole blood and brain tissue by reversed-phase liquid chromatography-tandem mass spectrometry. *J Anal Toxicol, 33*(7), 345-350. doi:10.1093/jat/33.7.345

Kelly, E., Sutcliffe, K., Cavallo, D., Ramos-Gonzalez, N., Alhosan, N., & Henderson, G. (2023). The anomalous pharmacology of fentanyl. *Br J Pharmacol, 180*(7), 797-812. doi:10.1111/bph.15573

Kest, B., Adler, M., & Hopkins, E. (2000). Sex differences in thermoregulation after acute and chronic morphine administration in mice. *Neurosci Lett, 291*(2), 126-128. doi:10.1016/s0304-3940(00)01393-8

Kest, B., Palmese, C., & Hopkins, E. (2000). A comparison of morphine analgesic tolerance in male and female mice. *Brain Res, 879*(1-2), 17-22. doi:10.1016/s0006-8993(00)02685-8

Kest, B., Palmese, C. A., Hopkins, E., Adler, M., & Juni, A. (2001). Assessment of acute and chronic morphine dependence in male and female mice. *Pharmacol Biochem Behav, 70*(1), 149-156. doi:10.1016/s0091-3057(01)00600-1

Kintz, P., Villain, M., Dumestre, V., & Cirimele, V. (2005). Evidence of addiction by anesthesiologists as documented by hair analysis. *Forensic Sci Int, 153*(1), 81-84. doi:10.1016/j.forsciint.2005.04.033

Kuczynska, K., Grzonkowski, P., Kacprzak, L., & Zawilska, J. B. (2018). Abuse of fentanyl: An emerging problem to face. *Forensic Sci Int, 289*, 207-214. doi:10.1016/j.forsciint.2018.05.042

Kurita, A., Miyauchi, Y., Ikushiro, S., Mackenzie, P. I., Yamada, H., & Ishii, Y. (2017). Comprehensive Characterization of Mouse UDP-Glucuronosyltransferase (Ugt) Belonging to the Ugt2b Subfamily: Identification of Ugt2b36 as the Predominant Isoform Involved in Morphine Glucuronidation. *J Pharmacol Exp Ther, 361*(2), 199-208. doi:10.1124/jpet.117.240382

Lauren, A. (1847). Sur la composition des alcalis organiques et de quelques combinaisons azolées. *Ann Chim Phys, 19*, 359-361.

Lawrence, A. J., Michalkiewicz, A., Morley, J. S., MacKinnon, K., & Billington, D. (1992). Differential inhibition of hepatic morphine UDP-glucuronosyltransferases by metal ions. *Biochem Pharmacol, 43*(11), 2335-2340. doi:10.1016/0006-2952(92)90311-6

Leal, T., Lebacq, J., Vanbinst, R., Lederman, C., De Kock, M., & Wallemacq, P. (2006). Successful protocol of anaesthesia for measuring transepithelial nasal potential difference in spontaneously breathing mice. *Lab Anim, 40*(1), 43-52. doi:10.1258/002367706775404480

Lipiński, P. F. J., Jaronczyk, M., Dobrowolski, J. C., & Sadlej, J. (2019). Molecular dynamics of fentanyl bound to mu-opioid receptor. *J Mol Model, 25*(5), 144. doi:10.1007/s00894-019-3999-2

Lowenstein, E., Hallowell, P., Levine, F. H., Daggett, W. M., Austen, W. G., & Laver, M. B. (1969). Cardiovascular response to large doses of intravenous morphine in man. *N Engl J Med, 281*(25), 1389-1393. doi:10.1056/NEJM196912182812503

Lunn, J. K., Stanley, T. H., Eisele, J., Webster, L., & Woodward, A. (1979). High dose fentanyl anesthesia for coronary artery surgery: plasma fentanyl concentrations and influence of nitrous oxide on cardiovascular responses. *Anesth Analg, 58*(5), 390-395.

Luster, B. R., Cogan, E. S., Schmidt, K. T., Pati, D., Pina, M. M., Dange, K., & McElligott, Z. A. (2020). Inhibitory transmission in the bed nucleus of the stria terminalis in male and female mice following morphine withdrawal. *Addict Biol, 25*(3), e12748. doi:10.1111/adb.12748

Macmadu, A., Carroll, J. J., Hadland, S. E., Green, T. C., & Marshall, B. D. (2017). Prevalence and correlates of fentanyl-contaminated heroin exposure among young adults who use prescription opioids non-medically. *Addict Behav, 68*, 35-38. doi:10.1016/j.addbeh.2017.01.014

Mahonski, S. G., Leonard, J. B., Gatz, J. D., Seung, H., Haas, E. E., & Kim, H. K. (2020). Prepacked naloxone administration for suspected opioid overdose in the era of illicitly manufactured fentanyl: a retrospective study of regional poison center data. *Clin Toxicol (Phila), 58*(2), 117-123. doi:10.1080/15563650.2019.1615622

Mather, L. E. (1983). Clinical pharmacokinetics of fentanyl and its newer derivatives. *Clin Pharmacokinet, 8*(5), 422-446. doi:10.2165/00003088-198308050-00004

Mayer, S., Boyd, J., Collins, A., Kennedy, M. C., Fairbairn, N., & McNeil, R. (2018). Characterizing fentanyl-related overdoses and implications for overdose response: Findings from a rapid ethnographic study in Vancouver, Canada. *Drug Alcohol Depend, 193*, 69-74. doi:10.1016/j.drugalcdep.2018.09.006

Meissner, W. (1819). Uber Pflanzenalkalien: II. Uber ein neues pflanzenalkali (alkaloid). *J Chem Phys, 25*(379-381).

Moe, J., Godwin, J., Purssell, R., O'Sullivan, F., Hau, J. P., Purssell, E., Curran, J., Doyle-Waters, M. M., Brasher, P. M. A., Buxton, J. A., & Hohl, C. M. (2020). Naloxone dosing in the era of ultra-potent opioid overdoses: a systematic review. *CJEM, 22*(2), 178-186. doi:10.1017/cem.2019.471

Murphy, P. B., Bechmann, S., & Barrett, M. J. (2024). Morphine. In *StatPearls*. Treasure Island (FL) ineligible companies. Disclosure: Samuel Bechmann declares no relevant financial relationships with ineligible companies. Disclosure: Michael Barrett declares no relevant financial relationships with ineligible companies.

Newman, M., Lynch, C., Connery, H., Goldsmith, W., Nurkiewicz, T., Raylman, R., & Boyd, J. (2024). Fentanyl overdose: Temporal effects and prognostic factors in SKH1 mice. *Basic Clin Pharmacol Toxicol, 134*(4), 460-471. doi:10.1111/bcpt.13984

Oiestad, E. L., Johansen, U., Oiestad, A. M., & Christophersen, A. S. (2011). Drug screening of whole blood by ultra-performance liquid chromatography-tandem mass spectrometry. *J Anal Toxicol, 35*(5), 280-293. doi:10.1093/anatox/35.5.280

Peirson, S. N., Brown, L. A., Pothecary, C. A., Benson, L. A., & Fisk, A. S. (2018). Light and the laboratory mouse. *J Neurosci Methods, 300*, 26-36. doi:10.1016/j.jneumeth.2017.04.007

Philadelphia, U. o. t. S. i. (2006). *Remington: The Science and Practice of Pharmacy.* (21 ed.). Philadelphia: Lippincott Williams & Wilkins.

Powers, N., Massena, C., Crouse, B., Smith, M., Hicks, L., Evans, J. T., Miller, S., Pravetoni, M., & Burkhart, D. (2023). Self-Adjuvanting TLR7/8 Agonist and Fentanyl Hapten Co-Conjugate Achieves Enhanced Protection against Fentanyl Challenge. *Bioconjug Chem, 34*(10), 1811-1821. doi:10.1021/acs.bioconjchem.3c00347

Puig, S., Shelton, M. A., Barko, K., Seney, M. L., & Logan, R. W. (2022). Sex-specific role of the circadian transcription factor NPAS2 in opioid tolerance, withdrawal and analgesia. *Genes Brain Behav, 21*(7), e12829. doi:10.1111/gbb.12829

Raffa, R. B., Pergolizzi, J. V., Jr., LeQuang, J. A., Taylor, R., Jr., Group, N. R., Colucci, S., & Annabi, M. H. (2018). The fentanyl family: A distinguished medical history tainted by abuse. *J Clin Pharm Ther, 43*(1), 154-158. doi:10.1111/jcpt.12640

Raleigh, M. D., Baruffaldi, F., Peterson, S. J., Le Naour, M., Harmon, T. M., Vigliaturo, J. R., Pentel, P. R., & Pravetoni, M. (2019). A Fentanyl Vaccine Alters Fentanyl Distribution and Protects against Fentanyl-Induced Effects in Mice and Rats. *J Pharmacol Exp Ther, 368*(2), 282-291. doi:10.1124/jpet.118.253674

Redford, A., & Powell, B. (2016). Dynamics of Intervention in the War on Drugs: The Buildup to the Harrison Act of 1914. *The Independent Review, 20*(4), 509-530.

Roy, S. D., & Flynn, G. L. (1988). Solubility and related physicochemical properties of narcotic analgesics. *Pharm Res, 5*(9), 580-586. doi:10.1023/a:1015994030251

Ruzycki, S., Yarema, M., Dunham, M., Sadrzadeh, H., & Tremblay, A. (2016). Intranasal Fentanyl Intoxication Leading to Diffuse Alveolar Hemorrhage. *J Med Toxicol, 12*(2), 185-188. doi:10.1007/s13181-015-0509-5

Schneider, E., & Brune, K. (1985). Distribution of fentanyl in rats: an autoradiographic study. *Naunyn Schmiedebergs Arch Pharmacol, 331*(4), 359-363. doi:10.1007/BF00500820

Schneider, E., & Brune, K. (1986). Opioid activity and distribution of fentanyl metabolites. *Naunyn Schmiedebergs Arch Pharmacol, 334*(3), 267-274. doi:10.1007/BF00508781

Sertürner, F. W. A. (1806). Darstellung der reinen Mohnsäure (Opiumsäure) nebst einer Chemischen Untersuchung des Opiums mit vorzüglicher Hinsicht auf einendarin neu entdeckten Stoff und die dahin gehörigen Bemerkungen. *J Pharme Ärzte, Apoth Chem., 14*, 47-93.

Smith, L. C., Bremer, P. T., Hwang, C. S., Zhou, B., Ellis, B., Hixon, M. S., & Janda, K. D. (2019). Monoclonal Antibodies for Combating Synthetic Opioid Intoxication. *J Am Chem Soc, 141*(26), 10489-10503. doi:10.1021/jacs.9b04872

Somerville, N. J., O'Donnell, J., Gladden, R. M., Zibbell, J. E., Green, T. C., Younkin, M., Ruiz, S., Babakhanlou-Chase, H., Chan, M., Callis, B. P., Kuramoto-Crawford, J., Nields, H. M., & Walley, A. Y. (2017). Characteristics of Fentanyl Overdose - Massachusetts, 2014-2016. *MMWR Morb Mortal Wkly Rep, 66*(14), 382-386. doi:10.15585/mmwr.mm6614a2

Spencer, M. R., Warner, M., Cisewski, J. A., Miniño, A., Dodds, D., Perera, J., and Ahmad, F. B. (2023). *Estimates of Drug Overdose Deaths Involving Fentanyl, Methamphetamine, Cocaine, Heroin, and Oxycodone: United States, 2021* (27). Retrieved from

Stanley, T. H. (1992). The history and development of the fentanyl series. *J Pain Symptom Manage, 7*(3 Suppl), S3-7. doi:10.1016/0885-3924(92)90047-l

Stanley, T. H. (2014). The fentanyl story. *J Pain, 15*(12), 1215-1226. doi:10.1016/j.jpain.2014.08.010

Stanley, T. H. (2014). The history of opioid use in anesthetic delivery. In E. I. Eger, 2nd, Saidman, L.J., and Westhorpe, R.N. (Ed.), *The Wondrous Story of Anesthesia*. New York: Springer.

Stout, P. R., Claffey, D. J., & Ruth, J. A. (1998). Fentanyl in hair. Chemical factors involved in accumulation and retention of fentanyl in hair after external exposure or in vivo deposition. *Drug Metab Dispos, 26*(7), 689-700.

Sutcliffe, K. J., Charlton, S. J., Sessions, R. B., Henderson, G., and Kelly, E. (2021). Fentanyl binds to the μ-opioid receptor via the lipid membrane and transmembrane helices. *bioRxiv*.

Sutter, M. E., Gerona, R. R., Davis, M. T., Roche, B. M., Colby, D. K., Chenoweth, J. A., Adams, A. J., Owen, K. P., Ford, J. B., Black, H. B., & Albertson, T. E. (2017). Fatal Fentanyl: One Pill Can Kill. *Acad Emerg Med, 24*(1), 106-113. doi:10.1111/acem.13034

System, N. F. L. I. (2017). *NFLIS Brief: Fentanyl and Fentanyl-Related Substances Reported in NFLIS, 2015–2016*. Retrieved from

Terman, G. W., Jin, W., Cheong, Y. P., Lowe, J., Caron, M. G., Lefkowitz, R. J., & Chavkin, C. (2004). G-protein receptor kinase 3 (GRK3) influences opioid analgesic tolerance but not opioid withdrawal. *Br J Pharmacol, 141*(1), 55-64. doi:10.1038/sj.bjp.0705595

Torralva, R., Eshleman, A. J., Swanson, T. L., Schmachtenberg, J. L., Schutzer, W. E., Bloom, S. H., Wolfrum, K. M., Reed, J. F., & Janowsky, A. (2020). Fentanyl but not Morphine Interacts with Nonopioid Recombinant Human Neurotransmitter Receptors and Transporters. *J Pharmacol Exp Ther, 374*(3), 376-391. doi:10.1124/jpet.120.265561

Trease, G. E. (1964). *Pharmacy in History*. London: Baillière, Tindall and Cox.

United Nations Office on Drugs and Crime. (2017). Global SMART Update: Fentanyl and its analogues - 50 years on. In (Vol. 17).

United States Drug Enforcement Administration. (2016). *Counterfeit Prescription Pills Containing Fentanyls: A Global Threat* (DEA-DCT-DIB-021-16).

United States Drug Enforcement Administration. Facts about Fentanyl. Retrieved from https://www.dea.gov/resources/facts-about-fentanyl

United States Drug Enforcement Administration. (2017). *2017 National Drug Threat Assessment*.

Vandenbosch, M., Pajk, S., Van Den Bogaert, W., Wuestenbergs, J., Van de Voorde, W., & Cuypers, E. (2022). Postmortem Analysis of Opioids and Metabolites in Skeletal Tissue. *J Anal Toxicol, 46*(7), 783-790. doi:10.1093/jat/bkab095

Varshneya, N. B., Hassanien, S. H., Holt, M. C., Stevens, D. L., Layle, N. K., Bassman, J. R., Iula, D. M., & Beardsley, P. M. (2022). Respiratory depressant effects of fentanyl analogs are opioid receptor-mediated. *Biochem Pharmacol, 195*, 114805. doi:10.1016/j.bcp.2021.114805

Vo, Q. N., Mahinthichaichan, P., Shen, J., & Ellis, C. R. (2021). How mu-opioid receptor recognizes fentanyl. *Nat Commun, 12*(1), 984. doi:10.1038/s41467-021-21262-9

Volkow, N. D. (2021). The epidemic of fentanyl misuse and overdoses: challenges and strategies. *World Psychiatry, 20*(2), 195-196. doi:10.1002/wps.20846

Warner, M., Trinidad, J. P., Bastian, B. A., Minino, A. M., & Hedegaard, H. (2016). Drugs Most Frequently Involved in Drug Overdose Deaths: United States, 2010-2014. *Natl Vital Stat Rep, 65*(10), 1-15.

Weinsanto, I., Laux-Biehlmann, A., Mouheiche, J., Maduna, T., Delalande, F., Chavant, V., Gabel, F. Darbon, P., Charlet, A., Poisbeau, P., Lamshöft, M., Van Dorsselaer, A., Cianferani, S., Parat, M. O., & Goumon, Y. (2018). Stable isotope-labelled morphine to study in vivo central and peripheral morphine glucuronidation and brain transport in tolerant mice. *Br J Pharmacol, 175*(19), 3844-3856. doi:10.1111/bph.14454

Welch, S. P., & Dewey, W. L. (1986). A characterization of the antinociception produced by intracerebroventricular injection of 8-(N,N-diethylamino)octyl-3,4,5-trimethoxybenzoate in mice. J Pharmacol Exp Ther, 239(2), 320-326.

Wicks, C., Hudlicky, T., & Rinner, U. (2021). Morphine alkaloids: History, biology, and synthesis. *Alkaloids Chem Biol, 86*, 145-342. doi:10.1016/bs.alkal.2021.04.001

Wiese, B. M., Liktor-Busa, E., Levine, A., Couture, S. A., Nikas, S. P., Ji, L., Liu, Y., Mackie, K., Makriyannis, A., Largent-Milnes, T. M., & Vanderah, T. W. (2021). Cannabinoid-2 Agonism with AM2301 Mitigates Morphine-Induced Respiratory Depression. *Cannabis Cannabinoid Res, 6*(5), 401-412. doi:10.1089/can.2020.0076

Yang, Z., Wang, L., Xu, M., Gu, J., Yu, L., & Zeng, S. (2016). Simultaneous analysis of gemfibrozil, morphine, and its two active metabolites in different mouse brain structures using solid-phase extraction with ultra-high performance liquid chromatography and tandem mass spectrometry with a deuterated internal standard. *J Sep Sci, 39*(11), 2087-2096. doi:10.1002/jssc.201600088

Zavala, C. A., Thomaz, A. C., Iyer, V., Mackie, K., & Hohmann, A. G. (2021). Cannabinoid CB(2) Receptor Activation Attenuates Fentanyl-Induced Respiratory Depression. *Cannabis Cannabinoid Res, 6*(5), 389-400. doi:10.1089/can.2020.0059

Zelcer, N., van de Wetering, K., Hillebrand, M., Sarton, E., Kuil, A., Wielinga, P. R., Tephly, T., Dahan, A., Beijnen, J. H., & Borst, P. (2005). Mice lacking multidrug resistance protein 3 show altered

morphine pharmacokinetics and morphine-6-glucuronide antinociception. *Proc Natl Acad Sci U S A, 102*(20), 7274-7279. doi:10.1073/pnas.0502530102

Zhan, B., Ma, H. Y., Wang, J. L., & Liu, C. B. (2015). Sex differences in morphine-induced behavioral sensitization and social behaviors in ICR mice. *Dongwuxue Yanjiu, 36*(2), 103-108. doi:10.13918/j.issn.2095-8137.2015.2.103

Zhu, P., Ye, Z., Guo, D., Xiong, Z., Huang, S., Guo, J., Zhang, W., Polli, J. E., Zhou, H., Li, Q., & Shu, Y. (2018). Irinotecan Alters the Disposition of Morphine Via Inhibition of Organic Cation Transporter 1 (OCT1) and 2 (OCT2). *Pharm Res, 35*(12), 243. doi:10.1007/s11095-018-2526-y

Zuccaro, P., Ricciarello, R., Pichini, S., Pacifici, R., Altieri, I., Pellegrini, M., & D'Ascenzo, G. (1997). Simultaneous determination of heroin 6-monoacetylmorphine, morphine, and its glucuronides by liquid chromatography--atmospheric pressure ionspray-mass spectrometry. *J Anal Toxicol, 21*(4), 268-277. doi:10.1093/jat/21.4.268

APPENDIX: METHOD VALIDATION TABLES

Table A1. Absolute Between-Run Accuracy (Bias)

	Accuracy (%Bias) (n = 14-15)			
Analyte	LLOQ	Low QC	Med QC	High QC
Fentanyl	11	4.1	7.0	10
Norfentanyl	3.7	1.3	0.46	3.1
4-ANPP	7.5	5.7	10	14
Morphine	4.2	1.0	6.6	10
Morphine-3-glucuronide	12	4.4	0.29	3.8
Morphine-6-glucuronide	10	2.9	1.4	4.4

LLOQ (lower limit of quantification): 1 ng/mL (fentanyl & 4-ANPP), 5 ng/mL (norfentanyl), 10 ng/mL (morphine), 50 ng/mL (morphine-3- and -6-glucuronide)
Low QC (low quality control): 3 ng/mL (fentanyl & 4-ANPP), 15 ng/mL (norfentanyl), 30 ng/mL (morphine), 150 ng/mL (morphine 3- and -6-glucuronide)
Med QC (medium quality control): 7.5 ng/mL (fentanyl & 4-ANPP), 40 ng/mL (norfentanyl), 75 ng/mL (morphine), 400 ng/mL (morphine 3- and -6-glucuronide)
High QC (high quality control): 75 ng/mL (fentanyl & 4-ANPP), 400 ng/mL (norfentanyl), 750 ng/mL (morphine), 4,000 ng/mL (morphine 3- and -6-glucuronide)

%Bias = relative bias = ((sample value—reference value)/reference value)(100)

Absolute Within-Run Accuracy (Bias)

Table A2.1: Run 1

	Accuracy (%Bias) (n = 5)			
Analyte	LLOQ*	Low QC	Med QC	High QC
Fentanyl	15	8.8	2.7	14
Norfentanyl	16	16	12	4.1
4-ANPP	7.6	3.5	6.2	8.0
Morphine	2.6	11	0.80	7.0
Morphine-3-glucuronide	30	6.4	9.0	1.6
Morphine-6-glucuronide	13	11	11	4.0

*Samples run with separate batch (10/3/23)

Table A2.2: Run 2

	Accuracy (%Bias) (n = 4-5)			
Analyte	LLOQ	Low QC	Med QC	High QC
Fentanyl	16	15	7.6	11
Norfentanyl	3.5	11	12	13
4-ANPP	16	20	15	18
Morphine	10	10	10	15
Morphine-3-glucuronide	11	19	18	8.8
Morphine-6-glucuronide	7.8	14	14	12

Table A2.3: Run 3

Accuracy (%Bias) (n = 5)				
Analyte	LLOQ	Low QC	Med QC	High QC
Fentanyl	2.3	6.5	11	5.0
Norfentanyl	8.8	8.7	4.3	2.8
4-ANPP	0.56	0.53	8.8	18
Morphine	5.2	4.6	10	10
Morphine-3-glucuronide	5.2	0.13	6.3	2.1
Morphine-6-glucuronide	8.8	6.0	5.0	1.5

LLOQ (lower limit of quantification): 1 ng/mL (fentanyl & 4-ANPP), 5 ng/mL (norfentanyl), 10 ng/mL (morphine), 50 ng/mL (morphine-3- and -6-glucuronide)
Low QC (low quality control): 3 ng/mL (fentanyl & 4-ANPP), 15 ng/mL (norfentanyl), 30 ng/mL (morphine), 150 ng/mL (morphine 3- and -6-glucuronide)
Med QC (medium quality control): 7.5 ng/mL (fentanyl & 4-ANPP), 40 ng/mL (norfentanyl), 75 ng/mL (morphine), 400 ng/mL (morphine 3- and -6-glucuronide)
High QC (high quality control): 75 ng/mL (fentanyl & 4-ANPP), 400 ng/mL (norfentanyl), 750 ng/mL (morphine), 4,000 ng/mL (morphine 3- and -6-glucuronide)

Table A3: Absolute Between-Run Precision

Mean ± SD ng/mL (%CV) (n = 14-15)				
Analyte	LLOQ	Low QC	Med QC	High QC
Fentanyl	1.1±0.17 (15)	3.1±0.50 (16)	8.0±0.52 (6.5)	82±5.4 (6.6)
Norfentanyl	5.2±0.59 (11)	15±2.3 (15)	40±4.5 (11)	413±36 (8.7)
4-ANPP	1.1±0.10 (10)	3.2±0.41 (13)	8.2±0.53 (6.4)	86±5.5 (6.4)
Morphine	10 ± 1.3 (13)	30±4.0 (13)	80±6.3 (7.8)	826±42 (5.1)
Morphine-3-glucuronide	56±8.4 (15)	157±18 (11)	399±55 (14)	4152±284 (6.9)
Morphine-6-glucuronide	55±4.1 (7.5)	154±21 (14)	394±47 (12)	4177±322 (7.7)

LLOQ (lower limit of quantification): 1 ng/mL (fentanyl & 4-ANPP), 5 ng/mL (norfentanyl), 10 ng/mL (morphine), 50 ng/mL (morphine-3- and -6-glucuronide)
Low QC (low quality control): 3 ng/mL (fentanyl & 4-ANPP), 15 ng/mL (norfentanyl), 30 ng/mL (morphine), 150 ng/mL (morphine 3- and -6-glucuronide)
Med QC (medium quality control): 7.5 ng/mL (fentanyl & 4-ANPP), 40 ng/mL (norfentanyl), 75 ng/mL (morphine), 400 ng/mL (morphine 3- and -6-glucuronide)
High QC (high quality control): 75 ng/mL (fentanyl & 4-ANPP), 400 ng/mL (norfentanyl), 750 ng/mL (morphine), 4,000 ng/mL (morphine 3- and -6-glucuronide)

Absolute Within-Run Precision

Table A4.1: Run 1

	Mean ± SD ng/mL (%CV) (n = 5)			
Analyte	LLOQ*	Low QC	Med QC	High QC
Fentanyl	1.1±0.051 (4.5)	2.7±0.43 (16)	7.7±0.53 (6.9)	85±3.6 (4.2)
Norfentanyl	5.8±0.12 (2.1)	13±2.3 (18)	35±1.5 (4.2)	384±24 (6.2)
4-ANPP	1.1±0.062 (5.8)	2.9±0.40 (14)	8.0±0.31 (3.9)	81±4.4 (5.4)
Morphine	9.7±1.9 (19)	27±4.8 (18)	76±3.9 (5.1)	803±42 (5.3)
Morphine-3-glucuronide	645±3.2 (5.0)	140±7.5 (5.3)	364±36 (10)	4062±182 (4.5)
Morphine-6-glucuronide	57±1.5 (2.6)	133±15 (11)	358±14 (4.0)	4158±231 (5.6)

*Samples run with separate batch (10/3/23)

Table A4.2: Run 2

	Mean ± SD ng/mL (%CV) (n = 4-5)			
Analyte	LLOQ	Low QC	Med QC	High QC
Fentanyl	1.2±0.26 (22)	3.4±0.34 (10)	8.1±0.32 (4.0)	83±2.5 (3.0)
Norfentanyl	5.2±0.39 (7.5)	17±0.81 (4.9)	45±2.5 (5.6)	450±21 (4.7)
4-ANPP	1.2±0.084 (7.3)	3.6±0.19 (5.3)	8.7±0.24 (2.8)	88±1.2 (1.4)
Morphine	11±0.54 (4.9)	33±1.3 (3.9)	82±6.7 (8.1)	861±20 (2.3)
Morphine-3-glucuronide	55±4.2 (7.6)	179±2.2 (1.2)	473±9.6 (2.0)	4353±343 (7.9)
Morphine-6-glucuronide	54±3.4 (6.4)	171±9.5 (5.5)	458±25 (5.5)	4495±229 (5.1)

Table A4.3: Run 3

Mean ± SD ng/mL (%CV) (n = 5)				
Analyte	LLOQ	Low QC	Med QC	High QC
Fentanyl	1.0±0.043 (4.2)	3.2±0.45 (14)	8.3±0.46 (5.5)	79±6.6 (8.3)
Norfentanyl	4.6±0.28 (6.1)	16±0.55 (3.4)	42±1.8 (4.3)	411±27 (6.5)
4-ANPP	0.99±0.093 (9.3)	3.0±0.16 (5.4)	8.2±0.64 (7.9)	89±5.3 (6.0)
Morphine	11±0.76 (7.2)	31±2.0 (6.4)	82±5.5 (6.7)	822±37 (4.6)
Morphine-3-glucuronide	47±5.6 (12)	150±6.9 (4.6)	375±32 (8.5)	4082±232 (5.7)
Morphine-6-glucuronide	54±5.8 (11)	159±15 (9.4)	380±28 (7.3)	3942±241 (6.1)

LLOQ (lower limit of quantification): 1 ng/mL (fentanyl & 4-ANPP), 5 ng/mL (norfentanyl), 10 ng/mL (morphine), 50 ng/mL (morphine-3- and -6-glucuronide)
Low QC (low quality control): 3 ng/mL (fentanyl & 4-ANPP), 15 ng/mL (norfentanyl), 30 ng/mL (morphine), 150 ng/mL (morphine 3- and -6-glucuronide)
Med QC (medium quality control): 7.5 ng/mL (fentanyl & 4-ANPP), 40 ng/mL (norfentanyl), 75 ng/mL (morphine), 400 ng/mL (morphine 3- and -6-glucuronide)
High QC (high quality control): 75 ng/mL (fentanyl & 4-ANPP), 400 ng/mL (norfentanyl), 750 ng/mL (morphine), 4,000 ng/mL (morphine 3- and -6-glucuronide)

Table A5: Recovery of Analytes

	%Recovery (n = 5)	
Analyte	Low QC	High QC
Fentanyl	66	93
Norfentanyl	101	139
4-ANPP	69	88
Morphine	77	90
Morphine-3-glucuronide	66	81
Morphine-6-glucuronide	52	62

Low QC (low quality control): 3 ng/mL (fentanyl & 4-ANPP), 15 ng/mL (norfentanyl), 30 ng/mL (morphine), 150 ng/mL (morphine 3- and -6-glucuronide)
High QC (high quality control): 75 ng/mL (fentanyl & 4-ANPP), 400 ng/mL (norfentanyl), 750 ng/mL (morphine), 4,000 ng/mL (morphine 3- and -6-glucuronide)

Table A6: Recovery of Internal Standards

Analyte	**%Recovery (n=10)**
Fentanyl-d_5	93
Norfentanyl-d_5	118
4-ANPP -d_5	85
Morphine-d_3	93
Morphine-3-glucuronide-d_3	84
Morphine-6-glucuronide-d_3	59

Table A7: Matrix Effect: Standard

Matrix Effect (n = 5)		
Analyte	Low QC	High QC
Fentanyl	45	15
Norfentanyl	15	5.7
4-ANPP	68	14
Morphine	19	11
Morphine-3-glucuronide	26	12
Morphine-6-glucuronide	26	15

Low QC (low quality control): 3 ng/mL (fentanyl & 4-ANPP), 15 ng/mL (norfentanyl), 30 ng/mL (morphine), 150 ng/mL (morphine 3- and -6-glucuronide)
High QC (high quality control): 75 ng/mL (fentanyl & 4-ANPP), 400 ng/mL (norfentanyl), 750 ng/mL (morphine), 4,000 ng/mL (morphine 3- and -6-glucuronide)

Table A8: Matrix Effect: Internal Standard

Analyte	Matrix Effect (n=10)
Fentanyl-d_5	22
Norfentanyl-d_5	8.7
4-ANPP-d_5	25
Morphine-d_3	13
Morphine-3-glucuronide-d_3	14
Morphine-6-glucuronide-d_3	17

Table A9: Analyte Stability under Different Storage Conditions

		Mean ± SD ng/mL (%CV) (n = 5)	
Analyte	Stability Test	Low QC	High QC
Fentanyl	Benchtop	2.9±0.38 (13)	82±6.9 (8.5)
	Freeze/Thaw	3.1±0.38 (12)	84±5.6 (6.7)
Norfentanyl	Benchtop	12±1.2 (10)	402±32 (8.0)
	Freeze/Thaw	13±1.2 (8.8)	421±30 (7.2)
4-ANPP	Benchtop	2.8±0.14 (4.9)	84±4.5 (5.4)
	Freeze/Thaw	2.9±0.61 (21)	81±5.9 (7.3)
Morphine	Benchtop	33±2.5 (7.8)	829±57 (6.9)
	Freeze/Thaw	34±1.6 (4.9)	836±38 (4.6)
Morphine-3-glucuronide	Benchtop	159±15 (9.5)	4620±414 (9.0)
	Freeze/Thaw	175±6.9 (4.0)	4692±239 (5.1)
Morphine-6-glucuronide	Benchtop	137±8.2 (6.0)	4086±361 (8.8)
	Freeze/Thaw	152±6.9 (4.6)	4082±227 (5.6)

Low QC (low quality control): 3 ng/mL (fentanyl & 4-ANPP), 15 ng/mL (norfentanyl), 30 ng/mL (morphine), 150 ng/mL (morphine 3- and -6-glucuronide)
High QC (high quality control): 75 ng/mL (fentanyl & 4-ANPP), 400 ng/mL (norfentanyl), 750 ng/mL (morphine), 4,000 ng/mL (morphine 3- and -6-glucuronide)

Analyte Stability Over Time

Table A10.1: 24 hours post-preparation

Mean ± SD ng/mL (%CV) (n = 5)				
Analyte	LLOQ	Low QC	Med QC	High QC
Fentanyl	0.92±0.033 (3.6)	2.9±0.30 (10)	8.1±0.71 (8.8)	79±8.9 (11)
Norfentanyl	4.4±0.14 (3.1)	16±0.44 (2.8)	41±2.5 (6.1)	435±20 (4.5)
4-ANPP	0.99±0.10 (10)	2.9±0.16 (5.4)	8.0±0.86 (11)	84±7.8 (9.3)
Morphine	10±1.2 (12)	32±1.1 (3.5)	85±2.8 (3.3)	839±38 (4.5)
Morphine-3-glucuronide	48±4.5 (9.3)	150±17 (11)	386±14 (3.8)	3866±328 (8.5)
Morphine-6-glucuronide	54±5.8 (11)	152±20 (13)	393±17 (4.4)	3814±251 (6.6)

Table A10.2: 48 hours post-preparation

Mean ± SD ng/mL (%CV) (n = 4-5)				
Analyte	LLOQ	Low QC	Med QC	High QC
Fentanyl	1.1±0.055 (5.1)	2.8±0.17 (5.9)	7.9±0.53 (6.7)	83±4.2 (5.1)
Norfentanyl	4.6±0.30 (6.6)	16±0.66 (4.2)	41±2.0 (4.9)	431±23 (5.3)
4-ANPP	0.90±0.11 (12)	3.2±0.38 (12)	7.9±0.38 (5)	90±4.7 (5.2)
Morphine	11±1.1 (11)	32±2.7 (8.2)	84±2.7 (3.2)	812±66 (8.2)
Morphine-3-glucuronide	51±4.8 (9.4)	159±20 (13)	436±23 (5.3)	3970±460 (12)
Morphine-6-glucuronide	56±5.7 (10)	153±15 (10)	441±26 (5.9)	4028±394 (10)

Table A10.3: 72 hours post-preparation

Mean ± SD ng/mL (%CV) (n = 5)				
Analyte	LLOQ	Low QC	Med QC	High QC
Fentanyl	1.0±0.079 (7.9)	3.1±0.18 (5.7)	8.2±0.60 (7.3)	76±5.7 (7.4)
Norfentanyl	5.3±0.55 (10)	17±0.45 (2.6)	42±2.3 (5.5)	421±15 (3.5)
4-ANPP	1.0±0.11 (11)	3.3±0.41 (13)	8.9±0.75 (8.4)	84±4.8 (5.7)
Morphine	10±1.4 (14)	33±2.4 (7.1)	84±5.9 (7.1)	825±62 (7.6)
Morphine-3-glucuronide	55±5.4 (10)	177±17 (9.4)	447±21 (4.8)	4262±268 (6.3)
Morphine-6-glucuronide	55±3.6 (6.6)	182±4.1 (2.3)	440±13 (2.9)	4316±369 (8.6)

LLOQ (lower limit of quantification): 1 ng/mL (fentanyl & 4-ANPP), 5 ng/mL (norfentanyl), 10 ng/mL (morphine), 50 ng/mL (morphine-3- and -6-glucuronide)
Low QC (low quality control): 3 ng/mL (fentanyl & 4-ANPP), 15 ng/mL (norfentanyl), 30 ng/mL (morphine), 150 ng/mL (morphine 3- and -6-glucuronide)
Med QC (medium quality control): 7.5 ng/mL (fentanyl & 4-ANPP), 40 ng/mL (norfentanyl), 75 ng/mL (morphine), 400 ng/mL (morphine 3- and -6-glucuronide)
High QC (high quality control): 75 ng/mL (fentanyl & 4-ANPP), 400 ng/mL (norfentanyl), 750 ng/mL (morphine), 4,000 ng/mL (morphine 3- and -6-glucuronide)

Absolute Accuracy (Bias) for Analyte Stability Over Time

Table A11.1: 24 hours post-preparation

	Accuracy (%Bias) (n = 5)			
Analyte	LLOQ	Low QC	Med QC	High QC
Fentanyl	7.6	3.5	7.5	5.2
Norfentanyl	11	5.9	1.9	8.7
4-ANPP	1.0	4.0	7.1	11
Morphine	1.1	7.2	14	12
Morphine-3-glucuronide	4.0	0.27	3.5	3.4
Morphine-6-glucuronide	7.7	1.5	1.8	4.7

Table A11.2: 48 hours post-preparation

	Accuracy (%Bias) (n = 4-5)			
Analyte	LLOQ	Low QC	Med QC	High QC
Fentanyl	6.6	6.7	5.0	10
Norfentanyl	7.2	5.9	2.7	7.7
4-ANPP	10	5.2	4.9	19
Morphine	7.5	7.6	12	8.3
Morphine-3-glucuronide	1.4	5.7	9.1	0.75
Morphine-6-glucuronide	11	1.7	10	0.70

Table A11.3: 72 hours post-preparation

Accuracy (%Bias) (n = 5)				
Analyte	LLOQ	Low QC	Med QC	High QC
Fentanyl	0.58	3.1	10	1.9
Norfentanyl	6.0	15	5.2	5.2
4-ANPP	4.0	8.4	18	13
Morphine	0.58	10	12	10
Morphine-3-glucuronide	10	18	12	6.6
Morphine-6-glucuronide	11	21	10	7.9

LLOQ (lower limit of quantification): 1 ng/mL (fentanyl & 4-ANPP), 5 ng/mL (norfentanyl), 10 ng/mL (morphine), 50 ng/mL (morphine-3- and -6-glucuronide)
Low QC (low quality control): 3 ng/mL (fentanyl & 4-ANPP), 15 ng/mL (norfentanyl), 30 ng/mL (morphine), 150 ng/mL (morphine 3- and -6-glucuronide)
Med QC (medium quality control): 7.5 ng/mL (fentanyl & 4-ANPP), 40 ng/mL (norfentanyl), 75 ng/mL (morphine), 400 ng/mL (morphine 3- and -6-glucuronide)
High QC (high quality control): 75 ng/mL (fentanyl & 4-ANPP), 400 ng/mL (norfentanyl), 750 ng/mL (morphine), 4,000 ng/mL (morphine 3- and -6-glucuronide)

Table A12.1: Fentanyl Quality Controls for 13 Experimental Matrices

	Mean ± SD ng/mL or ng/g (%CV)		
Sample type (n=3)	Low QC	Med QC	High QC
Whole Blood	3.2 ± 0.30 (9.4)	7.5 ± 0.72 (10)	80 ± 5.7 (7.2)
Brain	3.4 ± 0.039 (1.1)	7.9 ± 0.35 (4.4)	75 ± 5.4 (7.2)
Liver	3.2 ± 0.062 (1.9)	7.7 ± 0.35 (4.5)	69 ± 1.3 (1.8)
Heart	3.2 ± 0.066 (2.1)	8.4 ± 0.37 (4.4)	78 ± 7.1 (9.1)
Lung	3.3 ± 0.091 (2.8)	8.2 ± 0.42 (5.2)	76 ± 8.9 (12)
Kidney	3.4 ± 0.045 (1.3)	7.8 ± 0.80 (10)	76 ± 7.2 (10)
Spleen	2.9 ± 0.32 (11)	7.7 ± 0.35 (4.5)	80 ± 1.2 (1.6)
Small Intestine	3.02± 0.16 (5.1)	8.1 ± 0.42 (5.2)	80 ± 3.5 (4.4)
Large Intestine	3.0 ± 0.29 (10)	8.5 ± 0.87 (10)	72 ± 2.2 (3.1)
Stomach	3.4 ± 0.045 (1.3)	7.9 ± 0.24 (3.0)	77 ± 6.5 (8.4)
Muscle	3.3 ± 0.017 (0.51)	8.1 ± 0.25 (3.0)	82 ± 1.8 (2.3)
Fat	3.3 ± 0.054 (1.6)	8.3 ± 0.052 (0.63)	85 ± 0.52 (0.62)
Skin	2.7 ± 0.093 (3.5)	7.4 ± 0.49 (6.6)	79 ± 1.1 (1.3)

Table A12.2: Norfentanyl Quality Controls for 13 Experimental Matrices

	Mean ± SD ng/mL or ng/g (%CV)		
Sample type (n=3)	Low QC	Med QC	High QC
Whole Blood	13 ± 0.16 (1.2)	42 ± 2.5 (6.1)	431 ± 29 (6.7)
Brain	16 ± 0.71 (4.6)	38 ± 2.5 (6.5)	426 ± 11 (2.7)
Liver	14 ± 1.2 (8.7)	34 ± 0.78 (2.3)	344 ± 13 (3.8)
Heart	16 ± 2.5 (16)	45 ± 2.6 (5.8)	399 ± 23 (5.8)
Lung	14 ± 0.53 (3.8)	42 ± 4.5 (11)	358 ± 14 (3.9)
Kidney	15 ± 2.3 (16)	42 ± 4.8 (11)	409 ± 5.6 (1.4)
Spleen	16 ± 2.2 (14)	40 ± 1.1 (2.6)	405 ± 14 (3.4)
Small Intestine	18 ± 0.68 (3.9)	42 ± 0.24 (0.59)	414 ± 18 (4.4)
Large Intestine	17 ± 1.2 (7.3)	41 ± 0.14 (0.34)	366 ± 8.3 (2.3)
Stomach	18 ± 0.39 (2.2)	39 ± 1.2 (3.0)	392 ± 2.4 (0.60)
Muscle	15 ± 0.42 (2.8)	37 ± 0.19 (0.50)	391 ± 5.9 (1.5)
Fat	18 ± 0.42 (2.3)	41 ± 0.45 (1.1)	435 ± 5.9 (1.4)
Skin	13 ± 0.17 (1.4)	36 ± 1.7 (4.8)	403 ± 2.6 (0.65)

Table A12.3: 4-ANPP Quality Controls for 13 Experimental Matrices

	Mean ± SD ng/mL or ng/g (%CV)		
Sample type (n=3)	Low QC	Med QC	High QC
Whole Blood	3.1 ± 0.31 (10)	8.2 ± 0.22 (2.9)	77 ± 2.1 (2.8)
Brain	3.1 ± 0.21 (6.6)	8.7 ± 0.071 (0.82)	78 ± 11 (14)
Liver	3.0 ± 0.16 (5.4)	8.4 ± 0.38 (4.5)	74 ± 1.4 (1.9)
Heart	3.1 ± 0.31 (10)	8.6 ± 0.71 (8.2)	68 ± 2.1 (3.0)
Lung	3.3 ± 0.59 (18)	8.6 ± 0.33 (3.8)	71 ± 2.0 (2.8)
Kidney	3.0 ± 0.22 (7.5)	8.3 ± 0.37 (4.5)	83 ± 4.5 (5.5)
Spleen	2.7 ± 0.24 (9.1)	7.5 ± 0.16 (2.2)	71 ± 3.4 (4.8)
Small Intestine	3.0 ± 0.034 (1.1)	7.9 ± 0.016 (0.21)	82 ± 0.33 (0.40)
Large Intestine	3.7 ± 0.66 (18)	7.6 ± 0.19 (2.5)	69 ± 2.1 (3.0)
Stomach	3.1 ± 0.12 (3.7)	7.5 ± 0.26 (3.5)	75 ± 5.2 (7.0)
Muscle	3.0 ± 0.071 (2.3)	7.8 ± 0.25 (3.2)	74 ± 2.6 (3.5)
Fat	3.4 ± 0.18 (5.3)	7.5 ± 0.34 (4.6)	81 ± 1.2 (1.5)
Skin	2.5 ± 0.11 (4.4)	6.8 ± 0.12 (1.7)	73 ± 1.5 (2.0)

Table A12.4: Morphine Quality Controls for 13 Experimental Matrices

	Mean ± SD ng/mL or ng/g (%CV)		
Sample type (n=1-3)	Low QC	Med QC	High QC
Whole Blood	31 ± 3.1 (10)	76 ± 6.8 (8.8)	774 ± 88 (11)
Brain	34 ± 6.4 (19)	75 ± 4.5 (6.0)	794 ± 41 (5.1)
Liver	34 ± 2.2 (6.5)	73 ± 3.2 (4.3)	719 ± 33 (4.6)
Heart	27 ± 2.2 (8.0)	77 ± 0.94 (1.2)	735 ± 0 (0)
Lung	31±0 (0)		860 ±6.1 (0.71)
Kidney	33 ± 0 (0)	84 ± 0 (0)	800 ± 49 (6.1)
Spleen	31 ± 1.5 (4.9)	84 ± 4.7 (5.5)	775 ± 49 (6.4)
Small Intestine	30 ± 2.2 (7.3)	87 ± 5.7 (6.6)	758 ± 27 (3.5)
Large Intestine	31 ± 0.050 (0.16)	87 ± 8.4 (10)	699 ± 4.8 (0.68)
Stomach	35 ± 0.67 (1.9)	85 ± 0.54 (0.64)	811 ± 13 (1.6)
Muscle			658 ± 48 (7.3)
Fat	35 ± 0.24 (0.70)	86 ± 2.7 (3.2)	875 ± 12 (1.4)
Skin	31 ± 1.4 (4.4)	87 ± 0 (0)	821 ± 10 (1.2)

*Blank spaces denote QCs rejected due to severe deviation from acceptable levels of accuracy

Table A12.5: Morphine-3-β-D-glucuronide Quality Controls for 13 Experimental Matrices

	Mean ± SD ng/mL or ng/g (%CV)		
Sample type (n=3)	Low QC	Med QC	High QC
Whole Blood	155 ± 8.7 (5.6)	451 ± 27 (5.9)	4513 ± 496 (11)
Brain	165 ± 9.9 (6.0)	443 ± 20 (4.6)	4367 ± 249 (5.7)
Liver	176 ± 8.2 (4.7)	391 ± 52 (13)	3680 ± 151 (4.1)
Heart	163 ± 20 (12)	410 ± 47 (12)	3547 ± 441 (12)
Lung	167 ± 7.4 (4.4)	440 ± 35 (8.0)	4440 ± 418 (9.4)
Kidney	173 ± 17 (10)	402 ± 57 (14)	4237 ± 204 (4.8)
Spleen	151 ± 23 (15)	386 ± 13 (3.4)	3900 ± 270 (6.9)
Small Intestine	151 ± 9.3 (6.1)	399 ± 32 (7.9)	4270 ± 393 (9.2)
Large Intestine	184 ± 35 (19)	418 ± 4.6 (1.1)	3943 ± 259 (6.6)
Stomach	161 ± 12 (7.2)	412 ± 33 (8.0)	4310 ± 139 (3.2)
Muscle	172 ± 6.2 (3.6)	439 ± 29 (6.6)	4407 ± 62 (1.4)
Fat	164 ± 6.2 (3.8)	422 ± 28 (6.7)	4627 ± 175 (3.8)
Skin	138 ± 4.8 (3.5)	396 ± 11 (2.7)	4723 ± 117 (2.5)

Table A12.6: Morphine-6-β-D-glucuronide Quality Controls for 13 Experimental Matrices

	Mean ± SD ng/mL or ng/g (%CV)		
Sample type (n=1-3)	Low QC	Med QC	High QC
Whole Blood	174 ± 6.5 (3.7)	406 ± 49 (12)	4110 ± 200 (4.9)
Brain	169 ± 5.0 (2.9)	390 ± 12 (3.1)	4313 ± 46 (1.1)
Liver	160 ± 9.5 (5.9)	372 ± 25 (6.6)	3994 ± 307 (7.7)
Heart	150 ± 5.3 (3.5)	372 ± 5.9 (1.6)	3767 ± 254 (6.7)
Lung	132 ± 8.3 (6.3)	369 ± 24 (6.6)	4067 ± 171 (4.2)
Kidney	165 ± 16 (10)	429 ± 36 (8.4)	4090 ± 410 (10)
Spleen	133 ± 0 (0)	431 ± 14 (3.4)	4170 ± 128 (3.1)
Small Intestine	142 ± 10 (7.2)	419 ± 26 (6.2)	4070 ± 99 (2.4)
Large Intestine	144 ± 6.9 (4.8)	410 ± 10 (2.5)	3903 ± 296 (7.6)
Stomach	177 ± 1.7 (1.0)	442 ± 16 (3.6)	4457 ± 270 (6.0)
Muscle	163 ± 4.8 (2.9)	396 ± 11 (2.8)	4590 ± 134 (2.9)
Fat	176 ± 2.1 (1.2)	457 ± 3.8 (0.82)	4563 ± 152 (3.3)
Skin	136 ± 2.9 (2.2)	370 ± 19 (5.0)	4000 ± 29 (0.74)

Low QC (low quality control): 3 ng/mL (fentanyl & 4-ANPP), 15 ng/mL (norfentanyl), 30 ng/mL (morphine), 150 ng/mL (morphine 3- and -6-glucuronide)
Med QC (medium quality control): 7.5 ng/mL (fentanyl & 4-ANPP), 40 ng/mL (norfentanyl), 75 ng/mL (morphine), 400 ng/mL (morphine 3- and -6-glucuronide)
High QC (high quality control): 75 ng/mL (fentanyl & 4-ANPP), 400 ng/mL (norfentanyl), 750 ng/mL (morphine), 4,000 ng/mL (morphine 3- and -6-glucuronide)

Table A13.1: Fentanyl: Absolute Accuracy (Bias) in 13 Matrices.

	Accuracy (%Bias) (n = 3)		
Tissue	Low QC	Med QC	High QC
Whole Blood	5.7	0.62	6.8
Brain	14	5.2	0.044
Liver	6.4	2.9	8.0
Heart	5.1	12	4.0
Lung	9.4	10	0.76
Kidney	14	4.5	1.2
Spleen	2.8	3.3	6.2
Small Intestine	0.67	7.7	7.0
Large Intestine	1.0	13	4.5
Stomach	14	5.7	3.3
Muscle	10	7.6	9.1
Fat	10	11	13
Skin	11	1.0	5.1

Table A13.2: Norfentanyl: Absolute Accuracy (Bias) in 13 Matrices.

	Accuracy (%Bias) (n = 3)		
Tissue	Low QC	Med QC	High QC
Whole Blood	11	4.0	7.8
Brain	4.0	5.1	6.6
Liver	6.2	15	14
Heart	4.2	11	0.25
Lung	7.8	5.4	10
Kidney	2.2	5.2	2.2
Spleen	7.6	0.92	1.2
Small Intestine	17	4.2	3.5
Large Intestine	13	2.8	8.6
Stomach	18	2.4	2.1
Muscle	0.67	6.4	2.2
Fat	22	1.3	8.7
Skin	16	10	0.67

Table A13.3: 4-ANPP: Absolute Accuracy (Bias) in 13 Matrices.

	Accuracy (%Bias) (n = 3)		
Tissue	Low QC	Med QC	High QC
Whole Blood	2.9	9.1	2.7
Brain	4.4	16	4.5
Liver	1.3	12	1.5
Heart	4.9	15	9.4
Lung	10	15	5.2
Kidney	1.1	11	10
Spleen	11	0.62	4.7
Small Intestine	0.89	4.8	10
Large Intestine	25	2.0	8.1
Stomach	4/9	0	0.44
Muscle	1.3	3.4	1.8
Fat	14	0.089	7.6
Skin	18	9.4	2.8

Table A13.4: Morphine: Absolute Accuracy (Bias) in 13 Matrices.

	Accuracy (%Bias) (n = 1-3)		
Tissue	Low QC	Med QC	High QC
Whole Blood	4.3	2.0	3.2
Brain	12	0.36	5.8
Liver	14	2.6	4.2
Heart	10	2.2	2.0
Lung	1.7		15
Kidney	10	13	6.7
Spleen	4.2	12	3.3
Small Intestine	0.78	16	1.1
Large Intestine	3.5	16	6.8
Stomach	16	14	8.2
Muscle			12
Fat	16	15	17
Skin	13	16	19

*Blank spaces denote QCs rejected due to severe deviation from acceptable levels of accuracy

Table A13.5: Morphine-3-β-D-glucuronide: Absolute Accuracy (Bias) in 13 Matrices.

	Accuracy (%Bias) (n = 3)		
Tissue	Low QC	Med QC	High QC
Whole Blood	3.1	13	13
Brain	10	11	9.2
Liver	18	2.3	8.0
Heart	8.4	2.5	11
Lung	12	10	11
Kidney	16	0.42	5.9
Spleen	0.44	2.5	2.5
Small Intestine	0.67	0.17	6.8
Large Intestine	22	4.6	1.4
Stomach	7.3	2.9	7.8
Muscle	14	10	10
Fat	10	5.5	16
Skin	8.2	0.92	18

Table A13.6: Morphine-6-β-D-glucuronide: Absolute Accuracy (Bias) in 13 Matrices.

	Accuracy (%Bias) (n = 3)		
Tissue	Low QC	Med QC	High QC
Whole Blood	16	1.4	2.8
Brain	13	2.6	7.8
Liver	6.4	7.0	0.15
Heart	0.22	7.1	5.8
Lung	12	7.7	1.7
Kidney	10	7.3	2.3
Spleen	11	7.7	4.3
Small Intestine	5.3	4.8	1.8
Large Intestine	4.2	2.4	2.4
Stomach	18	11	11
Muscle	8.9	1.1	15
Fat	18	14	14
Skin	9.3	7.5	0

Low QC (low quality control): 3 ng/mL (fentanyl & 4-ANPP), 15 ng/mL (norfentanyl), 30 ng/mL (morphine), 150 ng/mL (morphine 3- and -6-glucuronide)
Med QC (medium quality control): 7.5 ng/mL (fentanyl & 4-ANPP), 40 ng/mL (norfentanyl), 75 ng/mL (morphine), 400 ng/mL (morphine 3- and -6-glucuronide)
High QC (high quality control): 75 ng/mL (fentanyl & 4-ANPP), 400 ng/mL (norfentanyl), 750 ng/mL (morphine), 4,000 ng/mL (morphine 3- and -6-glucuronide)

VITA

Rosamond Morgan Goodson was born on August 28th, 1994 in Savannah, Georgia. She graduated from Statesboro High School, Statesboro, Georgia in 2013 and received her Bachelor of Arts in Neuroscience and Music from Wesleyan College, Macon, Georgia in 2017. Afterwards, she enrolled at Virginia Commonwealth University, Richmond, Virginia, where she earned a Doctor of Philosophy in Pharmacology and Toxicology in 2024.